

DISSERTATION

PSEUDO PELGER-HUËT ANOMALIES AS POTENTIAL BIOMARKERS FOR ACUTE
RADIATION DOSE IN RHESUS MACAQUES (*MACACA MULATTA*)

Submitted by

Joshua Michael Hayes

Department of Environmental and Radiological Health Sciences

In partial fulfillment of the requirements

For a Doctor of Philosophy Degree

Colorado State University

Fort Collins, Colorado

Spring 2021

Doctoral Committee:

Advisor: Thomas E. Johnson

Susan Bailey

Alexander Brandl

John Walrond

Copyright by Joshua Michael Hayes 2021

All Rights Reserved

ABSTRACT

PSEUDO PELGER-HUËT ANOMALIES AS POTENTIAL BIOMARKERS FOR ACUTE RADIATION DOSE IN RHESUS MACAQUES (*MACACA MULATTA*)

The potential for malicious use of radiation, or radiation accidents could potentially lead to acute, high radiation doses to members of the public. Following an acute accidental exposure to high doses of radiation, medical intervention is pivotal to the survivability of the patient and the sooner the appropriate measures are taken the better the odds for survival. Early estimates of acute accidental radiation doses can be determined via biomarkers such as dicentric chromosome analysis or scenario reconstruction using computer software. However, both take valuable time, and can be expensive. Here, potentially faster, and cheaper quantitative biomarkers for radiation exposure were evaluated in acutely exposed Rhesus Macaques from the Wake Forest School of Medicine, Department of Comparative Medicine. Increased frequencies of abnormal neutrophils in peripheral blood, referred to as pseudo Pelger-Huët anomalies (PPHAs), have been shown to be potential biomarkers of radiation exposure in several scenarios, including the 1958 Y-12 criticality accident and the radium dial painters. We have confirmed the PPHA morphology to be present in Rhesus Macaques and a dose response curve, a biokinetics model, and determination of background prevalence of the morphology has been constructed utilizing peripheral blood smears. The dose response curve consists of macaques that received doses ranging from 0 Gy to 8.5 Gy (LD90/30) and a blood smear at a common time point post-irradiation. The biokinetics model utilized only 4 Gy exposures and blood smears taken periodically over 3.1 years post-

irradiation. Results show a linear correlation between PPHA concentration and acute radiation dose and the PPHA morphology appears stable over 3.1 years post-irradiation.

ACKNOWLEDGEMENTS

To Thomas Johnson, thank you for trusting me to be a free-range graduate student, but still being enough of a guide to keep me from falling flat on my face . . . more than once. I trust that our last 3 am email exchange about projects are not behind us, and that has nothing to do with time differences. I will get you that 12-dollar scotch and respect if I get to drive the toaster. Semper Gumby! To my Dad, I read your dissertation probably 3 times while trying to break the ice on my own. Once I finally hit a stride, you were always able to coach me back in line when I got frustrated and/or discouraged. Lastly, and most importantly, my wife told me that if I did not finish my dissertation this year, she would beat me senseless . . . so here we are. In all seriousness, this project would never have been completed without your endless support, insurmountable patience, and ability to keep me grounded when I get overwhelmed. Graduate school is finally almost behind us, and we are onto the next big adventure.

DEDICATION

I am dedicating this dissertation to Morgan Ladd Sneed (Oct 21, 1981 – Nov 18, 2020)
It was an honor to be your friend and to grow together in post military life.
I will see you on the other side.

TABLE OF CONTENTS

ABSTRACT.....ii

ACKNOWLEDGEMENTS.....iv

DEDICATION.....v

LIST OF TABLES.....ix

LIST OF FIGURES.....x

Chapter 1: Introduction and Literature Review..... 1

 Scope and Purpose of this Project.....1

 Definitions of Pertinent Terms.....4

 Ionizing Radiation, Biological Effects, & Relevant Real-World Cases.....6

 Purpose of Biodosimetry and Current Methods8

 The Hematopoietic System/Neutrophil Development.....13

 The Pseudo Pelger-Huët Anomaly: Morphology and Suspected Origin.....23

 The Pseudo Pelger-Huët Anomaly as a Biodosimeter.....28

 Rhesus Macaque: Species Information and Justification of Use in This Study.....32

Chapter 2: Methodology35

 IACUC Approval Statement.....35

 Studies Conducted Using Rhesus Macaques.....35

 Irradiation Protocols for Rhesus Macaques.....39

Pseudo Pelger-Huët Anomaly Quantification with Light Microscope.....	41
Risk and Mitigation of Bias.....	42
Data Analysis and Presentation.....	44
Chapter 3: Results.....	46
Pseudo Pelger-Huët Anomaly Baseline Precedence in Rhesus Macaques (non- irradiated)	46
Pseudo Pelger-Huët Anomaly Dose Response in Rhesus Macaques.....	47
Pseudo Pelger-Huët Anomaly Biokinetics/Persistence in Rhesus Macaques Post- Irradiation.....	50
Chapter 4: Discussion.....	55
Rhesus Macaque Baseline Prevalence of Pseudo Pelger-Huët Anomalies.....	55
Rhesus Macaque Dose Response of Pseudo Pelger-Huët Anomalies.....	55
Rhesus Macaques Biokinetics/Persistence Post Irradiation.....	57
Possible Reasons for PPHA Persistence When Compared to Other Biodosimetry - Methods.....	58
Ergonomic Hazards of this Study.....	60
Limitations of Results.....	60
Chapter 5: Conclusions and Recommendations for Future Research.....	62
Expanding Dose Response, Biokinetics, & Persistence.....	62
Validation of the Pseudo Pelger-Huët Against Current Methods.....	63

Molecular Characterization and Identifying Origin of the Pseudo Pelger-Huët Anomaly.....	63
Automation of Analysis for Efficiency in Mass Casualty Incidents.....	66
Conclusions.....	68
References.....	71
Appendix A: Colorado State University IACUC Inter-Institutional Agreement.....	79
Appendix B: Wake Forest School of Medicine IACUC Approval Letter.....	82
Appendix C: Occupational Safety and Health Zoonotic Concerns Agreement with Wake Forest School of Medicine.....	83
Appendix D: Chart of Hematopoietic Stem Cell Differentiation.....	87
Appendix E: Statement of Permission to Use Rhesus Macaque Images.....	88
Appendix F: Biokinetic/Persistence Models and Data for Individual Rhesus Macaque.....	89
Dose Response Data.....	89
Group 1 Biokinetics, Rhesus Macaques, Irradiation Date 10/16/2016 (4 Gy)	91
Group 2 Biokinetics, Rhesus Macaques, Irradiation Date 10/23/2016 (4Gy).....	97
Appendix G: Making A Blood Smear.....	103
Appendix H: Giemsa Staining Blood Smears.....	105

LIST OF TABLES

Table 1. Biodosimetry methods and the corresponding detection limits.....	13
Table 2. All rhesus macaques with associated demographic data.....	36
Table 3. Baseline prevalence of pseudo Pelger-Huët anomalies in rhesus macaques.....	46
Table 4. Averages of 0, 4, and 6.5 Gy rhesus macaques.....	48
Table 5. Rhesus Macaques dose response clustered by radiation dose.....	50
Table 6. Rhesus macaque biokinetics/persistence with n-10 averaged	54
Table 7. Rhesus macaques dose response.....	89
Table 8. Rhesus macaque biokinetics/persistence, average PPHA concentration of group 1	91
Table 9. Biokinetics/persistence for macaque 1962.....	92
Table 10. Biokinetics/persistence for macaque 1971.....	93
Table 11. Biokinetics/persistence for macaque 1974.....	94
Table 12. Biokinetics/persistence for macaque 1979.....	95
Table 13. Biokinetics/persistence for macaque 1982.....	96
Table 14. Rhesus macaque biokinetics/persistence, average PPHA concentration of group 2.....	97
Table 15. Biokinetics/persistence for macaque 1965.....	98
Table 16. Biokinetics/persistence for macaque 1973.....	99
Table 17. Biokinetics/persistence for macaque 1975.....	100
Table 18. Biokinetics/persistence for macaque 1976.....	101
Table 19. Biokinetics/persistence for macaque 1977.....	102

LIST OF FIGURES

Figure 1. Red blood cells, platelets, and a PPHA cell from Macaque 1905.....	15
Figure 2. Neutrophil from macaque 1905.....	17
Figure 3: Eosinophil from macaque 1905.....	20
Figure 4. Monocyte from macaque 1905.....	21
Figure 5. Basophil from macaque 1905.....	22
Figure 6: Lymphocyte from macaque 1905.....	23
Figure 7. Structure of the lamin-B receptor.....	25
Figure 8. Examples of pseudo Pelger-Huët anomalies.....	26
Figure 9: Example of a normal neutrophil next to a pseudo Pelger-Huët cell from macaque 1905.....	27
Figure 10. Images of rhesus macaques.....	34
Figure 11. Distribution of PPHAs in 0 Gy rhesus macaques.....	46
Figure 12. Rhesus macaques dose response.....	48
Figure 13. Rhesus macaques dose response with animals clustered by dose.....	49
Figure 14. Rhesus macaques average time to a steady increase in the prevalence of pseudo Pelger-Huët anomalies.....	51
Figure 15. Rhesus macaques biokinetics/persistence, n-10 overlay.....	53
Figure 16. Rhesus macaque biokinetics/persistence, average PPHA concentration	53
Figure 17. Hematopoietic stem cell differentiation.....	87
Figure 18. Rhesus macaque biokinetics/persistence, average PPHA concentration of group 1.....	91
Figure 19. Biokinetics/persistence diagram for macaque 1962.....	92

Figure 20. Biokinetics/persistence diagram for macaque 1971.....	93
Figure 21. Biokinetics/persistence diagram for macaque 1974.....	94
Figure 22. Biokinetics/persistence diagram for macaque 1979.....	95
Figure 23. Biokinetics/persistence diagram for macaque 1982.....	96
Figure 24. Rhesus macaque biokinetics/persistence, average PPHA concentration of group 2.....	97
Figure 25. Biokinetics/persistence diagram for macaque 1965.....	98
Figure 26. Biokinetics/persistence diagram for macaque 1973.....	99
Figure 27. Biokinetics/persistence diagram for macaque 1975.....	100
Figure 28. Biokinetics/persistence diagram for macaque 1976.....	101
Figure 29. Biokinetics/persistence diagram for macaque 1977.....	102
Figure 30. Placement of second slide in the process of creating a blood smear.....	103
Figure 31. Drawing back the top slide as to contact the blood drop.....	103
Figure 32. Placement of second slide in the process of creating a blood smear.....	104
Figure 33. GURR buffer tablets used in preparation of Giemsa stain.....	105
Figure 34. Giemsa stained blood smears.....	106

Chapter 1: Introduction & Literature Review

Scope and Purpose of this Project

This study is intended to expand upon the methodologies available to biodosimetrists for early and retrospective dose estimations for individuals that have been exposed to ionizing radiation. Radiation exposure can occur in several different ways to include but not limited to internal, external, chronic, acute, industrial accidents, environmental contamination, naturally occurring radioactive materials, criticality accidents, or combinations of the above. Considering the multiple scenarios for accidental radiation exposures that have happened and could happen, tools for early dose assessment are vital to proper triage of patients and ultimately medical treatment.

The pseudo Pelger-Huët anomalies (PPHA) assay is performed by taking a peripheral blood smear that has been stained with a nuclear staining dye such as Giemsa-Wright stain and evaluated using a light microscope to determine the percentage of neutrophils presenting the PPHA morphology. Previous research projects have shown promising results for chronic exposure from environmental sources, and preliminary data have been produced for acute exposure scenarios, but many questions have been left unanswered (Meehan, 2001 & Goans, 2015). Biological samples from acutely exposed rhesus macaques have been obtained to expand on the previously discovered evidence for the efficacy of the PPHA assay as a biomarker of radiation. This study hypothesizes that the PPHA assay will produce a statistically significant dose response model, and will have some degree of persistence following an irradiation incident.

Four specific aims were addressed in this study: (1) Establishing a baseline prevalence of PPHAs in the peripheral blood of rhesus macaques, (2) establishing a dose response curve across a variety of acute doses, (3) establishing a biokinetics and persistence model, (4) determining future study needs to utilize the PPHA assay for biodosimetry.

Part one of this study consists of establishing a baseline prevalence of PPHAs in peripheral blood of rhesus macaques. Goans et. al found that humans have a background prevalence of PPHAs of between $4.4 \pm 0.4\%$, so it was assumed that rhesus macaques have a background prevalence as well. Background radiation is an important consideration for both the baseline and the persistence of PPHAs, as PPHA morphology may be induced by chronic low dose exposure. The baseline prevalence of PPHAs in rhesus macaques was hypothesized to be above zero, but below the baseline of humans due the majority of the primates being irradiated at 5.2 ± 1.3 years of age, while humans were much older thus accumulating much higher lifetime doses from background radiation. Once again, correction factors for age could be required.

Part two of this study consists of establishing a dose response curve across a variety of acute radiation doses ranging from zero dose to 8.5 Gy (LD90/30) for the rhesus macaques (MacVittie, Farese, & Jackson, 2015). Goans et al. conducted a retrospective dose response study on 8 humans exposed to a mixed field of gamma rays and neutrons during the criticality accident at the Y-12 uranium enrichment facility in 1958 (Goans et. al, 2017). A dose response curve was constructed, however there was a small sample size, doses were estimated with dose reconstruction models lending to possible error, and the distribution of doses was split into a low dose cohort and a high dose cohort versus a spectrum. The limitations of the Goans et. al study was mitigated by using well characterized radiation doses to non-human primates, accumulating a large sample size, and seeking a spectrum of doses for a more robust dose response curve.

Part three of this study establishes a biokinetics and persistence model that illustrates how quickly the PPHA morphology manifests and how long PPHAs persist following exposure. In previous studies, biokinetics and persistence were briefly studied by Goans et al. Goans et al. irradiated non-human primates at the Armed Forces Radiobiology Research Institute (AFRRI) using a Co-60 source, and blood smears were taken to investigate how quickly the PPHA morphology began to rise in prevalence within the blood (Goans, 2015). Goans et al documented an increased frequency of PPHAs within 5 hours post exposure, but a peak prevalence was not documented and whether the prevalence persisted at that peak was not investigated. Persistence was retrospectively investigated by Goans et al. using the survivors of the Y-12 criticality accident, however, with a variety of doses received by the victims of the accident each persistence model only has $n=1$.

Part three of the study was accomplished using rhesus macaque blood smears taken at 18 different time points following exposure to a single, well characterized, acute radiation dose of 4 Gy then evaluated for PPHAs. The goal of evaluating multiple time points for PPHAs post-exposure is to provide insight into the time for the PPHA morphology to reach peak prevalence, and how persistent that prevalence is within the bounds of available samples (3.1 years post exposure).

The final part of this study consists of analyzing the collected data and extrapolating what further studies must be conducted to validate the PPHA morphology as a biomarker and to demonstrate that the PPHA assay can be utilized for biodosimetry. While the models built for this project will be more robust than previous studies, shortcomings remain. Future directions include analysis of more zero dose rhesus macaques to increase confidence in baseline, expansion of the dose response model by adding additional animals to increase a variety of

doses, extending the biokinetics model beyond the available 3.1 years of blood smears, and increasing frequency of blood smears taken immediately following irradiation to better characterize the induction of PPHAs. Additional anticipated areas of research that can be done to continue this project are to molecularly characterize the PPHA morphology, investigate other means of inducing PPHAs (chemical, viral, dietary, etc..), and investigating the efficacy of PPHA assay automation using metasystem microscopes that are currently in use for dicentric chromosome analysis.

Definitions of Pertinent Terms

Biokinetics – The movement of something inside of an organism, or of the organism itself (Ellapen & Swanepoel, 2017). In the context of the PPHA assay, biokinetics describes the mobilization of the anomalous neutrophils from the red bone marrow in the context of both the peak mobilization and how fast the mobilization reaches that peak in the peripheral blood following an irradiation event.

Prevalence – The proportion of a population that expresses a variable of interest at a specific time. The PPHA assay investigates the prevalence of neutrophils that present with the PPHA morphology as a percentage.

Persistence – The continuance in a course of action for a behavior, reaction, or effect despite any form of opposition that may be present. Following the increase in prevalence and subsequent peak of PPHAs in the peripheral blood, how long the PPHA morphology maintains that peak is investigated as the ‘persistence’ of the morphology.

Pelger-Huët anomalies (PHA) – a bilobed neutrophil that has variable shapes and sizes of the two lobes but is connected by a very thin bridge of nuclear material, often presenting with a dumbbell shape. Originates from a mutation on chromosome-1 that leads to a defect in the lamin-B receptor (Colella, 2012).

Pseudo Pelger-Huët anomalies (PPHA) – Presents with the same morphology as the PHA but is not caused by a mutation on chromosome-1. PPHAs are induced anomalies, by interaction of radiation with an unknown portion of the generation of granulocytes. The PPHA appears in all granulocytes (neutrophils, eosinophils, & basophils); however, the neutrophil is the most abundant white blood cell in peripheral blood making it the best choice for use in the PPHA assay (Colella, 2012).

Hematopoietic Stem Cells (HSC) – The progenitor cell that resides in the red bone marrow and can differentiate into all cells of the hematopoietic system (Spangrude, Heimfeld, & Weissman, 1988). Differentiation is determined by growth factors that bind to transmembrane receptors and induce intracellular pathways.

Neutrophils – A granulocyte that is a part of the innate immune system and can induce oxidative environments in bacterially infected tissues. The neutrophil is the most abundant white blood cell in the peripheral blood and contains a segmented nucleus (King, Toler & Woodell-May, 2018). The PPHA and PHA are both anomalous morphologies of the neutrophil.

Gray – A unit of measure that denotes radiation absorbed dose under the international system of units. The base units for a Gray are Joules per kg (ICRU Publication No. 51, 1993), which is energy deposited per unit mass. Gray is the unit of measure used for irradiation protocols for the rhesus macaques in this study.

Triage – a process by which severity of injuries imparted on patients is assessed and a priority is placed upon them for treatment based on their physical condition and the likelihood of survival with and without treatment. Early dose assessment is an important factor in triage for radiological accidents, and biodosimetry methodologies are one of many tools for assessment.

Ionizing Radiation, Biological Effects, & Relevant Real-World Cases

Pseudo Pelger-Huët anomalies present as an induced anomaly under multiple exposure scenarios and from multiple modalities of radiation warranting a brief explanation of the different types of radiation. Radiation can be placed into two distinct categories, ionizing radiation and non-ionizing radiation; both non-ionizing and ionizing radiation can be further subdivided into particle and electromagnetic radiation. Particle radiation includes neutrons, beta particles, alpha particles, protons, and heavy charged particles, while electromagnetic waves includes X-rays and gamma (γ) rays. Ionization is the basis for biological impacts of radiation, and the energy threshold required for ionization to occur is known as the ionization potential. Non-ionizing radiation is not capable of ionizing atoms from electromagnetic waves or particles because they are below the ionization potential. The deposition of non-ionizing radiation energy leads to heating and is not of interest to this study. Ionizing radiation, however, is inherently capable of depositing sufficient energy into matter to detach electrons from the atoms it interacts with, thereby ionizing that atom.

Alpha (α) particles are ejected from the nucleus and are identical to a helium nucleus, 2 protons and 2 neutrons. Examples of α -emitters include thorium 232, radium 226, uranium 238, and radon 222 (ICRU Publication No. 10b, 1964). Beta (β) particles are also ejected from the

nucleus and are either a negatively charged electron or a positively charged positron. Examples of β -emitters include tritium, sulfur-35, strontium-90, and carbon-14 (ICRU Publication No. 10b, 1964). Heavy charged particles are positively charged nuclei of elements including iron and carbon that have been stripped of some or all their orbital electrons. Heavy charged particles are most commonly components of space radiation and are a large contributor of dose to space exploration and research. X-rays and gamma-rays are high energy electromagnetic waves with wavelengths less than 200 nanometers. Both X-rays and gamma- (γ) rays frequently accompany α and β particles as they are emitted from a decaying radioactive atom. X-rays and gamma-rays differ from one another based on their origin in a decaying atom: X-rays are of orbital origin, while gamma-rays are of nuclear origin. Examples of wave radiation emitters include cobalt-60, barium-137m, and manmade sources of X-rays such as the accelerators used to irradiate the animals in this project (ICRU Publication No. 10b, 1964). Lastly, neutrons are commonly a product of a fission reaction in the core of a nuclear reactor. Fission occurs when a neutron impacts the nucleus of a fissile atom and the nucleus splits into two fission products generally with an atomic number of approximately 92 and 135 (ICRU Publication No. 10b, 1964). Examples of fissile radionuclides include uranium-235 and plutonium 239.

As previously stated, the basis for biological impacts of ionizing radiation is the ionization of matter. On a cellular and molecular level, ionizing radiation affects the functionality of the cell by damaging DNA within the nucleus or impeding other cellular functions through oxidative stress. DNA damage can be either direct or indirect ionization of the nucleic acid strand. Direct damage is responsible for approximately 30% of ionizing events damaging DNA, while indirect damage is responsible for approximately 70% of DNA ionizing events. Direct damage can occur from either particulates or electromagnetic waves and will pass

through the cytoplasm of the cell and impact the structure of DNA directly as the name implies. Indirect damage results in the generation of reactive oxygen species (ROS) as the tracks of radiation ionize the water molecules in the cytoplasm. Reactive oxygen species include hydrogen radicals (H•), hydroxyl radicals (OH•), and free electrons (e-), which can diffuse through the cytoplasm and cause ionizing events that will damage the DNA strand (Alizadeh, Sanz, Garcia, & Sanche, 2013).

Damage to one cell is often accompanied by damage to many other cells leading to visually recognizable tissue damage. Tissue is defined as one or more cell types working together for a common function, and damage to tissue is directly proportional to the dose that is absorbed by the tissue at low doses, and directly proportional to the square of the dose at high doses. Low doses generally result in sub-lethal damage that can be repaired with endogenous DNA repair mechanism but can still produce double strand DNA breaks. Higher doses can result in double strand breaks of DNA from clustered ionizing events that can result in mitotic cell death or apoptotic cell death. If this cell death is widespread due to a large dose or a concentrated field of irradiation it can result in deterministic effects like acute radiation syndrome and/or stochastic effects such as cancers. Currently the PPHA morphology can best be described as a stochastic effect because they have a baseline prevalence, and the possibility of their occurrence increases with increased radiation dose.

The Purpose of Biodosimetry and Current Methods

Biodosimetry is the science of using a biological, physiological, or chemical marker for the purposes of reconstructing a dose of ionizing radiation that was imparted on human tissues. While there are many techniques in use today the immense variety of scenarios in which people

can be exposed renders no one assay as the best method, let alone a standalone assay. Many factors to include detection limits, number of patients, other hazards to life and well-being of both patients and the caregivers, accessibility to necessary laboratory equipment, and cost all impact what assay is best for a situation. Emergency preparedness and research seeking to improve preparedness for radiological incidents or a nuclear disaster call for the ability to perform a number of different assays to include but not limited to electron paramagnetic resonance, dicentric chromosome analysis, gamma-(γ) H2AX foci analysis, micronuclei, lymphocyte depletion, premature chromosome condensation (PCC), time to emesis following exposure, and gene expression. Below is a short description of each of the preceding methods of biodosimetry, their strengths associated with that assay, limitations of the assays, and the detection limits (Table 1).

Electron Paramagnetic Resonance (EPR) – EPR has been widely used for the detection of free radicals and transition metals in many industries. It is used as a biodosimeter by detecting free radicals that are produced when radiation interacts with biological tissue. Free radicals produced in the aqueous environment of the cell only last in the nanosecond range. Free radicals produced in calcified tissue such as bone and teeth can trap the free radicals for much longer on a scale of 10^8 years (Swartz et. al, 2007). The EPR signal has also been shown to be present in the keratin fibers of fingernails but degrades with in several weeks (Symons, et al., 1995). EPR has been used in retrospective studies of victims of Nagasaki, Hiroshima, and Chernobyl.

Dicentric Chromosome Assay (DCA) – Dicentric chromosome analysis is conducted by culturing peripheral blood with the isolation of lymphocytes. Next, lymphocytes are stimulated to divide while adding a spindle fiber block to arrest the cells in metaphase

(Johnson & Rao, 1970). The result is a chromosome spread where dicentrics can be quantified to assess a dose. DCA is capable of being extremely accurate because of low background rates of dicentrics in humans, and it has been conducted on hundreds of humans allowing for a well characterized dose response curve. In a non-emergency setting the goal is to score between 500 and 1000 metaphase spreads, but in a triage situation this is far too time consuming. For emergency situations, the requirement is between 50 and 100 metaphase spreads to keep the standard deviation between 0.5 and 1.0 Gy (Sullivan, et al., 2013). Persistence is described as reliable between three and six months, when it becomes more reliable to quantify translocations via Fluorescent In-Situ Hybridization.

Gamma H2AX foci Assays (γ -H2AX) – A process of quantifying the γ -H2AX protein through either flow cytometry or fluorescent microscopy. The γ -H2AX protein accumulates at the site of double strand breaks and becomes phosphorylated in the process of DNA repair (Rogakau et al, 1998). The protein degrades rapidly so it is advised that blood be drawn and analyzed within 30 minutes to one-hour post exposure, but not to exceed one to two days (Rothkamm & Horn, 2009).

Cytokinesis Block (micronuclei) – A micronucleus is formed when a segment of a chromosome that has been broken via a double strand break fails to be incorporated into the daughter nuclei (Heddle, 1973). This is informative of a radiation dose because the frequency of double strand breaks is proportional to the radiation dose imparted on the individual. The result is a much smaller, but separate nucleus that remains within the cytoplasm of a daughter cell. The type of chromosome aberration is persistent with a half-life of one year. The samples are cultured in a similar manner as dicentric analysis although they do

not include a metaphase cell cycle block. The samples are then fixed and stained for viewing under light microscopy. The recommended quantity to count is 1 000 cells, but under triage situation as little as 200 could be counted in under 20 minutes (AFRRI, 2010).

Lymphocyte Depletion – Often referred to as a complete blood count (CBC) with differential, this is the method of estimating dose to a victim of an acute exposure to radiation (Guskova et al, 1988). This is informative of a radiation dose because following an acute exposure there are characteristic changes in the whole blood count that can be correlated with radiation dose estimates. The blood is smeared on a glass microscope slide, stained, and observed to find the differential count of neutrophils to lymphocytes. Often this process is done at specialized laboratories such as the Cytogenetic Biodosimetry Laboratory in Oak Ridge, TN. Blood needs to be drawn within 12 hours of exposure due to the short lifespan of granulocytes in the blood. The relative differential can fall off exponentially after 12 hours (Goans, 1997).

Premature Chromosome Condensation (PCC) – Is a method of viewing chromosomal aberrations without having to force lymphocytes through mitosis. The interphase lymphocytes are treated with chemical agents or mitotic Chinese hamster ovary (CHO) cells. The result is a condensation of interphase chromatin into chromosomes (in G1 or G2 cells) (Nishimoto, Eilen, & Basilico, 1978). The resulting visible aberrations to include dicentrics, translocations, and rings can be measured (in G2 cells). Double strand breaks are counted among the condensed chromatin and their frequency can be used to estimate a radiation dose. The same automated metaphase finder that is used in dicentric analysis can be used to analyze these data (Lindholm, et al., 2010). When PCC and DCA are

compared the same source found that DCA is best for exposures under 6 Gy, while PCC is best for exposures over 6 Gy.

Time to Emesis- A crude method of biodosimetry is estimating the magnitude of dose imparted on the individual by measuring the time from the irradiation incident to the time when emesis begins. Early data produced indicates that if the patient were to begin vomiting in less than 2 hours following the irradiation incident the whole-body radiation dose can be estimated at greater than 3 Gy, and if the time to vomiting is less than 1 hour the whole body radiation dose can be estimated at greater than 4 Gy (Demidenko, Williams, & Swartz, 2009). The International Atomic Energy Agency (IAEA) has published a reference table of similar values. Emesis 2 hours post Irradiation incident equates to a 2 Gy or less whole-body dose, and emesis between 1 and 2 hours post irradiation incident equates to a 2-4 Gy whole body dose (IAEA Safety Report Series no. 2).

Gene Expression – Gene expression is the systematic measurement of gene pathways that have been shown to be particularly radiosensitive in peripheral blood. Some examples include genes in the injury repair pathway and p53-dependent DNA repair pathway (Paul & Amundson, 2008). Techniques including polymerized chain reaction (PCR) and nuclease protection assay (NPA) have been used to form a data base in which gene sets taken from exposure victims can be compared to determine an exposure estimate. Samples should be taken from exposure victims within 48-72 hours following the incident because gene expression techniques become invalid after a week (Meadow et al., 2008).

Many of these biodosimetry assays require immense logistical requirements which highlights the need for methods that are low cost, quick, and accurate. The PPHA assay demonstrates the potential to fill these needs. It can be low cost because the necessary equipment

includes glass slides, a nuclear stain, coverslips, and a light microscope; all of which are common laboratory equipment. It can be quick because the microscope slide only takes a trained technician less than 15 minutes to evaluate, and in fact the longest portion of the assay is fixing and staining the blood sample on the slide. Lastly, the PPHA assay can also be accurate if the exact mechanism of origin is discovered and a system of repeated laboratory irradiation and evaluation of samples can occur to narrow down detection limits, much like what has been done with dicentric chromosome analysis. A list of the biodosimetry methods, associated dose limitations, and the location of original research validating them can be referenced in Table 1.

Table 1. Biodosimetry methods and the corresponding detection limits

Detection Limits of Biodosimetry Methods		
Method	Dose Range (Gy)	Reference
EPR	1 – 30	(Swartz et al. 2010)
DCA	.01 - 5	(Marcella, 2010)
γ -H2AX	0.5 - 5	(Riecke et al. 2010)
Micronuclei	0.3 – 5	(AFRRI, 2010)
Lymphocyte Depletion	0.5 – 10	(Goans et al. 1997) & (Blakely et al., 2010)
Premature Chromosome Condensation	0.2 - 20	(Lindholm, et al., 2010)
Gene Expression	0.1 – 5	(Paul & Amundson, 2008)

The Hematopoietic System and Neutrophil Development

Understanding of the PPHA requires a working knowledge of the hematopoietic system for which the PPHA is a part (see Appendix D for a flow chart of the process). All blood cells, including white and red, originate from hematopoietic stem cells in the bone marrow. There are two types of hematopoietic stem cells that exist in the bone marrow; long-term hematopoietic

stem cells that are self-renewing adult stem cells and short-term hematopoietic stem cells that differentiate into progenitor cells. Progenitor cells consist of the common lymphoid progenitor that give rise to T-lymphocytes and B-lymphocytes, while the common myeloid progenitor will give rise to red blood cells, megakaryocytes, monocytes, and granulocytes. Differentiation of stem cells is based on the introduction of different chemokines that bind to the cell and induce selection of a pathway. The PPHA is an anomalous neutrophil so the specific details of neutrophil development will be expanded upon, but the development of other types of cells will be briefly discussed.

If a sample of whole blood is placed in a cell preparation tube (CPT) and centrifuged it will separate into three distinct layers of tissue. The bottom layer is known as the hematocrit and comprises roughly 45% of blood volume. The bottom layer consists of a red blood cells that are small bi-concave discs containing no nucleus, numerous iron rich molecules known as hemoglobin, but no cellular protein or lipid synthesis machinery. The purpose of a red blood cells is to carry oxygen molecules to the tissues to be used in the production of adenosine triphosphate (ATP) in mitochondria. Since red blood cells contain no nucleus or protein manufacturing machinery the life span of these cells is normally 90-120 days. Red blood cells are the most abundant cell type in peripheral blood and can be seen in every image of a peripheral blood smear in this document. The upper layer of centrifuged blood is known as the blood plasma and comprises roughly 55% of the blood volume. Blood plasma is a liquid solution in which both white and red blood cells are suspended when the blood is mixed. The plasma consists of water with dissolved salts called electrolytes and proteins. The middle layer of the centrifuged blood is known as the buffy coat and comprises less than 1% of the total blood volume (Garraud & Tissot, 2018). The buffy coat contains all the white blood cells and platelets.

The plasma and buffy coat together contain the components of the immune system. The PPHAs and all other nucleated cellular components will be in the buffy coat. While white blood cells is a term that encompasses many different types of cells, platelets are the product of a cell known as a megakaryocyte that fractures into hundreds to thousands of membrane bound bags containing granules and cytoplasm (Garraud & Tissot, 2018). In addition to erythrocytes, blood platelets are visible in every cell image in this document, and they appear as small purple circles or blobs. Erythrocytes, a PPHA, and blood platelets can be seen in Figure 1.

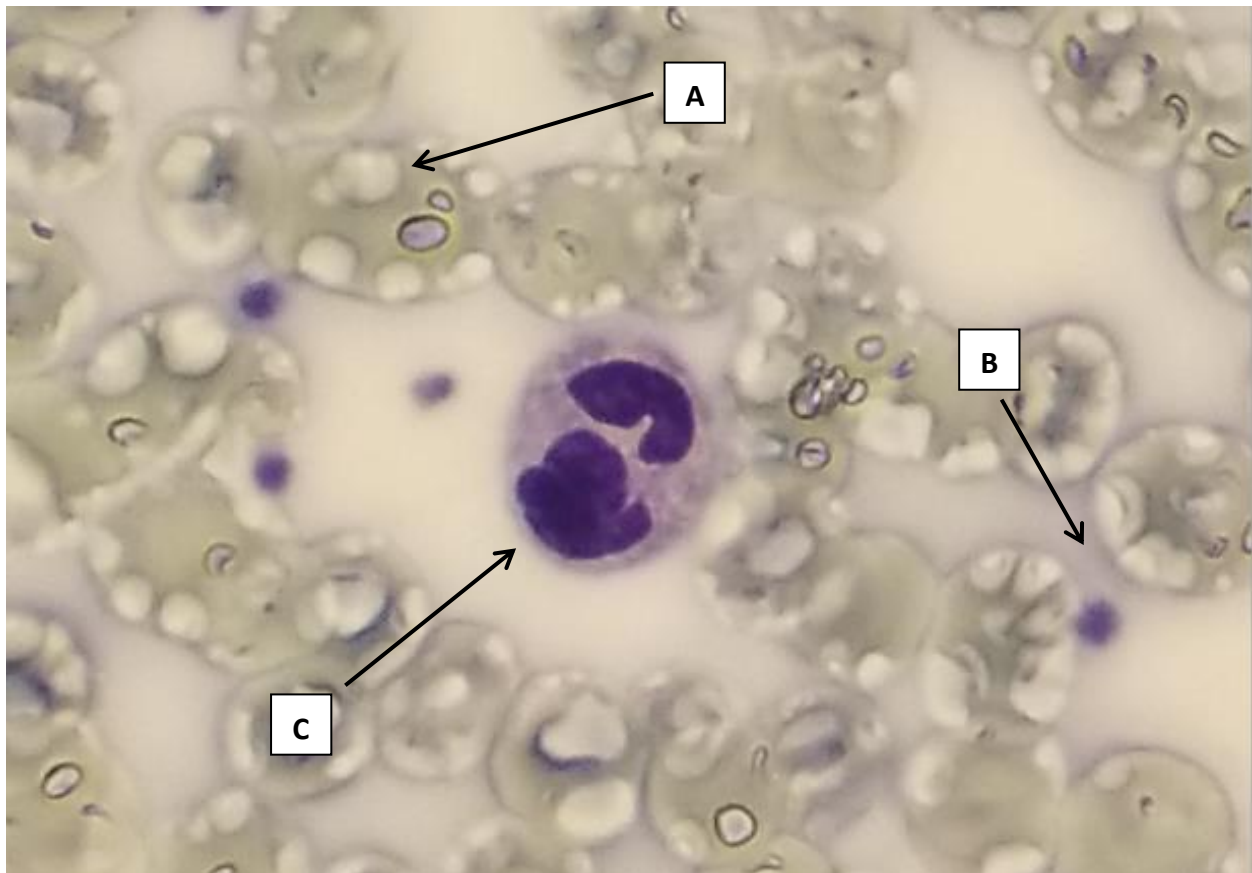


Figure 1. Red blood cells (A), platelets(B), and a PPHA cell (C) from Macaque 1905, blood smear taken on November 24, 2015.

The term hematopoiesis describes a process in the human body that contributes to the formation of blood. The process of hematopoiesis, the generation of blood, begins in the bone marrow with the hematopoietic stem cell (HSC) and the stromal support cells (Appendix D). HSCs can differentiate into erythrocytes (red blood cells), leukocytes (white blood cells), and platelets, and the differentiation of the HSC into one of these components is dependent upon which growth factors it receives. For example, if the body requires more red blood cells the kidney will release a molecule known as erythropoietin in response to low blood oxygen levels and when it binds to progeny of the HSC it will begin the process of erythropoiesis and at that point it is destined to become an erythrocyte.

The HSC is a pluripotent stem cell that further differentiates into two stem cell progeny, which ultimately further differentiate into all cellular components of the blood. A flow chart of HSC differentiation into all components of blood can be seen in Appendix D. The two stem cell progeny lines are the myeloid stem cells and the lymphoid stem cells. The myeloid stem cell undergoes one of three processes, erythropoiesis to generate red blood cells, thrombopoiesis to generate platelets, or leukopoiesis to generate cells of innate and adaptive immunity. The myeloid stem cell gives rise to several cells of importance that must be differentiated in the performance of a peripheral blood smear evaluation. The first cell type that the myeloid stem cell can differentiate into is the neutrophil. The neutrophil is a granulocyte and is the most abundant nucleated cell in the peripheral blood (Figure 2). Granulocytes migrate from the bone marrow and circulate in the blood where they eventually leave the blood vascular compartment and enter damaged tissue where they perform their function. Neutrophils will phagocytose foreign bodies and secrete oxidative materials such as hydrogen peroxide and free electrons. Neutrophils are polymorphonucleated and generally have between 3 and 7 lobes in their nucleus.

Neutrophils with less than 3 lobes are considered hypo-segmented and those with more than 5 are considered hyper-segmented. Both hypo- and hyper- segmented nuclei are abnormalities, with the bilobed nature of PPHAs being an anomaly. The neutrophil can be distinguished from the other granulocytes by its lack of darkly colored or reddish granules in the cytoplasm. While they do in fact have granules in the cytoplasm, they are full of molecules that are not visible under light microscopy, so they appear translucent. An immature form of neutrophil can be normally viewed in the peripheral blood and is called a band cell. The band cell has the beginning of the indentation that will lead to segmentation and has a horseshoe like appearance. A normal neutrophil can be seen in Figure 2.

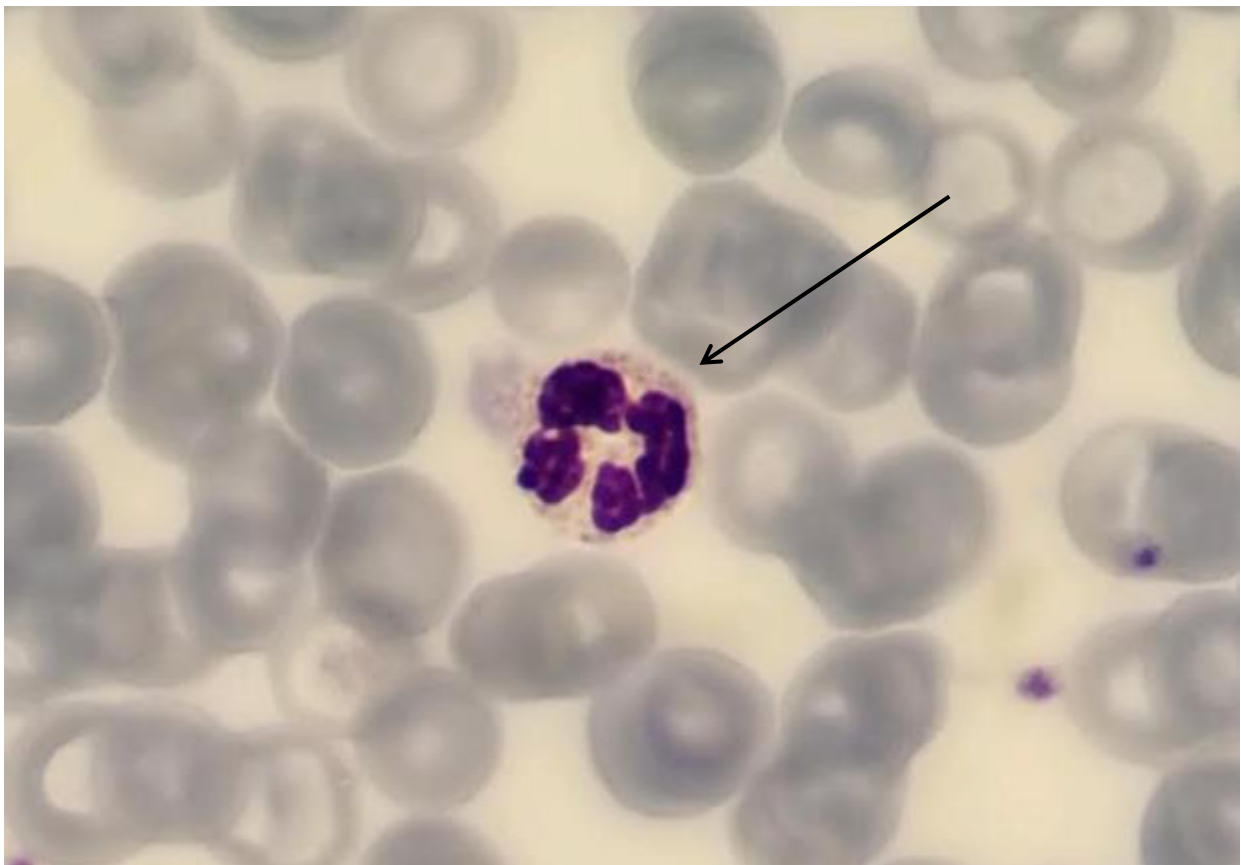


Figure 2. Neutrophil from Macaque 1905, blood smear taken on November 24, 2015.

With the introduction of interleukin-3 or interleukin-5 the myeloid stem cell will begin to differentiate into a basophil or an eosinophil, respectively. With interleukin-3 and the addition of granulocyte/macrophage-colony stimulating factor (G/M-CSF) the myeloid stem cell will differentiate into a granulocyte/macrophage progenitor cell (GMP). Additional introduction of granulocyte colony stimulating factor (G-CSF) or macrophage-colony stimulating factor (M-CSF) the GMP will differentiate into a neutrophil or a monocyte, respectively (Lieschke & Burgess, 1992). Upon differentiating into a neutrophil, the cell exists in an inactive form until activated by chemokines from the site of damaged tissue in the body.

When tissue is damaged it releases chemokines such as interleukin-23 (IL-23) and interferon gamma into the blood stream. Circulating neutrophils, once at the site of damaged tissue, bind to transmembrane proteins expressed on the apical membrane of the endothelial cells called selectins that allow for the neutrophils to attach and exit the blood vascular compartment via diapedesis. Once in the interstitial space, neutrophils have the capability of following a chemical gradient of chemokines in a near amoeboid manner using pseudopodia. The neutrophil proceeds to destroy micro-organisms via phagocytosis, degranulation, and neutrophil extracellular traps. Neutrophils contain granules that are filled with peroxides, alkaline phosphates, lysosomal proteins, proteases, and collagenases. Neutrophils will excrete these granules into the extra cellular space, as well as fuse the granules with the phagosome that is produced following phagocytosis of the microorganism. Neutrophil extracellular traps consist of the neutrophil excreting an extracellular matrix made of DNA and granule proteins that can ensnare microbes and inhibit the spread of infection and limit damage to the local tissue (Brinkmann, 2004). Neutrophils are thought to have a lifespan of approximately 8 hours in the blood stream, and the bone marrow is thought to produce upwards of 100 billion neutrophils per

day. Upon completion of their anti-microbial task the neutrophils are endocytosed by other phagocytic cells (dendritic cells and macrophages).

The concentration of mature neutrophils in the peripheral blood is regulated by a feedback loop generated by dendritic cells and macrophages. The stimulus for upregulation of granulopoiesis is given by the release of IL-23 from macrophages and dendritic cells. In turn, IL-23 stimulates secretion of interleukin-17 (IL-17) from T-cells, and IL-17 increases the levels of G-CSF. The subsequent flood of neutrophils to the peripheral blood and their phagocytic behavior reduces the production of IL-23, therefore reduces IL-17 and G-CSF, ultimately down-regulating granulopoiesis in a negative feedback type fashion (Vietinghoff & Ley, 2008). A diagram showing the negative feedback loop in granulopoiesis can be seen in Appendix D.

The second cell type into which myeloid stem cells differentiate is an eosinophil, a polymorphonucleated granulocyte whose function is to neutralize parasitic organisms within the body. Eosinophils can be distinguished from other cells in a peripheral blood smear by the many red granules present in the cell's cytoplasm and a multi-lobed nucleus. An eosinophil can be seen in Figure 3.

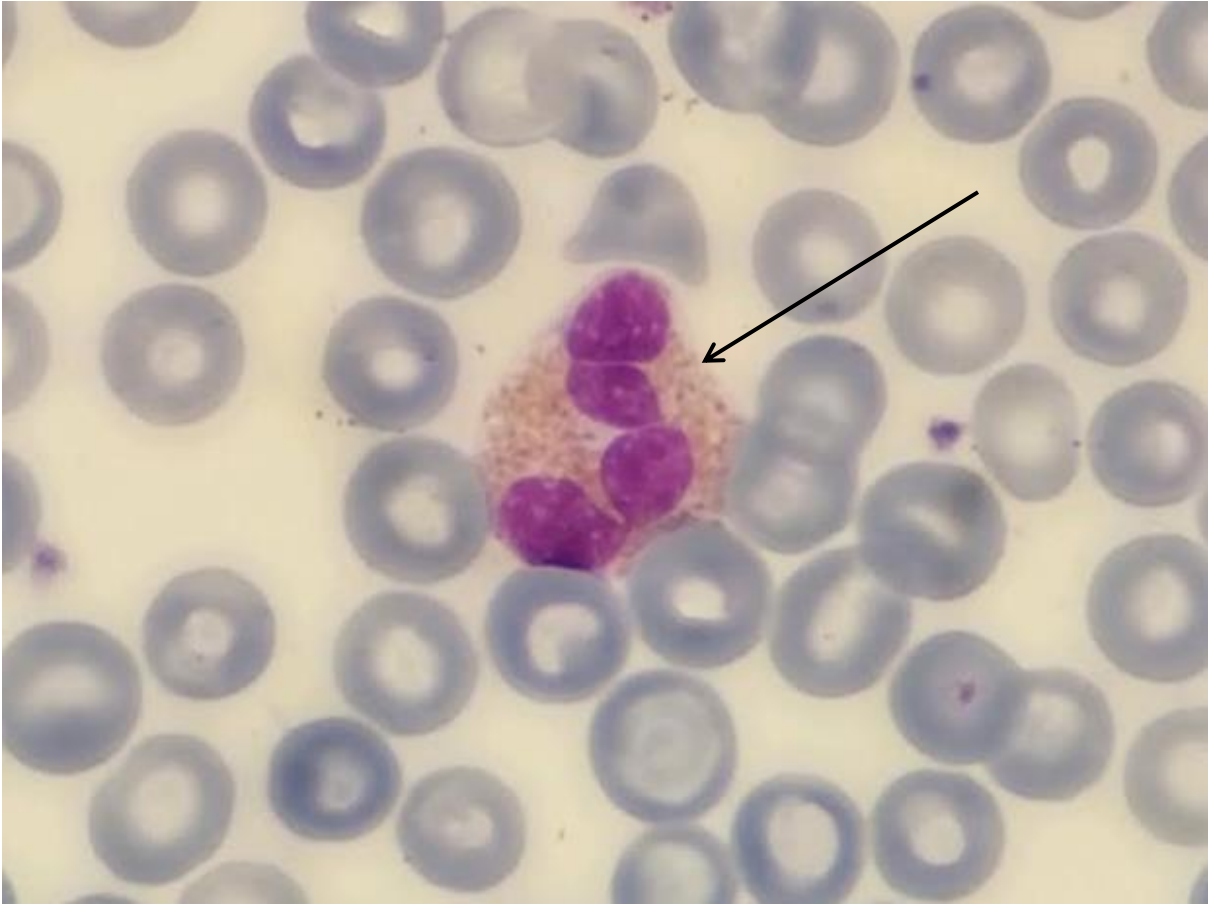


Figure 3: Eosinophil from Macaque 1905, blood smear taken on November 24, 2015.

The next type of cell into which myeloid stem cells can differentiate is a monocyte. Monocytes have a large nucleus that when stained appears bean-like in shape. Monocytes are the largest of the cells in a peripheral blood smear, but they can be difficult to differentiate them from lymphocytes when the nucleus does not have the characteristic bean shape. Monocytes leave the blood vascular compartment through a process called diapedesis and within the tissues they mature into a macrophage. Macrophages are essential to an inflammatory response due to their phagocytic nature, and essential to the adaptive immune response due to their ability to display antigen fragments on major histocompatibility type 2 receptors for interaction with T-lymphocytes known as CD4 cells. A monocyte can be seen on a peripheral blood smear in Figure 4.



Figure 4. Monocyte from Macaque 1905, blood smear taken on November 24, 2015.

The next cell type which myeloid stem cells can differentiate into is a basophil. Basophils, along with a histaminergic cell called a mast cell, helps initiate the inflammatory response. Basophil specifically will secrete molecules that are chemotactic towards eosinophils. Basophils create a chemical gradient that draws eosinophils to the site of inflammation. Basophils also secrete molecules that are broncho-constrictive. It is thought that basophils are partly responsible for initiating and maintaining an allergic response (Siracusa, Kim, Spergel, & Artis, 2013). Basophils are the rarest cell type in a peripheral blood smear and can be distinguished by its lobular nucleus and a multitude of darkly colored secretory granules. A basophil can be seen in a peripheral blood smear in Figure 5.

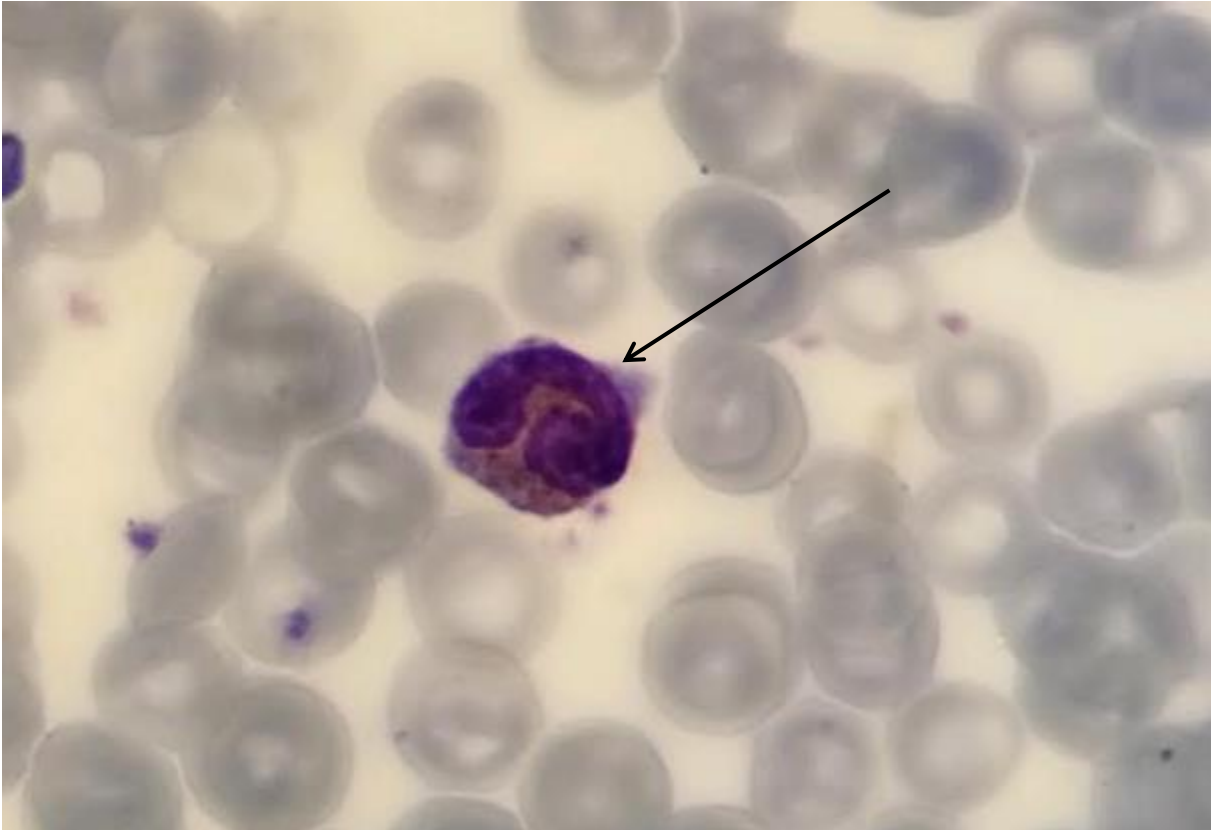


Figure 5. Basophil from Macaque 1905, blood smear taken on November 24, 2015.

In the lymphoid stem cell line, lymphoid stem cells undergo leukopoiesis to differentiate into B-lymphocytes and T-lymphocytes. B and T lymphocytes are responsible for a person's adaptive immunity. A lymphocyte is one of many cells that can be seen in a peripheral blood smear. When stained with Giemsa, lymphocytes appear to have a large round nucleus that takes up most of the cell's cytoplasm. B-lymphocytes are local to germinal regions in lymph nodes, gut associated lymphatic tissue, and the white pulp of the kidney. Any lymphocytes present in the peripheral blood are assumed to be T-lymphocytes. A lymphocyte from a peripheral blood smear in this study can be seen in Figure 6.



Figure 6: Lymphocyte from Macaque 1905, blood smear taken on November 24, 2015

A diagram of the hematopoietic stem cell differentiation including cell types and growth factors that induce the differentiation can be seen in Appendix D.

The Pseudo Pelger-Huët Anomaly: Morphology and Suspected Origin

Historically, there is a distinction between the Pelger-Huët Anomaly (PHA) and the pseudo Pelger-Huët anomaly (PPHA). The PHA can be observed in neutrophils, and any other granulocyte (neutrophils, eosinophils, and basophils). PPHAs are only quantified in neutrophils because neutrophils are the most abundant white blood cell in the peripheral blood. Counting the PPHA morphology in other granulocytes would be inefficient due to their low numbers in peripheral blood. PHAs are naturally occurring and were first described in 1928 by the German

physician, Karl Pelger, and were believed to be a sign of poor prognosis for tuberculosis (Pelger, 1928). However, in 1932 G.J Huët discovered PHAs were linked to an autosomal dominant mutation on the long arm of chromosome 1 (Huët, 1932). The mutation was in a gene that encodes for the lamin-B receptor, which is a membrane associated protein embedded in the inner nuclear membrane of the nuclear envelope. The lamin-B receptor has two functions that can be described by their location on the protein. The carboxyl terminus performs C14 sterol reductase activity which involves the breaking of carbon double bonds in cholesterol synthesis, while the amine terminus of the lamin-B receptor binds to an intermediate filament called lamin-B. Lamin-B in turn binds to the chromatin and provides structure to both the chromatin and the nucleoplasm (Holmer, Pezham, & Worman, 1998). The structure of the nucleus is incredibly important to granulocytes because a hyper-segmented nucleus makes it much easier for these cells to exit the blood vascular compartment via diapedesis. The structure of the nucleus also allows for ease in movement throughout tissues as the cell is migrating to areas undergoing the inflammation response (Colella, 2012). An image of the lamin-B receptor with the sterol reductase carboxyl terminus and the chromatin tethering amine terminus can be seen in Figure 7.

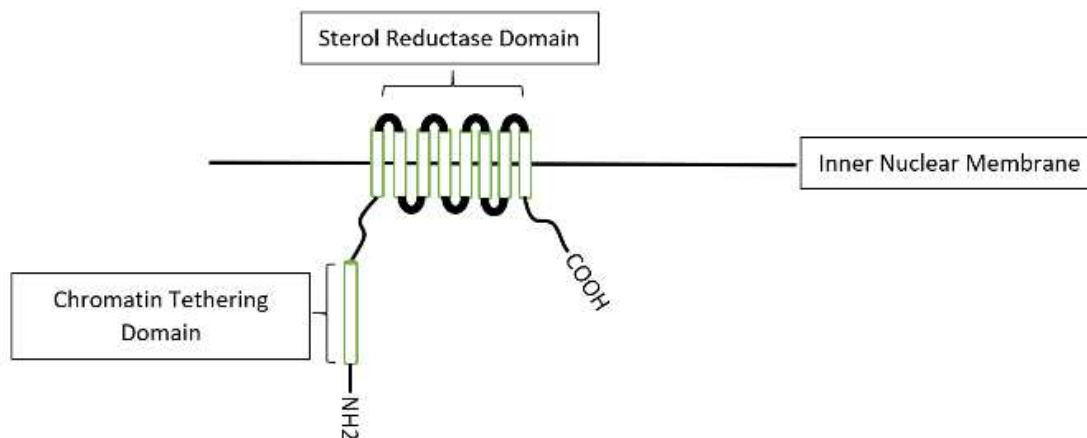


Figure 7. Structure of the lamin-B receptor (Hayes, 2018).

While the Pelger-Huët anomaly and pseudo Pelger-Huët anomalies can be seen in any granulocyte, PPHAs are only quantified in neutrophils because they are the most abundant leukocyte in peripheral blood. If the cell morphology is induced from an outside stimulus, such as an exposure to a toxin or ionizing radiation the cells are *pseudo* Pelger-Huët anomalies (PPHAs). PHAs and PPHAs are distinguishable from other neutrophils in a peripheral blood smear by two factors. The nucleus of the PPHA is bilobular with two lobes that can take on a number of different shapes and sizes, and the two segments are connected by a very thin mitotic bridge (Goans, Iddins, Ossetrova, Ney, & Daniak, 2015). While many of the images of PPHAs in this document display a perfectly round to bean-like structure of the two lobes, many of them present with an obscure shape that can be somewhat misleading to the evaluator. Several examples of PPHAs with the thin mitotic bridges can be seen in Figure 8.

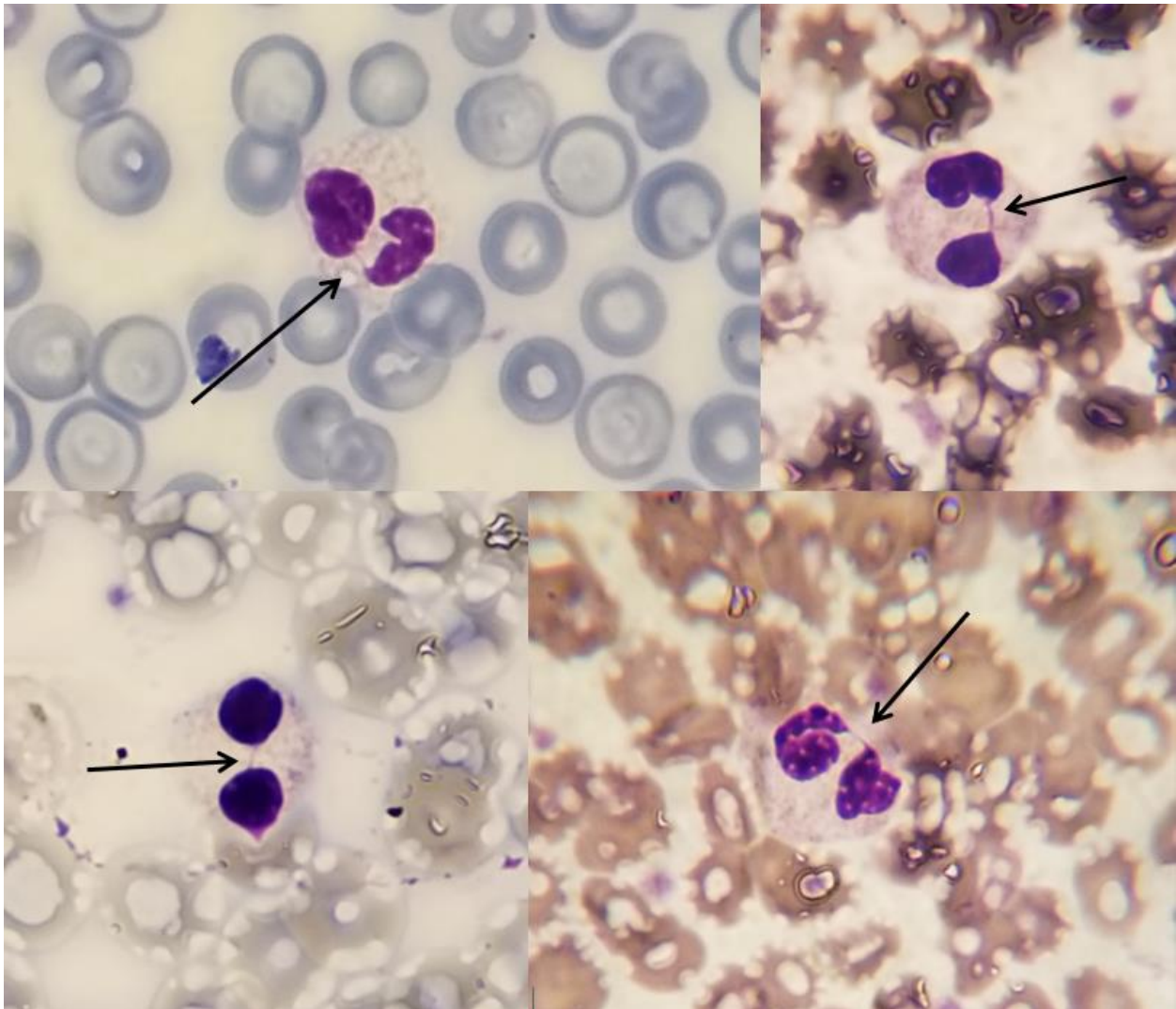


Figure 8. Examples of pseudo Pelger-Huët anomalies, and their various shapes of the two lobes. The thin bridge connecting the two lobes can be seen in each image (black arrow).

Some confusion can be experienced when differentiating PPHAs and immature neutrophils. Immature neutrophils remain in the bone marrow through interactions with the chemokine CXCL12 and its receptor CXCR4 (Vietinghoff & Ley, 2008). Immature neutrophils are rarely found in the peripheral blood but can escape the bone marrow during an inflammation response. Immature neutrophils in peripheral blood have a band-like morphology as opposed to a multilobed nucleus. In addition, if immature neutrophils enter the peripheral blood in a hypo-

segmented form they can be differentiated from PPHAs by the presence of Dohle bodies, fragments of the cells endoplasmic reticulum lost in development. It is possible that progenitor cells giving rise to granulocytes are impacted by radiation dose to produce the PPHA morphology. Progenitor cells are not terminally differentiated therefore they are more radiosensitive than the post-mitotic neutrophils. In addition, other granulocytes (basophils and eosinophils) often present with a bilobed morphology indicating that a common ancestor is being impacted. As previously stated, basophils and eosinophils are far less common in the peripheral blood under normal physiological conditions, so basophils and eosinophils are not informative biomarkers of radiation dose. A PPHA with an obscure shape to its two lobes and the most common morphology for a neutrophil can be seen in Figure 9.

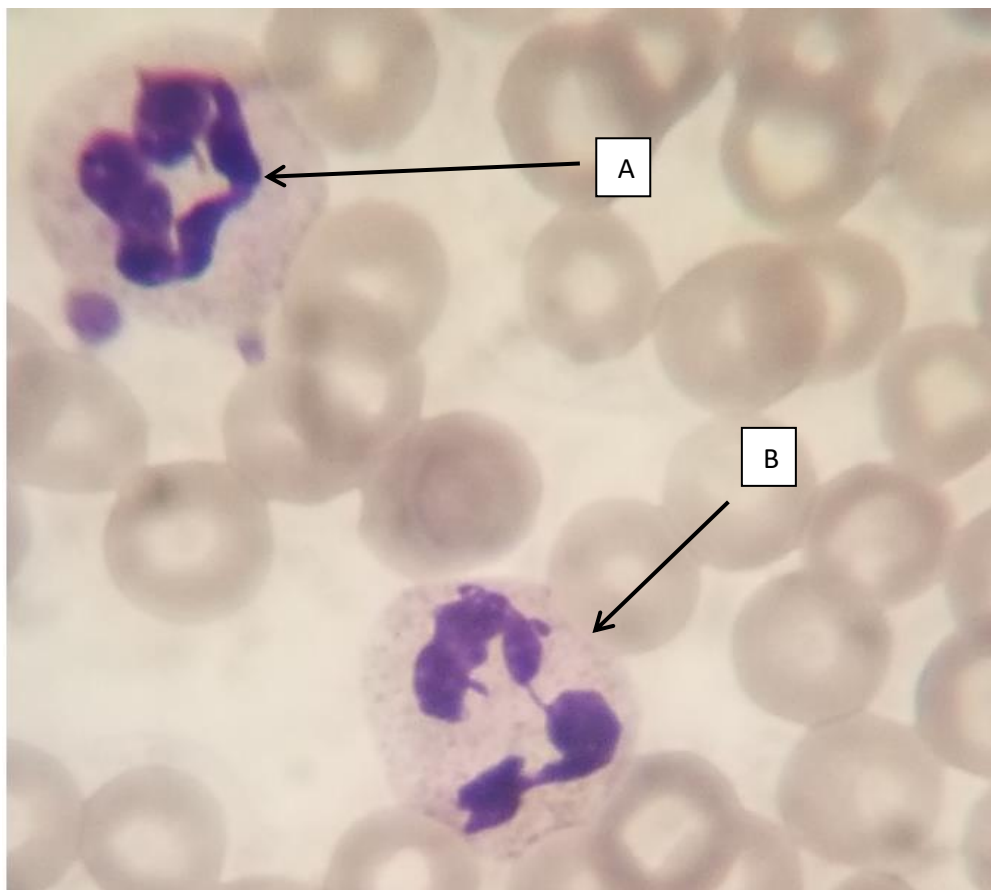


Figure 9. Example of a normal neutrophil (A), next to a Pseudo Pelger-Huët anomaly (B), from Macaque 1905, blood smear taken on November 24, 2015

Radiation could impact neutrophil progenitor cells in several possible ways to induce the PPHA morphology. First, the lamin-b receptor could be impacted either through direct interaction with the radiation or mutations generated on chromosome 1. Direct radiation interaction on chromosome 1 is unlikely since the lamin-b receptor is a small target for the radiation compared to the genome, and mutations would take longer to manifest than the cells have taken to experimentally be expressed in nonhuman primates (Goans, 2017). Second, the direct or indirect interaction of the radiation energy absorbed could result in DNA DSBs, impacting the stability of neutrophil progenitor cell's genome, and inhibiting the ability of the nucleus to fully segment. Neutrophils are the most abundant white blood cells in the peripheral blood and are therefore the largest target amongst nucleated blood cells, so it is possible that neutrophils would be most commonly expressing a bilobed morphology due to hypothesized mechanisms. Identifying the composition of the bridge between the lobes of the PPHA (Figure 8) could help determine the cause of the morphology. The PPHA bridge could be a hypo-segmentation of the nucleus. Alternatively, the PPHA bridge could represent a failure to complete cytokinesis during the cell cycle of the neutrophil progenitor cells due to a dicentric chromosome being stretched between the two lobes.

The Pseudo Pelger-Huët Anomaly as a Biodosimeter in Previous Research

There are several examples of PPHAs being used in research as potential biomarkers of radiation dose; here they will be summarized individually, and conclusions highlighted.

Japanese wild boar and large Japanese field mice (2017)– Wild Boar (*Sus scrofa leucomystax*) and large Japanese field mice (*Apodemus Speciosus*) were used as sentinel species of

opportunity from within the exclusion zone of the Fukushima Daiichi nuclear disaster area. The wild boar and mice were chronically exposed to low dose environmental radiation because of the deposition of long-lived fission fragments and fission products in the environment surrounding the Fukushima Dai-ichi nuclear reactors. Free-ranging wild boar and field mice were live captured and lifetime dose estimations calculated using muscle radiocesium burden and external dose estimations combined with an observed effective half-life for contamination. The large Japanese field mice ($n=20$) were live captured in areas with ambient dose rates ranging from 0.1 microSieverts/hour ($\mu\text{Sv/h}$) to 50 mSv/hr and no PPHA morphologies were observed in their peripheral blood. Japanese wild boar ($n=38$) were live captured in areas with ambient dose rates ranging from 0.1 $\mu\text{Sv/h}$ to 25 mSv/h and a dose response curve was constructed (Hayes, 2018). A linear relationship between estimated lifetime dose and PPHA frequencies in peripheral blood was found. Limitations of this study include estimated radiation doses, unknown environmental factors that impact the animal's health, and unknown additional exposures besides radiation.

South African Bats (2001) – A study conducted in South Africa utilized a resident population of bats (Chiroptera) in an abandoned mine. The background radiation within the mine was orders of magnitude above normal background because the ore inside contained high concentrations of a mineral known as monazite. Monazite contains an abundance of thorium-232 and its progeny. The bats were divided into 3 populations: controls that were exposed to normal terrestrial background radiation, a low dose area of the monazite mine with dose rates of 20 $\mu\text{Sv/h}$, and a high dose area of the mine with dose rates of 100 $\mu\text{Sv/h}$. Peripheral blood smears were taken from the bats, among other samples and

whole blood counts were performed. Only 100 total cells were counted across all types of white blood cells and within that, the percentage of neutrophils that displayed the PPHA morphology was calculated to be 0.27% in the controls, 12.67% in the low dose areas, and 22.66% in the high dose areas (Meehan, 2001). Limitations in this study include estimated radiation doses, unknown environmental factors that could impact health, and an exceptionally low count of neutrophils from which the prevalence of PPHAs was calculated.

Y-12 criticality accident victims, 2015 – The Radiation Emergency Assistance Center/Training Site (REAC/TS) conducted a retrospective study of the 1958 Y-12 criticality accident. The accident occurred when a group of radiation workers were pouring uranyl nitrate solution used in the extraction of enriched uranium from solid waste, into a 55-gallon drum believed to be empty. The barrel contained water, and the uranyl nitrate containing approximately 2.1 kg of uranium 235 went critical (McLaughlin, Monahan, Pruvost, Frolov, Ryazanov, & Sviridox, 2000). Eight workers received doses ranging from 0.288 Sv to 4.61 Sv (28.8 to 461 rem). Archived slides taken from the victims at the time of the accident and several years following were obtained by REAC/TS and were evaluated by counting 300 neutrophils and calculating the percentage of cells that had the PPHA morphology. The exposures that occurred from the Y-12 criticality accident were separated into 2 cohorts, high dose cohort with $n=5$ and a low dose cohort with $n=3$. Thirteen percent PPHAs were found in the high dose cohort, 6.8% PPHAs in the low dose cohort, and 3.6% PPHA background in the control group (Goans, Iddins, Ossetrova, Ney, & Daniak, 2015). Limitations in this study include estimated radiation doses, small sample size, and an unevenly distributed spectrum of doses.

Radium watch dial painters, 2018 – REAC/TS conducted another retrospective biodosimetry study on the radium watch dial painters from the first half of the 20th century. Radium was a commonly used material for creating illuminated dials for watch faces and airplane instrumentation. Radium is a long-lived radionuclide that is a biological analog for calcium, resulting in bone deposition of the nuclide. Prior to the abolishment of radium dial painting in 1955, dial painters would maintain a fine tip on paint brushes by wetting the brush with their mouths and thus ingesting radium. Archived blood slides from 166 dial painters with bone marrow doses ranging from 1.5-6,750 mGy were evaluated by REAC/TS (Goans, Toohey, Iddins, McComish, Tolmachev, & Dainiak, 2018). The resulting data displayed a sigmoidal relationship between bone marrow dose and PPHA prevalence. Limitation to this study include estimated radiation doses.

Non-human Primates 2016– The Armed Forces Radiobiology Research Institute (AFFRI) exposed 10 Rhesus macaques to whole body irradiation (1.0, 3.5, 5.0, 6.5, and 8.5 Gy) using a Cobalt-60 source at a dose rate of 600 mGy min⁻¹, with 2 macaques at each dose point. Each animal served as its own control and two additional macaques were used as true controls for the experiment. Blood smears were taken prior to irradiation and continued to be taken post irradiation with the first one at 5 hours post and the last at 60 days. A linear dose response was found, but with no statistical difference between the 1 Gy macaques and the 0 Gy macaques. Increased frequencies of PPHAs in peripheral blood was observed at 5 hours post irradiation, and peaked several days following. PPHAs remained at an increased level through the end of the 60-day experiment (Ossetrova et al. 2016). Limitations to this experiment include a small samples size in each dose cohort and a short period of observation for the persistence of PPHAs.

PHAs in dogs, rabbits, and cats in veterinary literature various dates (Supuka & Parkanyl, 2014 & Vale, Tomaz, Sousa, & Soto-Blanco, 2011)- PHAs have been reported in many animals in veterinary journals as genetic disorders much like humans. Animals were excluded from being considered to have PHAs if the animals had any infectious diseases, neoplastic diseases, or drug exposures because those were factors thought to induce PPHAs in the peripheral blood (Latimer, Rakich, & Thompson, 1985). Radiation was not mentioned as a source of PPHAs in these studies, however several other sources of PPHAs illustrate the possibility of confounding variables influencing the prevalence of PPHAs.

Rhesus Macaques: Species Information and Justification of Use in This Study

Rhesus Macaques (*Macaca mulatta*) are a small to medium sized non-human primate with an average weight of 7.7 kg (17 pounds) for males and 5.4 kg (12 pounds) for females, an average height of 53.3 cm (21 inches), and an average lifespan of 25 years. They are the most widespread species of non-human primates geographically on the planet with a natural home range in Asia from Afghanistan to the eastern shores of Vietnam and China. The animals are remarkably adaptable to a variety of climates, altitudes, and terrains throughout this entire region. The animals have even thrived in areas like coastal islands off the coast of Florida where small zoos were destroyed in hurricanes and the animals were free to roam. Lastly, these animals have an immense population in the wild that results in them being listed as ‘least concern’ for their conservation status (Singh, Kumar, & Kumara, 2020).

Their large populations, no conservation concerns, ease of acquisition, and most importantly their similarity to humans, both anatomically and physiologically, causes the rhesus

macaques to be a common non-human primate used in scientific research. More importantly the animals are an excellent model for translational research, and multiple studies have been conducted utilizing this species throughout history ranging from psychological research to radiation research. Specifically, the blood physiology is identical to humans making the animals a perfect model for researching the PPHA morphology (Yu, et. al, 2019).

Regardless of the type of research macaques need a place to live out their lives once projects are concluded. This necessitates facilities like, in the Section on Comparative Medicine, located at the Thomas B Clarkson Campus in Winston-Salem, North Carolina where macaques and other non-human primate species can reside for the remainder of their lives. Rhesus macaques used in this study were all residents, or former residents, of the Wake Forest School of Medicine, Department of Comparative Medicine. While there, the animals are housed in large facilities inside enclosures that have stainless steel walls that are open from floor to ceiling for the macaques to move around freely on a multitude of platforms and ropes intended to keep the animals entertained. The cages are built side by side with the cage doors facing the interior walkway of the buildings which provides access to the animals by handlers for feeding, veterinary care, and cage cleaning. Macaques are inherently social animals, so two animals are kept per cage to promote pair bonding and reduce stress to the animal that would be induced by solidarity. While social, the macaques are also highly territorial, so the walls separating the cages are solid walls which prevents direct interaction between neighboring cages, therefore mitigating stress to the animal. Lastly, each enclosure has access to an outside enclosure that is only accessible by the two animals in the one enclosure. Rhesus macaques that are residing at the Wake Forest School of Medicine, Department of Comparative Medicine, in the Section on Comparative Medicine, located at the Thomas B Clarkson Campus in Winston-Salem, North

Carolina can be seen below in Figure 10 (see written permission for use of these images is in Appendix E).



Figure 10. Rhesus Macaques, Photos courtesy of the Wake Forest School of Medicine, Department of Comparative Medicine.

Chapter 2: Methodology

IACUC Approval

This study was approved by the IACUC of Colorado State University on December 20, 2019 with a Colorado State University IACUC Inter-Institutional Agreement with the Wake Forest School of Medicine, Department of Comparative Medicine, in the Section on Comparative Medicine, located at the Thomas B Clarkson Campus in Winston-Salem, North Carolina (see Appendix A). Animal handling, care, and samples being provided by Wake Forest School of Medicine were under the IACUC of the providing institution themselves (see Appendix B). Furthermore, safe handling and occupational hazard associated with non-human primates were clearly communicated and understood by the receiving institution and consent to handling samples was demonstrated by signing an occupational safety and health zoonotic concerns agreement with the Wake Forest School of Medicine (see Appendix C).

Studies Conducted Using Rhesus Macaques Blood Smears

Three distinct PPHA studies were conducted using the blood smears obtained from Wake Forest School of Medicine, Department of Comparative Medicine, in the Section on Comparative Medicine, located at the Thomas B Clarkson Campus in Winston-Salem, North Carolina: a baseline prevalence of the PPHA morphology in non-irradiated macaques, a dose response curve, and a biokinetics/persistence study. Blood smears used in the study were selected from an archive of samples that have been taken as part of periodic wellness testing on

the primates at the center. Samples had been archived at the time that they were taken, and undisturbed until the time of this project. There were two distinct cohorts of animals that the smears were drawn from, the X-15 and the X-10 cohorts. X-15 was part of a previous study that looked at the impacts of radiation dose on gross blood cell counts over the lifetime of the animals, while the X-10 cohort was merely the repository of other rhesus macaques that were living or had lived at the facility and their blood smears were taken during annual health checkups. All evaluated macaques from both cohorts were used for the dose response model, the 4 Gy macaques from the X-15 cohort were used for biokinetics/persistence model, and all macaques that received 0 Gy of dose, regardless of which cohort they were a part, were used in the calculation of the baseline prevalence. A table of all macaques, the doses they received, the cohort from which they were drawn, and of which studies they were a part can be seen in Table 2.

Table 2. All rhesus macaques with associated animal IDs, cohort, doses received, and which study applies to each.

Rhesus Macaque Animal ID	Cohort	Acute Dose (Gy)	Studies Conducted (✓= Macaque in Study / X= Macaque not in Study)		
			Dose Response	Biokinetics/ Persistence	Baseline Prevalence
1962	X-15 (Group 1)	0	✓	✓	✓
1965	X-15 (Group 2)	0	✓	✓	✓
1971	X-15 (Group 1)	0	✓	✓	✓
1973	X-15 (Group 2)	0	✓	✓	✓
1974	X-15 (Group 1)	0	✓	✓	✓
1975	X-15 (Group 2)	0	✓	✓	✓
1976	X-15 (Group 2)	0	✓	✓	✓
1977	X-15 (Group 2)	0	✓	✓	✓
1979	X-15 (Group 1)	0	✓	✓	✓
1982	X-15 (Group 1)	0	✓	✓	✓
1960	X-15	0	✓	✓	✓

1967	X-15	0	✓	✓	✓
1968	X-15	0	✓	✓	✓
1969	X-15	0	✓	✓	✓
1970	X-15	0	✓	✓	✓
1972	X-15	0	✓	✓	✓
2061	X-10	0	✓	✗	✓
2065	X-10	0	✓	✗	✓
1962	X-15 (Group 1)	4	✓	✓	✗
1965	X-15 (Group 2)	4	✓	✓	✗
1971	X-15 (Group 1)	4	✓	✓	✗
1973	X-15 (Group 2)	4	✓	✓	✗
1974	X-15 (Group 1)	4	✓	✓	✗
1975	X-15 (Group 2)	4	✓	✓	✗
1976	X-15 (Group 2)	4	✓	✓	✗
1977	X-15 (Group 2)	4	✓	✓	✗
1979	X-15 (Group 1)	4	✓	✓	✗
1982	X-15 (Group 1)	4	✓	✓	✗
2058	X-10	4	✓	✗	✗
2059	X-10	4	✓	✗	✗
2060	X-10	4	✓	✗	✗
2062	X-10	4	✓	✗	✗
2063	X-10	4	✓	✗	✗
2064	X-10	4	✓	✗	✗
2067	X-10	4	✓	✗	✗
1892	X-10	6.4	✓	✗	✗
1884	X-10	6.5	✓	✗	✗
1885	X-10	6.5	✓	✗	✗
1886	X-10	6.5	✓	✗	✗
1904	X-10	6.5	✓	✗	✗
1906	X-10	6.5	✓	✗	✗
1917	X-10	6.5	✓	✗	✗
1919	X-10	6.5	✓	✗	✗
2056	X-10	6.5	✓	✗	✗
1910	X-10	8	✓	✗	✗
2053	X-10	8	✓	✗	✗
1905	X-10	8.5	✓	✗	✗

The baseline prevalence of the PPHA morphology was determined by evaluating 18 macaques that were non-irradiated. Six of the X-15 cohort were non-irradiated, while the 10 that were irradiated contributed blood smears from prior to their irradiation date. In total, 16 macaques contributed blood smears from the X-15 cohort, and 2 additional macaques that were non-irradiated were taken from the X-10 cohort. All values generated were averaged and a standard deviation was calculated.

For the dose response study, samples were chosen based on an arbitrary time frame of approximately 200 days post irradiation. The decision to have a narrow time frame was made because the persistence of the PPHA morphology was unknown at the time of selection, so all smears needed to be in the same stage of persistence, or lack of persistence. The selection of the 200-day time frame was simply the availability of macaques with a spectrum of doses from which blood smears had been taken. The archive of blood smears consisted of nearly 100 microscope slide boxes and over 8,100 blood smears, all with relatively no organization scheme. Slide boxes were all removed from storage and organized first chronologically in accordance with the blood smears that they contained. The predetermined list of blood smears at the 200-day time frame were sorted and placed into a separate slide box brought to Wake Forest from Colorado State University and subsequently transported back to Colorado. Only 27 of the original 50 selected blood smears were located. However, an additional 20 blood smears were added from the 4 Gy irradiated macaques in the X-10 cohort for a total samples size of 47 macaques. Ten blood smears were the pre-irradiation samples, and 10 blood smears were approximately 200 days post irradiation. The exact time post irradiation was not known until after the completion of the biokinetics/persistence study since it was blinded.

For the biokinetics/persistence study, blood smears were taken from the Wake Forest's X-15 cohort. The cohort consisted of 10 non-irradiated macaques and 10 macaques that were irradiated in October 2016 with a 4 Gy dose. Four of the 10 non-irradiated macaques had succumbed due to comorbidities and were excluded from this study. The remaining 16 macaques (10 irradiated and 6 non-irradiated), all had blood smears taken periodically from 6 days prior to irradiation to 1124 days post irradiation totaling 19 time points over 3 years and 1 month. Samples were taken on a biweekly basis for the first 2 months, but to minimize effects of anesthetizing agents on the health of the animal the time frame between smears was spread out to as far as 6 months by the conclusion of the study. The irradiated animals were fixed into 2 groups that were separated merely by the irradiation date. Group 1 consisted of macaques 1962, 1971, 1974, 1979, and 1982, while group 2 consisted of macaques 1965, 1971, 1975, 1976, and 1977. Irradiation dates were October 16, 2016 and October 23, 2016, respectively. Group information can be seen in Table 2.

Irradiation Protocols for Rhesus Macaques

The control and irradiated animal samples used for this study were obtained from Wake Forest School of Medicine, University of Maryland, University of Illinois, Armed Forces Radiobiology Research Institute, Lovelace Respiratory Research Institute, Citox Labs, and Primate Products. Irradiated animals received 0 to 8.5 Gy total body radiation under IACUC oversight at their prior institution using one of two strategies: (1) linear accelerator-derived photons at a nominal mean energy of 2 MeV, delivered at 80 cGy/minute as a split dose given half anterior-posterior and half posterior-anterior; or (2) Cobalt 60-derived gamma irradiation

delivered simultaneously, bilaterally at 60 cGy/min. These are potentially lethal doses: the LD 10/30 for rhesus macaques is ~5.5 Gy, the LD 50/30 is ~6.7 Gy, and the LD 90/30 is 8 Gy (MacVittie, Farese, Jackson, 2015). Surviving animals were subsequently transferred to Wake Forest School of Medicine Center for Comparative Medicine Research for long-term monitoring post-radiation. Irradiation methods, supportive care strategies, and acute effects for many animals donated to this cohort have been recently reported (Farese, Cohen, Katz, Smith, Jackson, Cohen, et al., 2012 & Yu, Lindeblad, Lyubimov, Neri, Smith, Szilagyi, et al., 2015)

After arrival at Wake Forest, all animals were monitored twice daily by trained veterinary technical laboratory staff to assure animal well-being and social stability. Any evidence of illness was classified using a nonhuman primate-specific modification of the Children's Clinical Oncology Group toxicity criteria (Uckun FM, Yanishevski Y, Tumer N, Waurzyniak B, Messinger Y, Chelstrom LM, et al., 1997). Sick animals were promptly evaluated by one of seven institutional veterinarians independent of the research team, two of whom are board-certified by the American College of Laboratory Animal Medicine.

Animals consumed a diet of laboratory chow (Purina LabDiet Monkey Diet 5038, Richmond, IN, USA) that was supplemented with fresh fruits and vegetables and with water as often as necessary or desired by the animal. They were housed socially in indoor-outdoor pens whenever possible, or in group cages if necessary, for safe handling or medical care. Care was taken to ensure the animals in the groups were compatible. Environmental enrichment, including fruits/vegetables, toys, puzzles, climbing and hiding environments, was provided continuously on a rotating basis. Behavioral well-being was additionally monitored, and recommendations made as needed by an independent behavioral management team. All animals were trained to

cooperate in handling procedures, to minimize stress. Sampling was scheduled so that the animals were sedated the minimum number of times required for data collection.

All macaques undergo computed tomography (CT) scans as a part of wellness checkups on various intervals. Animals in the X-10 cohort received CT scans upon arrival at the Wake Forest School of Medicine, Department of Comparative medicine, and X-15 animals received CT scans in May 2016, April 2018, and March 2020. The effective dose for the CT scans ranged from 9-37 mGy across all macaques. The dose received from the CT was inconsequential compared to the animal's acute doses and so was not considered a significant factor in PPHA frequency.

Pseudo Pelger-Huët Anomaly Quantification with Light Microscope

All blood smears were fixed with methanol, air dried, stained using Giemsa-Wright stain, and subsequently air dried again. Slide staining was performed the day of the sample collection, and at necropsy in the case of deceased animals, in all cases (see Appendix G and H). Certain slides were presented with a slightly different coloration, and it was determined that the same stain was used just at a different concentration. Coloration differences had no impact on the ability to evaluate the slides.

Blood smears were manually inspected under an Olympus BH-2 light microscope at 40x magnification. The slide was placed on the stage and low viscosity Thermo Scientific Resolve™ microscope immersion oil was used to maximize clarity of evaluation. The slide was first quickly inspected for clarity of staining, quality of cells, and ultimately the ability to continue

with the PPHA analysis. Once the slide was determined to be readable, the neutrophils were counted in a sweeping back and forth scan that was systematic in nature to ensure that cells were not counted more than once. A count of neutrophils was kept until a PPHA was encountered. At that time, the number of neutrophils counted, including the PPHA, was recorded in a laboratory notebook using Arabic numerals. The microscope magnification was then increased to 100x for closer inspection of the suspected PPHA. If it was determined to be a PPHA, an image was taken using a 12 megapixel Galaxy S8+ smartphone with a Gosky microscope lens smartphone camera adapter, and the PPHA was recorded in the laboratory notebook as a hashmark on a different line below the neutrophil count. This process was continued until the cumulative count of neutrophils, including PPHAs, reached 300 cells. To ensure that the gross cell count did not fall under or exceed 300, every time the number of neutrophils was recorded, the same number was added to a gross count on a calculator. This process was repeated for every blood smear evaluated in the exact same fashion to maintain consistency in methodology. Following evaluation, slides were removed from the microscope stage and placed face down on a paper towel to allow the immersion oil to evaporate overnight. Once determined to be oil free, the slides were removed from the paper towel, and the evaluations were reconciled with the sample identification number and recorded on a spreadsheet for later analysis.

Risk of Bias in Analysis, and Steps to Mitigate Bias

When evaluating blood smears manually there is an inherent risk of bias by the evaluator for considering neutrophils to be PPHAs when they are ultimately not (false positive, type 1 error). Several steps were taken to mitigate this risk of bias in the analysis and the data produced.

For the dose response study, animal IDs were known by the evaluator at the time of evaluation, but radiation doses were blinded until after the last animal was evaluated. All cell counts were kept in a laboratory notebook and data were not transcribed into a digital spreadsheet for evaluation until all relevant slides were evaluated. The exception to this was the 10 macaques that were in the X-10 cohort and were included in the dose response with blood smears prior to their irradiation (0 Gy) and blood smears approximately 200 days post irradiation (4 Gy). The animals that overlapped between the biokinetics/persistence and the dose response studies were not added to the dose response until the biokinetics/persistence was complete.

For the biokinetics and persistence study, since all animals had the same dose, the only means of preventing bias was to blind the dates the animals were evaluated and include several 0 Gy macaques. The X-15 cohort that was provided by Wake Forest contained 10 macaques that received 4 Gy, 6 macaques that received 0 Gy, and 1000 blood smears across 10 slide boxes (Table 2). The boxes of blood smears were labeled with the window of time that corresponded to the blood smears they contained. A piece of tape was placed over these labels and the boxes were randomly placed out of order. In addition, when slides were pulled for evaluation the following day, a small piece of tape was placed over the date on the label on the slide itself. As the slides were reconciled the following day, the tape was removed, and the handwritten data were transcribed to a spreadsheet accordingly. Complete models of the biokinetics and persistence study were not constructed until the conclusion of the microscope analysis, and the final macaque data were recorded on the digital spreadsheet.

Lastly, an image was taken of every PPHA found. All images were reconciled and labeled with the associated macaque the day after evaluation at the same time the data and slides

were reconciled and added to the spreadsheet. Images were inspected one by one on a large computer monitor to allow for close inspection of the cell's morphology. All cells that were erroneously determined as PPHAs were annotated in the laboratory notebook and the digital spreadsheet. At the conclusion of every week, all images were reviewed once again, data on the spreadsheet were checked against the laboratory notebook, and microscope slides were returned to the appropriate box and placed in a complete pile. Time stamp labels on the slide boxes were not removed until all 10 slide boxes were placed in the complete pile so process of elimination and assumptions were not made on the time of slides being evaluated last.

Data Analysis

All values and figures were calculated and generated using Microsoft Excel spreadsheets. Furthermore, data collected for the dose response, biokinetics/prevalence, and baseline studies were compiled in mutually exclusive spreadsheets in Microsoft Excel. Samples were not sorted by cohort (X-10/X-15), but by the studies in which they were involved, as indicated by Table 2, and they were entered into each spreadsheet that corresponded with the different studies. For each sample, the number of PPHAs observed in a blood smear was compared to the total number of neutrophils counted to determine a percentage of cells with the PPHA morphology. Total neutrophil counts included the number of PPHAs, in lieu of PPHAs + 300 normal neutrophils, because the latter would produce a ratio instead of a percentage. Once every macaque for the dose response study was evaluated for PPHAs, the percentages were reconciled with the doses and a dose response was produced. Since the dose response had multiple animals clustered at 0, 4, and 6.5 Gy, a box and whiskers plot was constructed to display the distribution of data within

the cohorts. A Student's t-test was performed between 0 and 4 Gy, 0 and 6.5 Gy, and 4 and 6.5 Gy to evaluate the data for statistical significance.

Biokinetics/persistence involved 10 animals separated into 2 groups that were distinct from one another only by irradiation date (Appendix F). For this reason, a graph for each group ($n=5$ each) was constructed that displays the average of each time point since irradiation and the standard deviation of that day. Since the 10 irradiated macaques were segregated into 2 groups and their irradiation dates were offset by 7 days, the compiled data were normalized between the 2 groups to 'weeks post irradiation' as opposed to 'days post irradiation'. An average of all 10 macaques was plotted as a function of weeks post irradiation and the standard deviation of that time point displayed. An individual biokinetics/persistence curve that is plotted as PPHA percentage as a function of days post irradiation was constructed for all 10 macaques. Only one blood smear was available per macaque per time point so there is no standard deviation displayed. Lastly, all 10 individual graphs were overlaid onto one single graph to display the PPHA percentage of all macaques as a function of days post irradiation. No standard deviation was reported, due to only one blood smear per day, per macaque being available for analysis. The prevalence of the PPHA morphology in 0 Gy rhesus macaques was compiled following completion of the biokinetics/persistence and the dose response studies for the calculation of a baseline prevalence. There was a complete overlap of the 0 Gy macaques and the other studies leading to the compilation of baseline animals to occur last. Once compiled an average and standard deviation were calculated.

Chapter 3: Results

Pseudo Pelger-Huët Anomaly Baseline Prevalence in Rhesus Macaques (non-irradiated)

The baseline prevalence of the PPHA morphology in the Rhesus Macaques was determined to be $0.58 \pm 0.46\%$ with a lower limit of 0% and an upper limit of 1%. Baseline prevalence data took on a log-normal distribution. The distribution of baseline percentages of PPHAs can be seen in Figure 11, and the Macaque identification numbers with the individual percentage of neutrophils presenting with the PPHA morphology can be seen in Table 3.

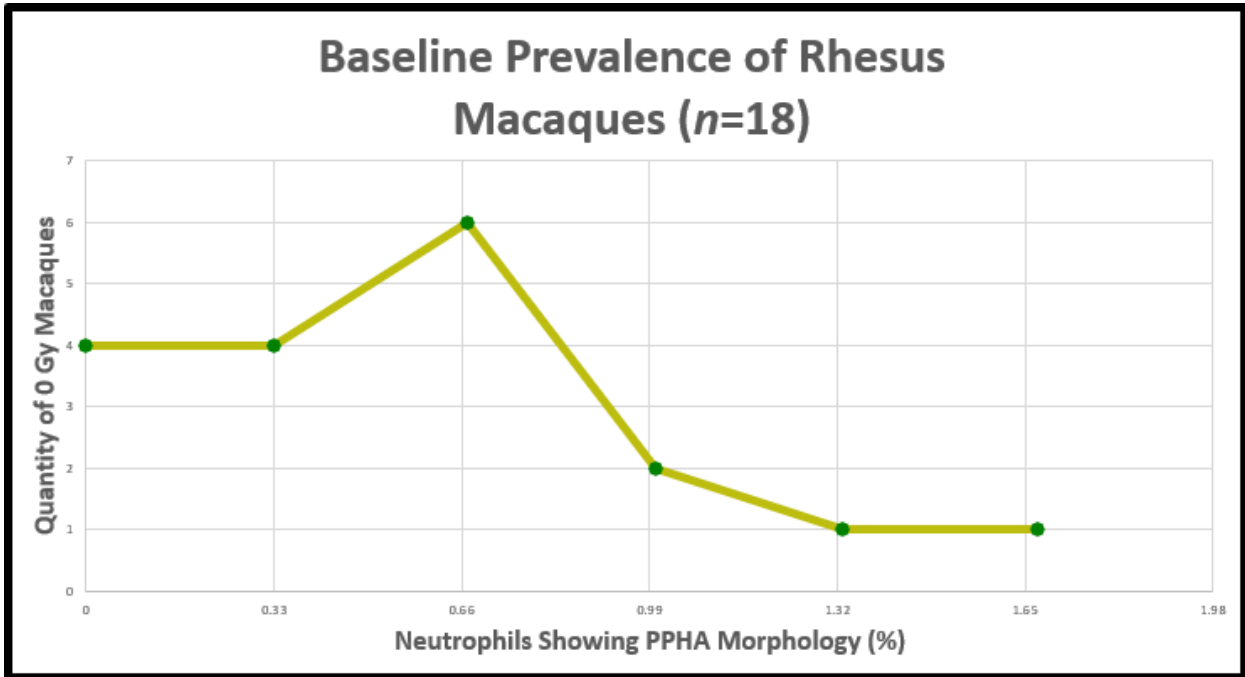


Figure 11. Distribution of the percentage of neutrophils presenting with PPHA morphology in 0 Gy dose rhesus macaques.

Table 3. Baseline prevalence of pseudo Pelger-Huët anomalies in rhesus macaques.

Macaque ID	Radiation Dose (Gy)	% PPHA
1962	0.00	1.00
1965	0.00	1.67
1971	0.00	0.00
1973	0.00	1.33
1974	0.00	0.00

1975	0.00	0.67
1976	0.00	1.00
1977	0.00	0.33
1979	0.00	0.67
1982	0.00	0.00
1960	0.00	0.33
1967	0.00	0.00
1968	0.00	0.72
1969	0.00	0.33
1970	0.00	0.67
1972	0.00	0.33
2061	0.00	0.67
2065	0.00	0.67
Average PPHA %		0.58 ± 0.46%

Pseudo Pelger-Huët Anomaly Dose Response in the Rhesus Macaques

A linear dose response relationship was found between the percentage of neutrophils that presented the PPHA morphology and the acute radiation dose administered to the Macaque. The linear trendline displayed a positive correlation between PPHAs and radiation dose with an R^2 of 0.88. Blood smears for the dose response were taken from the animals at an average of 198 ± 8.2 days following irradiation including the macaques used from the biokinetic/s/persistence study. Data points in the dose response graph are displayed as semi-translucent so that data points with multiple animals appear darker. Each animal had only one blood smear available for analysis, so no average or standard deviation is reported. The dose response model and corresponding linear regression line can be seen in Figure 12. All data points on the dose response model were intentionally semi-translucent to show where multiple macaques are at a single data point. Macaque identification numbers, days post irradiation the smear was taken, whole body radiation

dose, and the corresponding percentage of neutrophils that presented with the PPHA morphology can be seen in Appendix F.

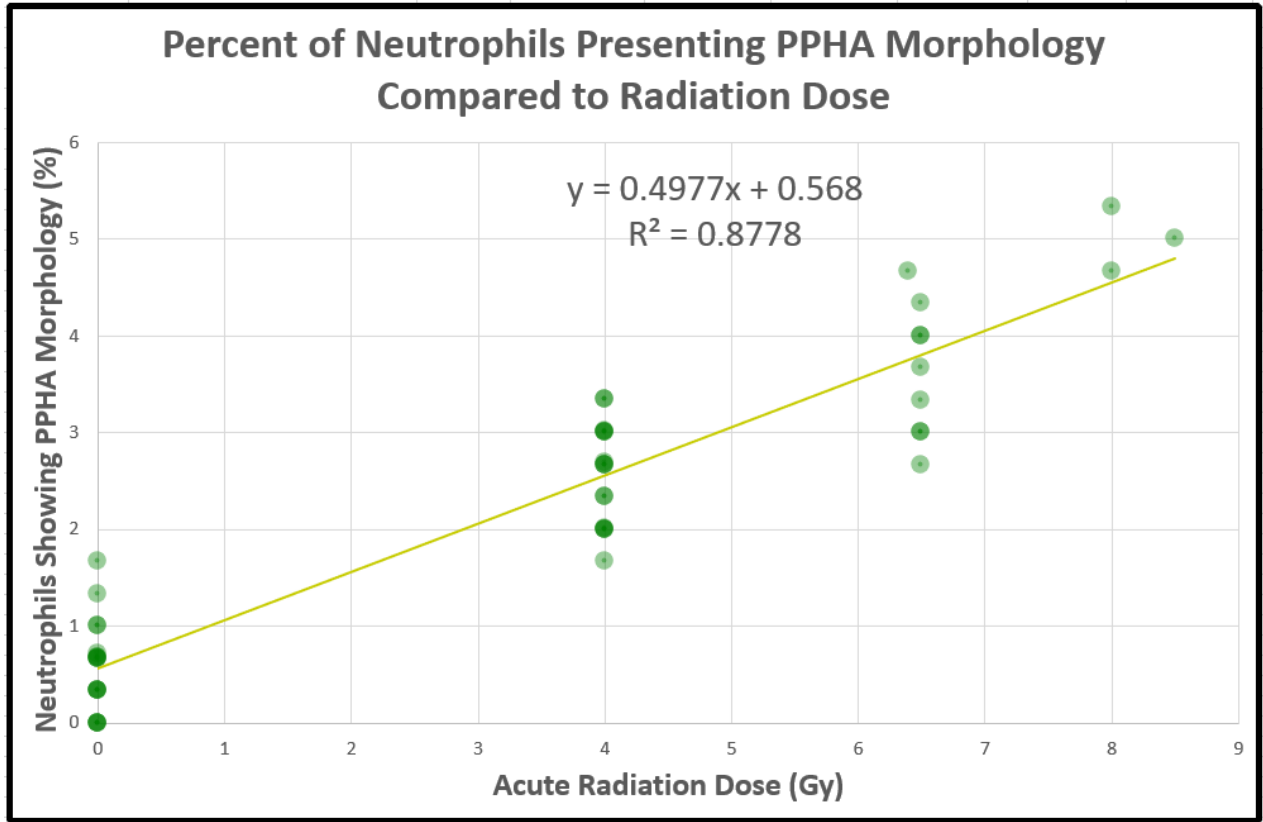


Figure 12. Rhesus Macaques dose response displaying a linear relationship between the percentage of neutrophils presenting the PPHA morphology and acute radiation dose.

Dose response samples were clustered at 0, 4, and 6.5 Gy, and only 4 doses were outside those categories. The number of animals and distribution of data can be seen in Table 4.

Table 4. Averages of 0, 4, and 6.5 Gy rhesus macaques.

	n	Average PPHA (%)
0 Gy	18	0.58 ± 0.46%
4 Gy	17	2.57 ± 0.51%
6.5 Gy	8	3.50 ± 0.59%

The upper limit of the 0 Gy macaques was larger than the lower limit of the 4 Gy macaques, and the averages of the 4 Gy and the 6 Gy macaques were less than two standard deviation from one another so Student t-tests were performed to test for statistically significant differences. The 0 Gy and 4 Gy cohorts were statistically different at the 95% confidence level, with a p-value of 1.34×10^{-13} . The 4 Gy cohort and the 6.5 Gy cohort were statistically different at the 95% confidence level, with a p-value of 5.34×10^{-4} (Figure 13).

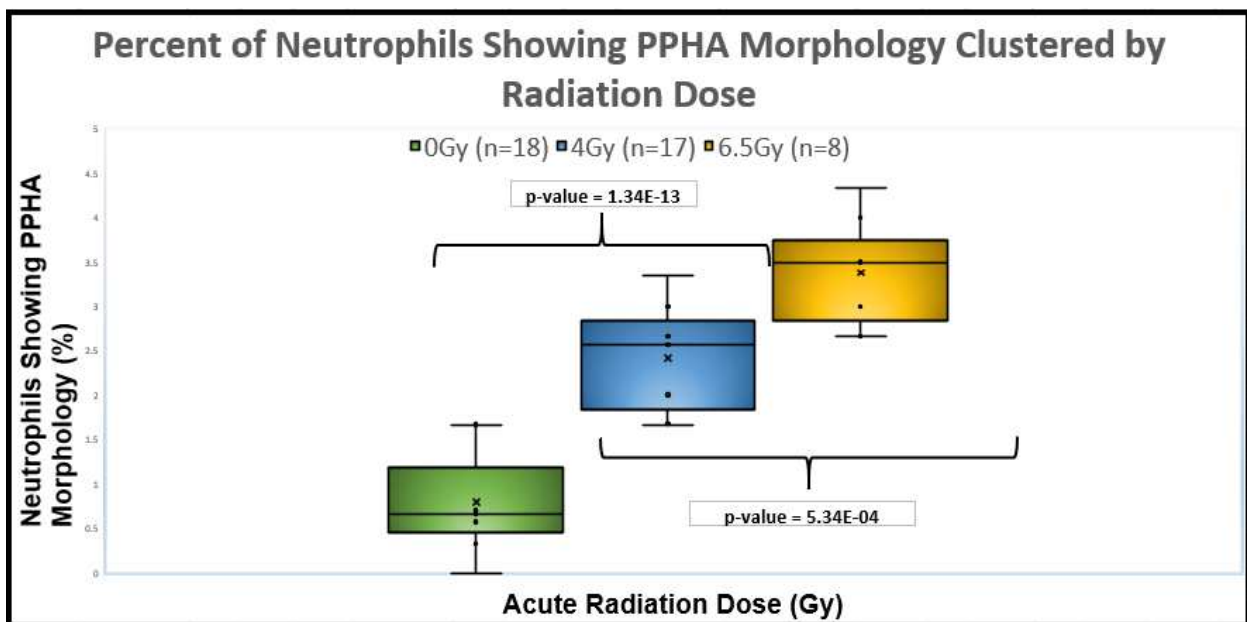


Figure 13. Rhesus macaque dose response with animals clustered by dose (0 Gy, 4 Gy, and 6.5 Gy). Upper and lower limits of recorded values are denoted with the upper and lower whiskers on each plot.

The standard deviation of each cohort was expected to increase with increasing radiation dose due to the inherently random nature of damage due to ionizing radiation. In addition, cellular repair mechanisms respond at different rates in different individuals leading to an increased variance of outcomes. The standard deviation only increased minimally with increasing dose. Data associated with the box and whiskers plot above can be seen below in Table 5.

Table 5. Rhesus Macaques dose response clustered by radiation dose.

Animals Clustered by Dose					
0 Gy Dose		4 Gy Dose		6.5 Gy Dose	
Animal ID	%PPHA	Animal ID	%PPHA	Animal ID	%PPHA
1962	1.00	1962	2.00	1884	3.00
1965	1.67	1965	3.34	1885	2.67
1971	0.00	1971	3.01	1886	4.33
1973	1.33	1973	3.00	1904	3.67
1974	0.00	1974	2.01	1906	4.00
1975	0.67	1975	3.34	1917	3.33
1976	1.00	1976	2.34	1919	3.00
1977	0.33	1977	3.00	2056	4.00
1979	0.67	1979	2.69	Average	3.50 ± 0.59%
1982	0.00	1982	2.00		
1960	0.33	2058	2.67		
1967	0.00	2059	2.67		
1968	0.72	2060	2.33		
1969	0.33	2062	2.67		
1970	0.67	2063	3.00		
1972	0.33	2064	2.00		
2061	0.67	2067	1.67		
2065	0.67	Average	2.57 ± 0.51%		
Average	0.58 ± 0.46%				

Pseudo Pelger-Huët Anomaly Biokinetics/Persistence Model in Rhesus Macaques Post-irradiation

The 10 animals in the biokinetics/persistence study were evaluated for PPHAs prior to irradiation and post irradiation. Rhesus macaques acted as their own controls in this experiment,

and the average baseline percentage of PPHAs used for comparison with post irradiation PPHA percentages was calculated using only the 10 rhesus macaques irradiated with 4 Gy in the X-15 cohort (Table 2). The 8 additional animals that received 0 Gy of irradiation were not factored into the baseline average for the biokinetics/persistence study. The average baseline percentage of PPHAs for control samples was $0.73 \pm 0.58\%$. The earliest time point following irradiation that was available for analysis was 24-48 hours post-irradiation. The average prevalence of the PPHA morphology 24-48 hours post-irradiation was $1.94 \pm 1.03\%$, which is an increase of 233% from pre-irradiation. The next data point was 1.2 weeks post-irradiation, and the average prevalence of the PPHA morphology was $2.80 \pm 0.60\%$, which is an increase of 350% from the baseline. Following one-week post-irradiation, the prevalence plateaued and was relatively constant. The increase in the prevalence of the PPHA morphology and up to 4 weeks post-irradiation can be seen in Figure 14.

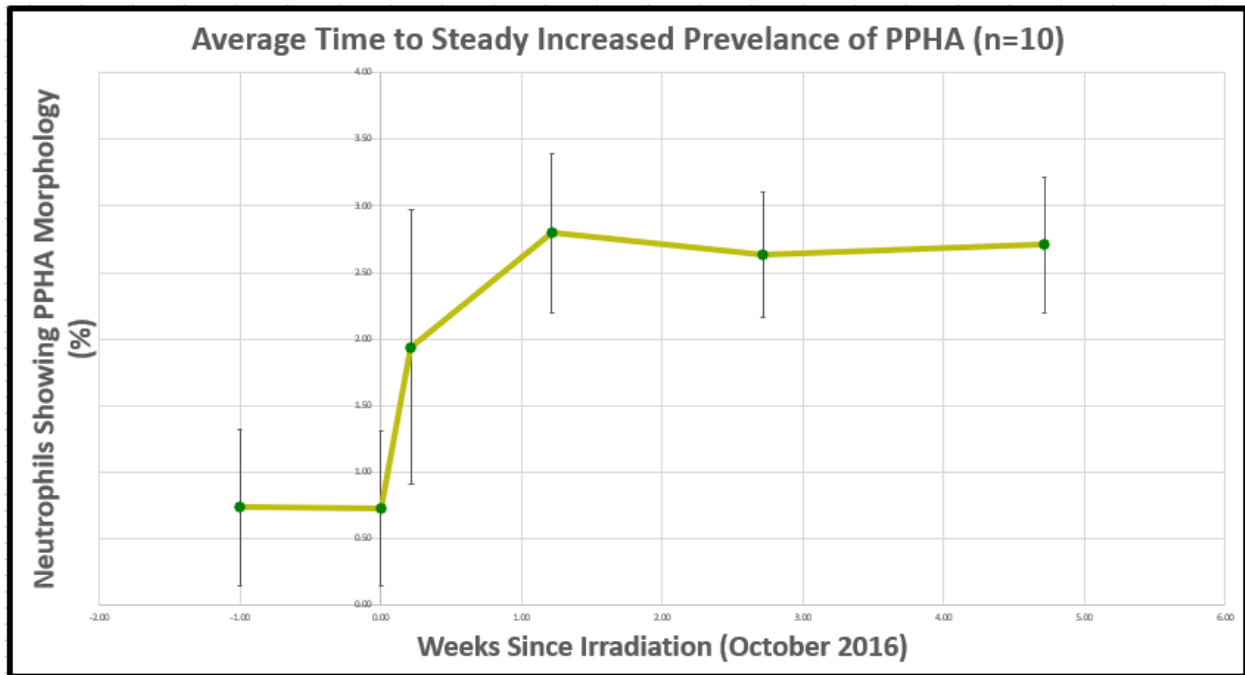


Figure 14. Rhesus macaques average time to a steady increase in the prevalence of pseudo Pelger-Huët anomalies as a function of weeks post irradiation.

The last time point evaluated for each macaque had an average increased prevalence of PPHAs of $2.7 \pm 0.28\%$ which is a 338% increase from the pre-irradiation average PPHA prevalence of $0.73 \pm 0.58\%$. When the average of the last time point is compared with the average of 1.2 weeks post irradiation (when the prevalence plateaued) a change of only -0.1% PPHA prevalence is observed over 3 years. The change in prevalence from 1.2 weeks post-irradiation to 3.1 years post irradiation is less than one standard deviation, indicating a negligible change in the prevalence and a persistence of the PPHA morphology to 3 years post irradiation. Furthermore, an average was taken of all PPHA evaluations across all animals in the study from the start of the prevalence plateau (1.2 weeks post-irradiation) through the end of the study (3.1 years post-irradiation), and the average PPHA percentage was $2.7 \pm 0.33\%$ which is a 338% increase from the pre-irradiation average.

All individual graphs and the averages segregated by group according to radiation date can be found in Appendix F. An overlay of the 10 independent biokinetics curves can be seen in Figure 15, an average of the 10 animals can be seen in Figure 16, and data associated with the average of all 10 animals can be seen in Table 6.

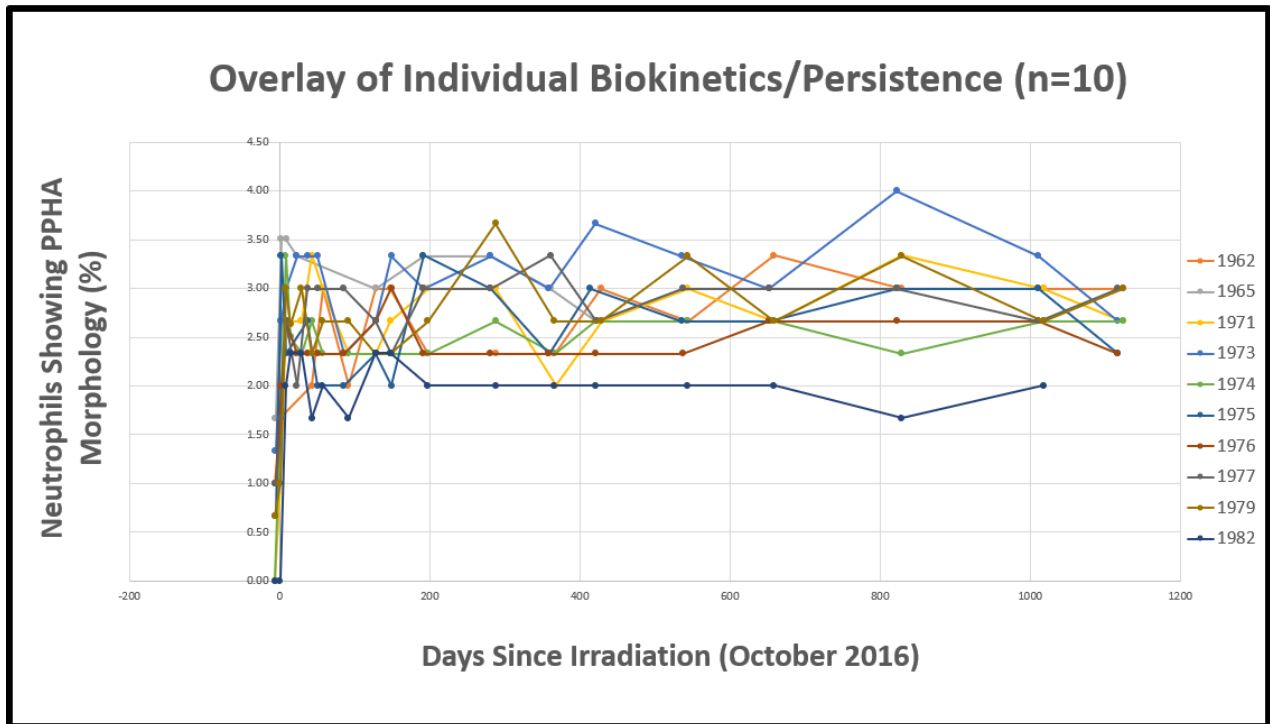


Figure 15. Rhesus macaques biokinetics/persistence with 10 subject animals overlaid.

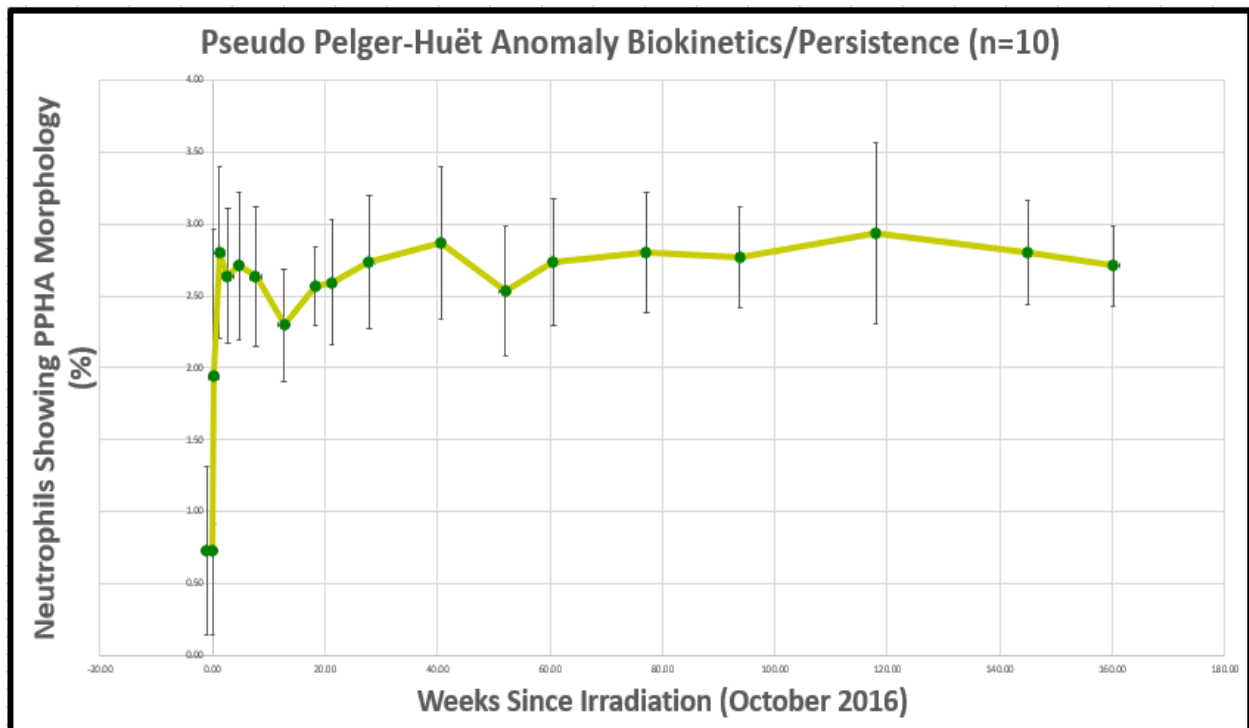


Figure 16. Rhesus macaque biokinetics/persistence, average PPHA concentration by weeks post irradiation.

Table 6. Rhesus macaque biokinetics/persistence with n=10 averaged at weeks post irradiation.

Average Biokinetics/Persistence Group 1&2 (n=10)		
Weeks Post Irradiation	Average PPHA (n=10)	Std. Dev. (±)
-1.00	0.73	0.58
0.00	0.73	0.58
0.22	1.94	1.03
1.22	2.80	0.60
2.72	2.64	0.47
4.72	2.71	0.51
7.71	2.63	0.48
12.72	2.30	0.39
18.29	2.57	0.27
21.22	2.59	0.43
27.86	2.73	0.47
40.64	2.87	0.53
52.07	2.53	0.45
60.64	2.73	0.44
77.14	2.80	0.42
93.77	2.77	0.35
117.93	2.93	0.62
144.93	2.80	0.36
160.20	2.71	0.28

Chapter 4: Discussion

Rhesus Macaques Baseline Prevalence of PPHAs (Non-irradiated)

The baseline prevalence of the PPHA morphology in rhesus macaques was found to be $0.58 \pm 0.46\%$ ($n=18$). Goans et al. reported a background percentage of PPHAs in humans to be $4.4 \pm 0.4\%$ ($n=16$) (Goans, 2017). A baseline prevalence of PPHAs is indicative that there are other causes for the PPHA morphology to be present in the peripheral blood besides an acute radiation dose that was investigated in this study. Furthermore, the average baseline is larger by several percent in humans, but the standard deviation is similar at a 0.06% difference, implying a common origin for the baseline PPHAs. A probable cause of the baseline prevalence is age related and due to the accumulation of radiation dose from background radiation sources. Rhesus Macaques have a life expectancy of approximately 25 years and the average age of the zero Gy dose animals when blood smears were taken was 5.2 ± 1.3 years old. An average age of the humans in the control group was not reported by Goans et. al, but were given as equivalent to the exposed radiation workers in the retrospective study of the Y-12 criticality accident. The individuals exposed in the accident were of working-class age and were much older than 5.2 years (Goans, 2017). The humans investigated for baseline prevalence were much older than the rhesus macaques studied, and this is a likely explanation for the much higher background prevalence of PPHAs in humans than in the macaques. The change in baseline prevalence of PPHAs as an organism ages warrants further investigation into how background radiation impacts the baseline prevalence, and correction factors for age will be necessary.

Rhesus Macaques Dose Response

The dose response study found a positive correlation between the percentage of neutrophils present in the peripheral blood with a PPHA morphology and acute radiation dose. A linear trendline of PPHA cells and radiation dose yielded an R-squared of 0.88. The blood smears available to use were all archived samples, and since the biokinetics was unknown for the PPHA morphology following an acute radiation dose, the spectrum of radiation doses were limited to those available in a small window of time following the irradiation event. The largest spread of doses inside the narrowest available timeframe included 6 dose cohorts (0, 4, 6.4, 6.5, 8, and 8.5 Gy) that were taken at 198 ± 8 days post irradiation. The 6.4, 8, and 8.5 Gy cohorts only contained 4 rhesus macaques total, so they are a part of the dose response model (Figure 12) but were removed from the box and whiskers plot (Figure 13). A Student's t-test confirmed a statistically significant difference between the 0 and 4 Gy cohorts, and the 4 and 6.5 Gy cohorts.

Detection limits and minimum dose for response could not be determined in this study. A statistical difference between the baseline macaques and the 4 Gy macaques was found, but there were no animals sampled between 0 and 4 Gy due to a lack of availability in the window of time chosen. With the results of the biokinetics study showing that the maximum prevalence of the PPHAs was reached in 1.2 weeks and persistence was observed after that, future samples can be analyzed and added to the dose response outside of the 198 ± 8 day window to fill the gaps between the dose cohorts. Additionally, LD 50/30 for rhesus macaques is reported to be 6.7 Gy, while LD 50/30 for humans is 3.5 Gy (MacVittie, Farese, Jackson, 2015). A lower LD 50/30 in humans demonstrates the need for determination of lower limits of detection so that decisions can be made during the triage phase following a mass casualty incident.

Rhesus Macaques Biokinetics/Persistence (Post-irradiation)

Rapid increase of the PPHA morphology indicates that it can be used for quick estimation of dose, and persistence to 3 years demonstrates that it can be used for retrospective dose estimation as well. However, only two blood smears were taken between irradiation and the peak PPHA percentage being reached, 1 day and 8 days post irradiation (Figure 14). In the first day, nearly a 3-fold increase of PPHAs was reported going from a baseline of 0.7% to 1.9%. In the next week, the PPHA percentage increased further to a 4-fold increase of 2.8% (Table 6). To characterize the rise in prevalence of the PPHA morphology more accurately, blood smears need to be taken at regular intervals until the reported values plateau. The estimated blood sampling interval for PPHA in future studies should be approximately 5 hours, based on Goans et. al reporting a rise in PPHA quantities in as little as 5 hours. Methods of extracting blood from the animal will need to be determined with the well-being of the animal's health in mind. The frequent handling and extraction of biological samples can cause a significant amount of stress and may lead to premature death.

A trendline was drawn between the irradiation date and one day post irradiation ($y = 5.6279x + 0.73$) and when the maximum value of 2.8% PPHAs was entered into the trendline equation, the interpolated time to reach maximum PPHA concentration is estimated to be 62 hours post irradiation if the rate of increase was constant (Figure 14). A 5-hour interval of sampling would result in 13 time points until the plateau is reached. Unfortunately, additional sampling was not possible as this was a retrospective study, and future research would require different animals. However, the 10 macaques in the biokinetics study are still alive with samples being taken periodically, so the persistence models can be extended from 3.1 years to 4 years post irradiation as of December 2020 (Figure 15 and 16).

Possible Reasons for PPHA Persistence When Compared to Other Biodosimetry Methods

The dicentric chromosome assay (DCA) and translocations are currently very well calibrated in biodosimetry, while the PPHA assay is still a novel approach. There were no DCAs conducted on the animals in this study, but the persistence of the PPHA can be compared with the biokinetics/persistence of dicentric chromosomes and translocations. Most of the dicentric chromosome data that have been produced are from acute radiation exposures like the ones received by the rhesus macaques in this study. The DCA is persistent in human peripheral blood from between three months to six months post exposure. Past the 6-month timepoint translocations were far more effective at estimating dose through Fluorescent In-situ Hybridization (FISH) techniques and fluorescent microscopy (Romm, et al., 2009). Dicentric chromosomes are an unstable aberration because they do not persist beyond cell division, whereas translocations, that are easily detected, can pass through mitosis and carry on the mutation to the daughter cells (Romm, et al., 2009).

Studies conducted on 16 individuals that survived the Goiania, Brazil radiological incident had DCAs performed to determine the half-life of dicentric chromosomes in peripheral lymphocytes. Humans exposed to over one Gy exhibited a dicentric chromosomes half-life of 110 days, with an elongation of up to 470 days as time progressed over a 6-year study (Ramolho, Curado, & Natarajan, 1995). The elongation of the half-life of lymphocytes expressing dicentrics is possibly due to a variability in lifespan of T-lymphocytes. It is still widely debated what the lifespan of the various subsets of T-lymphocytes are and the turnover rate is highly variable and unknown, potentially ranging between several days to several years (Ramolho, Curado, & Natarajan, 1995). This indicates that in the beginning, short lived T-lymphocytes

would die off quickly exhibiting a fast removal rate, but eventually leaving the long-lived T-lymphocytes to elongate the removal rate over time.

PPHAs present themselves in granulocytes versus T-lymphocytes, and granulocytes have an average lifespan in the blood of around 8 hours (Ramolho, Curado, & Natarajan, 1995).

PPHAs have persisted in rhesus macaques for 3 years despite the extremely short lifespan of neutrophils because the cells suspected of being affected by radiation are progenitor cells and hematopoietic stem cells in the bone marrow. The exact mechanism that causes the formation of PPHAs is unknown, but there are two possibilities for PPHA proliferations. First, a mutation in chromosome one impacts translation of the lamin-b receptor and degrades the integrity of the nuclear membrane. Second, a physical interaction of radiation with chromatin causes a bridge being formed and the cell is unable to complete cytokinesis or unable to fully segment.

In the case of chromosome one mutation, the hematopoietic stem cells would be affected. Hematopoietic stem cells can be long-lived, allowing for mutations to persist for potentially decades. The undifferentiated hematopoietic stem cells are far more radiosensitive than post-mitotic neutrophils so hematopoietic stem cells are more likely to be impacted by a mutation. A mutation could account for the persistency of the PPHA morphology while a dicentric chromosome in the hematopoietic stem cells would result in cell death. However, non-human primates have presented the PPHA morphology in as little as 5 hours post irradiation, which is very quick for a hematopoietic stem cell mutation to manifest (Goans, 2017). An argument for a physical interaction of the radiation with immature neutrophils could cause chromatin bridges to form and potentially lead to hypo-segmentation of the granulocyte nuclei. Given that there are on average 100 billion neutrophils produced by the bone marrow daily, there is a large potential

for interaction with developing cells that are post mitotic and maturing with the help of chemokines and other cellular messengers.

Ergonomic Hazards of this Study

This study was conducted using a light microscope on a bench top. Each blood smear took between 20 and 45 minutes to evaluate for the PPHA assay, and total time spent performing PPHA assays was estimated to be about 500 hours. The amount of time using the microscope, the chair available for use, and the height of the microscope when compared to the height of the evaluator all presented with ergonomic hazards. Severe neck and back pain was common, and long periods of evaluation were not possible which impacted the pace at which blood smears were evaluated negatively. All ergonomic hazards were mitigated at the 100-hour mark of analysis and the pace of evaluation was able to speed up drastically due to reduced neck and back pain. An ergonomic chair with lumbar support and adjustable height was purchased. Lumbar support mitigated lower back pain, while the adjustable height of the chair and placing the microscope on several textbooks to elevate it removed the upper back and neck pain. Additionally, a pad was added to the bench top to mitigate pressure on elbows and subsequent numbness in hands from pressure directly to the ulnar nerve.

Limitations of Results

The presence of the PPHA morphology in peripheral blood smears may be useful as an inexpensive and effective biomarker of acute radiation exposure. However, the relationship between the percentages of neutrophils that display the PPHA morphology and acute radiation

dose needs strengthening to ensure confidence in the macaque models and translation to humans in a mass casualty incident. The dose response is limited by the small number of cohorts that were available for evaluation. The biokinetics study was limited because blood smears were taken at only two time points in the first week following irradiation. Lastly, the persistence model was only evaluated to 3.1 years and a point where the peripheral prevalence of PPHAs begins to drop was not found.

In addition, the lack of other biodosimetry methods in the current sample population is concerning because assays such as the dicentric chromosome assay are the currently accepted standard of bio-dosimetry and would need to be conducted in parallel to validate the PPHA assay as a biomarker of acute radiation dose. Secondly, the differentiation of the PPHA from normal neutrophils is conducted purely from visual inspection, which can be very subjective. While images were taken to verify the decisions, a molecular characterization and the origin of the PPHA morphology could make determining what is a PPHA and what is a normal neutrophil much more consistent.

Chapter 5: Conclusions & Recommendation for Future Research

Expanding Dose Response, Biokinetics, & Persistence

For future work, additional archived blood smears from the Wake Forest School of Medicine, Department of Comparative medicine can be obtained and evaluated for PPHAs to expand on models constructed in this study. The X-10 cohort has over 8100 blood smears archived, and only 37 were evaluated for the construction of the dose response model in the window of 198 ± 8 days post irradiation. The results of the persistence study indicate that evaluation in such a small window of time is unnecessary, so the dose response can be expanded using additional blood smears from additional monkeys outside of the originally time point of 198 ± 8 days post irradiation.

Future studies should evaluate the X-10 cohort for blood smears taken in the first week post exposure to further define the time for an increased prevalence of PPHAs to occur post-irradiation. Initial searches of the X-10 cohort indicate that some primates had several smears taken in the first 72 hours post irradiation. Evaluation of more blood smears will better define PPHA response during the first week following irradiation, helping to determine the lower limits of detection, and derive correction factors for the ‘time since irradiation’ for PPHA assays conducted in the first 48-72 hours after an acute radiation dose.

As the 10 macaques from the X-15 cohort age, blood smears will continue to be taken at 6-month intervals. Evaluation of the X-15 cohort for PPHAs over time will build upon the biokinetics/persistence models constructed in this study. In addition to the X-15 biokinetics/persistence macaques, the macaques from the X-10 cohort had periodic blood smears taken as a part of periodic health checkups. Blood smears from the X-10 cohort can be selected

and persistence models of the PPHA morphology can be built for different doses besides 4 Gy and for periods as long as 15 years.

Validation of the Pseudo Pelger-Huët Anomaly Against Current Methods

Additional research is required to validate the PPHA morphology as a biomarker of radiation exposure. Trends have been illustrated in bats, humans, boar, and now rhesus macaques but PPHAs have not been compared to other forms of biodosimetry. A parallel study needs to be conducted where multiple methods of biodosimetry are performed and compared to the PPHA assay to validate the method. For validation, dicentric chromosome assays (DCAs) from peripheral lymphocytes would be analyzed in tandem with the whole blood taken from rhesus macaques. Further characterization of the initial increase in PPHA prevalence in the first several days post irradiation would maximize the efficiency of this study. DCAs should be performed on peripheral blood in tandem with PPHA assays when the PPHA persistence plateau has been reached in the biokinetics model. In addition to DCAs, that have a half-life in the peripheral blood of 110 days, translocations should be determined, as they are far more stable aberrations passed to daughter cells during cell division (Ramolho, Curado, & Natarajan, 1995). DCAs can be used to validate PPHAs for the first several months post irradiation and translocations can be used to validate long term persistence.

Molecular Characterization and Pinpoint Origin of the Pseudo Pelger-Huët Anomaly

Rhesus macaques are frequently used as translational models for biomarkers since their blood physiology is nearly identical to humans and they are abundantly available. Radiation

doses were well characterized in this study, however, in many exposure scenarios the doses are merely estimated, so a correlation between PPHA assays and DCAs is necessary. If the PPHA assay is validated against the dicentric chromosome analysis (DCA), further studies should be done on hematopoietic stem cells (HSC) from rhesus macaques. The movement of the PPHA assay forward with HSCs would require funding that would require the justification provided by this validation with DCA. The use of HSCs would help to discover where in the process of granulopoiesis the damaging event takes place that causes the PPHA morphology to occur. This insight would narrow the scope of work to help determine what that damaging event is, whether it be a double strand break, a mutation, or any other mechanism that would cause a change in the nuclear morphology.

A consensus has been reached on the necessity of a bi-lobed structure to consider the cells a PPHA, however there is still debate on what comprises the thin nuclear bridge that connects the two lobes. As previously discussed, PHAs are caused by a mutation on chromosome 1 that encodes for the lamin-B receptor. This mutation disrupts the integrity of the structural components in the nucleus and results in the abnormal morphology (Collela & Hollensead, 2012). PPHA prevalence has been observed to increase in 5 hours post irradiation in previous experiments, and in the first 24 hours here (Goans, Iddins, Ossetrova, Ney, & Dainiak, 2017). The rapid manifestation of the PPHA morphology is contradictory to the idea that a mutation is responsible, however since neutrophils are rapidly produced in the bone marrow and sent to the peripheral blood a mutation could be the cause. Further investigation of the composition of the PPHA bridge must be conducted. One possible approach is to use electron microscopy to image the bridge, and another could be to use fluorescent probes. If the bridge is

comprised of a dicentric chromosome being pulled between two segmentations a centromere probe could be utilized.

Furthermore, if the PPHA morphology is caused by ionizing radiation generating a double strand break in the genome of the cell, hematopoietic stem cells could be used as a diagnostic tool. Cultured HSCs would be induced into differentiation and irradiated at different stages. However, the cells will not be harvested at each stage but instead allowed to mature as neutrophils. When harvested, the white blood cells (WBC) can be isolated from red blood cells using a hypotonic solution or serum separation tubes. This is intended to increase the concentration of WBCs on the slide for faster and consistent analysis. Using the cytopsin technique the WBCs will adhere to a glass slide and then subsequently be fixed with methanol. Fluorescent In Situ Hybridization (FISH) would allow for an analysis of the nuclear region of cells with the added insight of segregating the chromatin. The fluorescence can be analyzed using a computer program called Metafer and a metasystems microscope that reads the differential fluorescent probes on the chromatin and produces a computer-generated image that color codes the chromatin. The bridge connecting the bilobed structure would then be characterized to determine which chromatin are contained in the bridge, if a dicentric chromosome is present, and if it is a random event or not. A metasystems microscope and Metafer programing is available to this project through collaborations with Oak Ridge Associate Universities and the Biodosimetry lab with the International Atomic Energy Agency.

Lastly, if a mutation is responsible for the PPHA morphology, experiments can be conducted to look for consistent mutations in the genome of PPHAs, and consistent changes in proteins produced by them during granulopoiesis. PHAs are caused by a defect in the lamin-B receptor gene, so Western blotting and DNA-polymerized chain reaction may be utilized to

image the lamin-b receptor and the lamin-b receptor gene, respectively. First, the experiment would need to be conducted in-vitro with excised hematopoietic stem cells grown in medium so that the differentiation can be controlled. Colony stimulating factors and interleukins would be selectively given to induce differentiation of the hematopoietic stem cells. At each stage of differentiation, an irradiated cohort would be harvested and analyzed to be compared to an unirradiated cohort. Some cells from each cohort would be pulverized using a Sonicator and evaluated for the lamin-b receptor using Western blot. In addition, the genome can be sequenced using DNA-PCR to investigate mutations directly. This experiment would also provide insight into which stage of differentiation is most likely to be causing the PPHA morphology to occur.

Automation of Analysis for Efficiency in Mass Casualty Incidents

For the PPHA assay to be used as a fast and effective biomarker in a mass casualty incident the need for an automated high throughput system is clear. Existing technology can be modified and eventually optimized to perform this task. Metasystems microscopes and the corresponding Metafer software is already being optimized for high throughput dicentric chromosome assays with Oak Ridge Associated Universities in Oak Ridge, Tennessee, and soon to be installed at the biodosimetry laboratory for the International Atomic Energy Agency in Seibersdorf, Austria. However, there are many challenges to face when using the metasystems microscope for a cellular assay versus a genomic assay.

First, DCAs are prepared in such a way that there is inherently a monolayer thickness of the sample that is being analyzed. When the metasystems microscope analyzes the DCA slide, it is manually focused in several random locations on the slide and then the microscope scans it automatically taking pictures of chromosome spreads that are thought to have dicentric

chromosomes by the Metafer software. As the microscope completes a slide, it can automatically change to a new slide and analyze the slide thoroughly. Blood smears are inherently not a monolayer of thickness. To achieve the monolayer of thickness of cells, red blood cells can be lysed and the cytopsin technique that was previously discussed could be used to evenly distribute the remaining white blood cells on a glass slide.

Secondly, the size and shape of the PPHA morphology needs to be clearly defined for visual inspection. If automation is functioning correctly, any cell with two lobes and a thin bridge between them will need to be photographed by the microscope, and a human worker will need to verify the cells are PPHAs. Thickness of the thin bridge connecting the two lobes of PPHAs needs to be exactly characterized for the automation to correctly identify PPHA cells. As the metasystems microscope is scanning, it can be taught to take pictures of anything that is below a certain thickness. However, the thickness of the bridge can match the thickness of bridges connecting the lobes of a normal neutrophil, so in addition to bridges the number of lobes would also need to be identified. The number of lobes would be a challenge to automate because the PPHA lobes are not all perfectly round lobes as portrayed in literature. There is a risk of bias that has been generated by the skewing of the PPHA imagery in the literature due to utilizing the most photogenic PPHA cells, rather than illustrating the variety of shapes that manifest.

Lastly, consistency is paramount when it comes to developing the PPHA assay. A standardized approach to extracting the blood sample, performing the blood smear, drying, fixing, staining, and isolating white blood cells would be required.

Conclusions

In conclusion, our hypothesis was proven correct that the pseudo Pelger-Huët anomaly (PPHA) , through the following four specific aims addressed in this study, has definitively been proven to be a biomarker for acute radiation dose in rhesus macaques: (1) Established a baseline prevalence of PPHAs, in the peripheral blood of rhesus macaques, (2) established a dose response curve across a variety of acute doses, (3) established a biokinetics and persistence model, and (4) determined future studies required to validate and optimize the PPHA assay for use as a method of biodosimetric analysis.

The PPHA assay is performed by taking a peripheral blood smear that has been stained with a nuclear staining dye such as Giemsa-Wright stain and evaluated using a light microscope to determine the percentage of neutrophils presenting the PPHA morphology. Previous research projects have produced preliminary data for acute radiation exposure scenarios, but many questions were left unanswered (Goans, 2015). Biological samples from acutely exposed rhesus macaques were obtained to answer many of these questions, and PPHA assays were performed on them to expand on the previously discovered evidence for the efficacy of the PPHA assay as a biomarker of radiation.

Part one of this study consisted of establishing a baseline prevalence of PPHAs in the peripheral blood of rhesus macaques. The baseline prevalence was found to be $0.58 \pm 0.46\%$ ($n=18$). Background radiation is an important consideration for both the baseline and the persistence of the PPHA assay, as PPHA morphology is thought to be induced by chronic low dose radiation exposures as well. Age may be a large factor in the efficacy of the PPHA assay and correction factors could be required. Previous research found that humans have a background prevalence of PPHAs of $4.4 \pm 0.4\%$. The baseline prevalence of PPHAs in rhesus

macaques was much lower than that of human, but the standard deviation of the data was only 0.06% different. This difference in baseline PPHA prevalence is likely due to the rhesus macaques only being on average 5.2 years old when blood smears were taken, while control humans were adults over 18 years old. An older age leads to a larger accumulation of dose from background radiation, therefore changing the baseline prevalence dramatically with a change in age of the victim. The baseline change in PPHAs over time necessitates the investigation of correction factors for age in future research.

Part two of this study consisted of establishing a dose response curve across a variety of acute doses ranging from zero Gy dose to 8.5 Gy (LD90/30) for the rhesus macaques (MacVittie, Farese, & Jackson, 2015). A dose response curve was constructed ($n = 47$) and a strong correlation was found between the percentage of neutrophils in the peripheral blood that presented with the PPHA morphology and acute radiation dose, with an R-squared of 0.88. Rhesus macaque blood was analyzed for increasing PPHA cells clustered at 0 Gy ($n=18$), 4 Gy ($n=18$), and 6.5 Gy ($n=8$), so a Student's t-test was performed between 0 and 4 Gy, and 4 and 6.5 Gy. A statistically significant difference was found in both Student t-tests.

Part three of this study established a biokinetics and persistence model that illustrates how quickly the PPHA morphology manifests and how long they are persistent following acute radiation exposure. Ten rhesus macaques were exposed to a single 4 Gy dose at a rate of 80 cGy min^{-1} and blood smears taken at 19 different time points following exposure. One blood smear was taken prior to irradiation so each animal acted as its own control. The prevalence of the PPHA morphology increased sharply and reached a maximum level at 8 days post irradiation. The maximum PPHA level plateaued and was persistent at this level until the end of available blood smears at 3.1 years post irradiation.

This study was intended to expand upon the methodologies available to biodosimetrists for early and retrospective radiation dose estimations for individuals that have been exposed to acute doses of ionizing radiation. While the models built for this project are more robust than previous studies, shortcomings are present. The dose response model has dose cohorts versus a spectrum, the first week post-irradiation needs to be characterized further, and the persistence was not observed past 3 years so a time related reduction of the PPHA morphology in peripheral blood was not found. Future projects will include analysis of more zero dose rhesus macaques to increase confidence in baseline, an expansion of the dose response model by adding additional animals to increase a variety of doses, extending the biokinetics model beyond the available 3.1 years of blood smears, and increasing frequency of blood smears taken immediately following irradiation to better characterize the initial peak of PPHA prevalence. Additional anticipated areas of research that can be done to continue this project are to molecularly characterize the PPHA morphology, seek to validate the PPHA assay with dicentric chromosome analysis, and investigating the efficacy of PPHA assay automation using metasystem microscopes that are currently in use for dicentric chromosome analysis.

References

- Alizadeh, E., Sanz, A. G., Garcia, G., & Sanche, L. (2013). Radiation Damage to DNA: The Indirect Effect of Low Energy Electrons. *J Phys Chem Lett*, 4(5), 820-825.
<https://doi.org/10.1021/jz4000998>
- Armed Forces Radiobiology Research Institute (AFRRI) Medical management of radiological casualty's handbook. AFRRI; Bethesda, MD, USA: 2010. Online 3rd Edition.
- Brinkmann, V., Reichard, U., Goosmann, C., Fauler, B., Uhlemann, Y., Weiss, D. S., Weinrauch, Y., & Zychlinsky, A. (2004). Neutrophil extracellular traps kill bacteria. *Science*, 303(5663), 1532-1535. <https://doi.org/10.1126/science.1092385>
- Carrano, A. V., & Heddle, J. A. (1973). The fate of chromosome aberrations. *J Theor Biol*, 38(2), 289-304. [https://doi.org/10.1016/0022-5193\(73\)90176-8](https://doi.org/10.1016/0022-5193(73)90176-8)
- Colella, R., & Hollensead, S. C. (2012). Understanding and recognizing the Pelger-Huet anomaly. *Am J Clin Pathol*, 137(3), 358-366.
<https://doi.org/10.1309/AJCP3G8MDUXYSCID>
- Demidenko, E., Williams, B. B., & Swartz, H. M. (2009). Radiation Dose Prediction Using Data on Time to Emesis in the Case of Nuclear Terrorism. *Radiation Research*, 171(3), 310-319. <https://doi.org/Doi.10.1667/Rr1552.1>
- International Atomic Energy Agency (1998). *Diagnosis and treatment of radiation injuries*. Vienna, Austria
- Ellapen, T. & Swanepoel, M. (2017). Evolution of the profession of biokinetics. *South African Journal for Research in Sport, Physical Education and Recreation*. 39. 41-49.

- Farese, A. M., Cohen, M. V., Katz, B. P., Smith, C. P., Jackson, W., 3rd, Cohen, D. M., & MacVittie, T. J. (2012). A nonhuman primate model of the hematopoietic acute radiation syndrome plus medical management. *Health Phys*, 103(4), 367-382.
<https://doi.org/10.1097/HP.0b013e31825f75a7>
- Garraud, O., & Tissot, J. D. (2018). Blood and Blood Components: From Similarities to Differences. *Front Med (Lausanne)*, 5, 84. <https://doi.org/10.3389/fmed.2018.00084>
- Goans, R. E., Holloway, E. C., Berger, M. E., & Ricks, R. C. (1997). Early dose assessment following severe radiation accidents. *Health Phys*, 72(4), 513-518.
<https://doi.org/10.1097/00004032-199704000-00001>
- Goans, R. E., Holloway, E. C., Berger, M. E., & Ricks, R. C. (2001). Early dose assessment in criticality accidents. *Health Phys*, 81(4), 446-449. <https://doi.org/10.1097/00004032-200110000-00009>
- Goans, R. E., Iddins, C. J., Christensen, D., Wiley, A., & Dainiak, N. (2015). Appearance of pseudo-Pelger Huet anomaly after accidental exposure to ionizing radiation in vivo. *Health Phys*, 108(3), 303-307. <https://doi.org/10.1097/HP.000000000000183>
- Goans, R. E., Iddins, C. J., Ossetrova, N. I., Ney, P. H., & Dainiak, N. (2017). The Pseudo-Pelger HuEt Cell-A New Permanent Radiation Biomarker. *Health Phys*, 112(3), 252-257.
<https://doi.org/10.1097/HP.0000000000000618>
- Goans, R. E., Toohey, R. E., Iddins, C. J., McComish, S. L., Tolmachev, S. Y., & Dainiak, N. (2019). The Pseudo-Pelger huet Cell as a Retrospective Dosimeter: Analysis of a Radium Dial Painter Cohort. *Health Phys*, 117(2), 143-148.
<https://doi.org/10.1097/HP.0000000000000831>

- Goans, R. E., & Waselenko, J. K. (2005). Medical management of radiological casualties. *Health Phys*, 89(5), 505-512. <https://doi.org/10.1097/01.hp.0000172144.94491.84>
- Guskova AK, et al. (1988). Acute radiation effects in victims of the Chernobyl nuclear power plant accident. In: *Sources, Effects and Risks of Ionizing Radiation*, United Nations Scientific Committee on the Effects of Atomic Radiation (UNSCEAR). New York: UNSCEAR, appendix.
- Heddle, J. A. (1973). A rapid in vivo test for chromosomal damage. *Mutat Res*, 18(2), 187-190. [https://doi.org/10.1016/0027-5107\(73\)90035-3](https://doi.org/10.1016/0027-5107(73)90035-3)
- Holmer, L., Pezhman, A., & Worman, H. J. (1998). The human lamin B receptor/sterol reductase multigene family. *Genomics*, 54(3), 469-476. <https://doi.org/10.1006/geno.1998.5615>
- Hayes J (2018). The Pseudo Pelger-Huet Anomaly as a Potential Biomarker for Chronic Low-Dose Radiation Exposures of *Sus Scrofa Leucomystax* and *Apodemus Speciosus*. (Masters Thesis)
- Huët G.J., (1931) Familial anomaly of leukocytes. *Nederl Tijdschr Genneesk* 75;5956-5959.
- ICRU No. 51 Quantities and Units in Radiation Protection Dosimetry, 1993. International Commission on Radiation Units and Measurements (ICRU), Bethesda, MD.
- ICRU No. 10b Physical Aspects of Irradiation, 1964. International Commission on Radiation Units and Measurements (ICRU), Bethesda, MD.
- Johnson, R. T., & Rao, P. N. (1970). Mammalian cell fusion: induction of premature chromosome condensation in interphase nuclei. *Nature*, 226(5247), 717-722. <https://doi.org/10.1038/226717a0>

- King, W., Toler, K., & Woodell-May, J. (2018). Role of White Blood Cells in Blood- and Bone Marrow-Based Autologous Therapies. *Biomed Res Int*, 2018, 6510842.
<https://doi.org/10.1155/2018/6510842>
- Latimer, K. S., Rakich, P. M., & Thompson, D. F. (1985). Pelger-Huet anomaly in cats. *Vet Pathol*, 22(4), 370-374. <https://doi.org/10.1177/030098588502200412>
- Lieschke, G. J., & Burgess, A. W. (1992). Granulocyte colony-stimulating factor and granulocyte-macrophage colony-stimulating factor (2). *N Engl J Med*, 327(2), 99-106.
<https://doi.org/10.1056/NEJM199207093270207>
- Lindholm, C., Stricklin, D., Jaworska, A., Koivistoinen, A., Paile, W., Arvidsson, E., Deperas-Standylo, J., & Wojcik, A. (2010). Premature chromosome condensation (PCC) assay for dose assessment in mass casualty accidents. *Radiat Res*, 173(1), 71-78.
<https://doi.org/10.1667/RR1843.1>
- MacVittie, T. J., Farese, A. M., & Jackson, W., 3rd. (2015). The Hematopoietic Syndrome of the Acute Radiation Syndrome in Rhesus Macaques: A Systematic Review of the Lethal Dose Response Relationship. *Health Phys*, 109(5), 342-366.
<https://doi.org/10.1097/HP.0000000000000352>
- Mclaughlin TP, Monahan SP, Pruvost NL, Frolov VV, Ryazanov BG, Sviridox VI. (2000). A review of criticality accidents. Los Alamos, NM: Los Alamos National Laboratory; LA-13638.
- Meadows, S. K., Dressman, H. K., Muramoto, G. G., Himburg, H., Salter, A., Wei, Z., Ginsburg, G. S., Chao, N. J., Nevins, J. R., & Chute, J. P. (2008). Gene expression signatures of

- radiation response are specific, durable and accurate in mice and humans. PLoS One, 3(4), e1912. <https://doi.org/10.1371/journal.pone.0001912>
- Meehan, K.A. (2001). Effects of Exposure to Continuous Low Doses of Ionising Radiation (Unpublished Doctoral Dissertation). Cape Town/Cape Technikon.
- Nikolakaki, E., Mylonis, I., & Giannakouros, T. (2017). Lamin B Receptor: Interplay between Structure, Function and Localization. *Cells*, 6(3). <https://doi.org/10.3390/cells6030028>
- Nishimoto, T., Eilen, E., & Basilico, C. (1978). Premature of chromosome condensation in a ts DNA- mutant of BHK cells. *Cell*, 15(2), 475-483. [https://doi.org/10.1016/0092-8674\(78\)90017-x](https://doi.org/10.1016/0092-8674(78)90017-x)
- Ossetrova, N. I., Blakely, W. F., Nagy, V., McGann, C., Ney, P. H., Christensen, C. L., Koch, A. L., Gulani, J., Sigal, G. B., Glezer, E. N., & Hieber, K. P. (2016). Non-human Primate Total-body Irradiation Model with Limited and Full Medical Supportive Care Including Filgrastim for Biodosimetry and Injury Assessment. *Radiat Prot Dosimetry*, 172(1-3), 174-191. <https://doi.org/10.1093/rpd/ncw176>
- Paul, S., & Amundson, S. A. (2008). Development of gene expression signatures for practical radiation biodosimetry. *Int J Radiat Oncol Biol Phys*, 71(4), 1236-1244. <https://doi.org/10.1016/j.ijrobp.2008.03.043>
- Pelger K. (1928). Demonstrate van een paar zeldzaamvoorkomend de typen v an bloedlichaapjes en bespreking der patienten n, *Nederl Tijdschr Geneesk* 72:1178; (in German).
- Ramalho, A. T., Curado, M. P., & Natarajan, A. T. (1995). Lifespan of human lymphocytes estimated during a six year cytogenetic follow-up of individuals accidentally exposed in

- the 1987 radiological accident in Brazil. *Mutat Res*, 331(1), 47-54.
[https://doi.org/10.1016/0027-5107\(95\)00049-o](https://doi.org/10.1016/0027-5107(95)00049-o)
- Rogakou, E. P., Pilch, D. R., Orr, A. H., Ivanova, V. S., & Bonner, W. M. (1998). DNA double-stranded breaks induce histone H2AX phosphorylation on serine 139. *J Biol Chem*, 273(10), 5858-5868. <https://doi.org/10.1074/jbc.273.10.5858>
- Romm, H., Oestreicher, U., & Kulka, U. (2009). Cytogenetic damage analysed by the dicentric assay. *Ann Ist Super Sanita*, 45(3), 251-259.
- Rothkamm, K., & Horn, S. (2009). gamma-H2AX as protein biomarker for radiation exposure. *Ann Ist Super Sanita*, 45(3), 265-271.
- Singh, M.; Kumar, A. & Kumara, H. N. (2020). "Macaca mulatta". IUCN Red List of Threatened Species. **2020**: e.T12554A17950825.
- Siracusa, M. C., Kim, B. S., Spergel, J. M., & Artis, D. (2013). Basophils and allergic inflammation. *J Allergy Clin Immunol*, 132(4), 789-801; quiz 788.
<https://doi.org/10.1016/j.jaci.2013.07.046>
- Spangrude, G. J., Heimfeld, S., & Weissman, I. L. (1988a). Purification and characterization of mouse hematopoietic stem cells. *Science*, 241(4861), 58-62.
<https://doi.org/10.1126/science.2898810>
- Sullivan, J. M., Prasanna, P. G., Grace, M. B., Wathen, L. K., Wallace, R. L., Koerner, J. F., & Coleman, C. N. (2013). Assessment of biodosimetry methods for a mass-casualty radiological

Supuka, P., & Parkanyl, V. (2014). Homozygous Pelger-Huet anomaly in three different crossbred rabbits: A case report. *Veterinami Medicina*, 59(2), 95-101. doi:10.17221/7319-VETMED

Swartz, H. M., Burke, G., Coey, M., Demidenko, E., Dong, R., Grinberg, O., Hilton, J., Iwasaki, A., Lesniewski, P., Kmiec, M., Lo, K. M., Nicolalde, R. J., Ruuge, A., Sakata, Y., Sucheta, A., Walczak, T., Williams, B. B., Mitchell, C., Romanyukha, A., & Schauer, D. A. (2007). In Vivo EPR For Dosimetry. *Radiat Meas*, 42(6-7), 1075-1084. <https://doi.org/10.1016/j.radmeas.2007.05.023>

Symons M, Handra, H., & Wyatt J (1995), Electron Paramagnetic Resonance Spectra of Irradiated Finger-nails: A Possible Measure of Accidental Exposure, *Radiation Protection Dosimetry*, Volume 58, Issue 1, Pages 11–15, <https://doi.org/10.1093/oxfordjournals.rpd.a082591>

Uckun, F. M., Yanishevski, Y., Tumer, N., Waurzyniak, B., Messinger, Y., Chelstrom, L. M., Lisowski, E. A., Ek, O., Zeren, T., Wendorf, H., Langlie, M. C., Irvin, J. D., Myers, D. E., Fuller, G. B., Evans, W., & Gunther, R. (1997). Pharmacokinetic features, immunogenicity, and toxicity of B43(anti-CD19)-pokeweed antiviral protein immunotoxin in cynomolgus monkeys. *Clin Cancer Res*, 3(3), 325-337.

Vale, A. M., Tomaz, L. R., Sousa, R. S., & Soto-Blanco, B. (2011). Pelger-Huet anomaly in two related mixed-breed dogs. *J Vet Diagn Invest*, 23(4), 863-865. <https://doi.org/10.1177/1040638711407891>

von Vietinghoff, S., & Ley, K. (2008). Homeostatic regulation of blood neutrophil counts. *J Immunol*, 181(8), 5183-5188. <https://doi.org/10.4049/jimmunol.181.8.5183>

Yu, J. Z., Lindeblad, M., Lyubimov, A., Neri, F., Smith, B., Szilagyi, E., Halliday, L., MacVittie, T., Nanda, J., & Bartholomew, A. (2015). Subject-Based versus Population-Based Care after Radiation Exposure. *Radiat Res*, 184(1), 46-55. <https://doi.org/10.1667/RR13918.1>

Yu, W., Hao, X., Yang, F., Ma, J., Zhao, Y., Li, Y., Wang, J., Xu, H., Chen, L., Liu, Q., Duan, S., Yang, Y., Huang, F., & He, Z. (2019). Hematological and biochemical parameters for Chinese rhesus macaque. *PLoS One*, 14(9), e0222338. <https://doi.org/10.1371/journal.pone.0222338><https://doi.org/10.1371/journal.pone.0222338>

8

APPENDIX A: COLORADO STATE UNIVERSITY IACUC INTER-INSTITUTIONAL AGREEMENT

**Colorado State University
Institutional Animal Care and Use Committee
Inter-Institutional Agreement
(CSU IACUC IIA)**

This form should be completed when animal work will take place at an institution other than Colorado State University (CSU) and:

- CSU is funding animal use activity or purchasing live vertebrate animals¹—either directly or through a subcontract or subaward
- Or CSU representatives are directly participating in the work involving animals.

Such collaboration has the potential to cause uncertainty involving animal use. Therefore, this form is designed to serve as a written agreement between CSU and the Collaborating Institution addressing the responsibility for animal care and use, animal ownership, and IACUC² review and oversight.

Please complete the applicable fields on this document and email the partially completed agreement and required attachments to: RICRO_IACUC@mail.colostate.edu

Name of CSU Investigator: Thomas E. Johnson
Name of Collaborating Institution Point of Contact: J. Mark Cline
Name of Collaborating Institution Providing IACUC Oversight: Wake Forest School of Medicine
Collaborating Institution USDA Registration # (as applicable): 825
Collaborating Institution PHS Animal Welfare Assurance# (as applicable): D16-00248(A3391-01)
Collaborating Institution AAALAC Accreditation Status (as applicable): Accredited September 13, 2017 Accredited #00008

The Officials signing below agree that Colorado State University (CSU) will rely on the designated IACUC of Wake Forest School of Medicine for the review and continuing oversight of its use of animals for the project described below:

This agreement covers the following specific IACUC protocol(s) at the *Collaborating Institution*:
Grant/Award/ Project Title: Radiation Countermeasures Long Term Response of Rhesus Macaques
Grant/Award/Project Principal Investigator: J. Mark Cline
Sponsor/Funding Agency (if any): NIH/NIAID
Sponsor Contract/Award Number (if any): U19 A167798
IACUC Protocol³ Principal Investigator: J. Mark Cline
IACUC Protocol Title: Radiation Countermeasures Long Term Response of Rhesus Macaques
IACUC Protocol Number: A 19-028
IACUC Protocol Approval Date: Tuesday, October 22, 2019

¹ Animals are defined here as live vertebrate animals used for the purposes of research, teaching, and/or testing.

² IACUC or equivalent body that performs this review and oversight

³ IACUC Protocol or equivalent document

Please check all that apply:

- The animals involved in the activity will be owned by the Collaborating Institution.
- The animals involved in the activity will be owned by Colorado State University but housed at the Collaborating Institution.
- Free-ranging, wild animals will be used in their natural habitat.
- Other (please describe): Click here to enter text.

Please provide a brief description of the nature of the collaboration in the space below.

Peripheral blood smears that have been taken and since archived by the collaborating institution are useable for a radiation biomarker study that is being conducted at CSU. Only fixed tissue will be needed by researchers at CSU and no contact will be made directly with the Rhesus Macaques. In addition, the work that will be conducted at CSU with the samples provided by Wake Forest will be funded by NIOSH/CDC and not the NIH funding listed in the IACUC protocol.

Please attach *official documentation of approval by the Collaborating Institution IACUC* to this document.

Grant – Protocol Congruency

If funded by a subaward or subcontract on a US Public Health Service (PHS) sponsored project⁴, the Collaborating Institution certifies the animal use as described in the protocol and grant are congruent:

Yes No ~~Both~~ *gmc*

The CSU IACUC also requires that the Collaborating Institution provide, as applicable:


- Documentation of IACUC approval for modifications to the approved protocol as well as triennial reviews of the protocols;
- Prompt notification of review and reporting of⁵:
 - any unexpected/adverse events that occur during the conduct of the research activities associated with this IIA that directly impact animal welfare,
 - any incidents of noncompliance with PHS Policy, the *Guide for the Care and Use of Laboratory Animals*, or any suspension of this activity by the IACUC;
- CSU requires that the collaborating institution provide notification of change in PHS Assurance status or AAALAC, International Accreditation status;
- For institutions not located in the US, a copy of the approved animal care and use protocol.

CSU IACUC may review the attached documentation and determine if a duplicative review is warranted or this form is sufficient to ensure animal welfare.

⁴ PHS agencies: National Institutes of Health (NIH), Food and Drug Administration (FDA), Center for Disease Control and Prevention (CDC), Health and Human Services Biomedical Advanced Research and Development Authority (HHS BARDA), Veterans Affairs (VA), and National Science Foundation (NSF).

⁵ Guidance on Prompt Reporting to OLAW under the PHS Policy on Humane Care and Use of Laboratory Animals: <https://grants.nih.gov/grants/guide/notice-files/NOT-OD-05-034.html>

CSU Signatures:


Signature of CSU Investigator Date: 21 Nov 19

Thomas E. Johnson


Print Name of CSU Investigator


Signature of Signatory Official for CSU Date: 12/20/19

Alan Rudolph, MBA, PhD^a

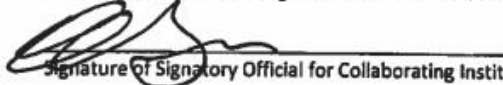
CSU Vice President for Research and Institutional Official (IO)

Collaborating Institution Signatures:


Signature of Collaborating Institution IACUC Protocol PI Date: 11/27/19

J. Mark Cline

Print Name of Collaborating Institution IACUC Protocol PI


Signature of Signatory Official for Collaborating Institution Date: 12/17/19

Christa Johnson

Print Name of Signatory Official for Collaborating Institution

^a Christa Johnson, PhD, Associate Vice President for Research, signature delegate for the IO.

APPENDIX B: WAKE FOREST SCHOOL OF MEDICINE IACUC APPROVAL LETTER



Office of Research

ANIMAL CARE AND USE COMMITTEE
ASSURANCE A3391-01

MEMORANDUM

To: J. Cline, D.V.M., Ph.D.
Comparative Medicine

From: Paul Czoty, Ph.D., Chair
Animal Care and Use Committee

Date: 6/14/2019

Subject: Animal Protocol: A19-028
<p>Radiation Countermeasures Long Term Response of Rhesus Macaques</p>

Official Approval Date: 6/14/2019

The Animal Care and Use Committee has concluded that the animals in your study will be appropriately used, will receive acceptable levels of care, will not be subjected to pain or distress needlessly, and will, if necessary, be terminated in a humane manner.

When ordering the animals for the above referenced study, please refer to the "A" number assigned to your project by the Animal Care and Use Committee. Since this is a replacement protocol, please transfer the animals currently in your care to the new protocol number using the Transfer Request forms for rodents or non-rodents (see <http://www1.wfubmc.edu/ARP/forms/>).

Committee approval is for a period of twelve months with a renewal allowed for two additional years. You will be sent a reminder memorandum three months prior to the anniversary date requesting the status of this protocol. Please notify the Office of Research when the project is terminated.

Non-Federal Research Sponsorship: If this protocol is related to a contract you may have reporting responsibilities to the sponsor. We encourage you to review the terms of the contract or contact the sponsor. This protocol replaces A16-094 which was terminated on 6/14/2019.

Paul Czoty, Ph.D.

APPENDIX C: OCCUPATIONAL SAFETY AND HEALTH ZOOLOGIC CONCERNS
AGREEMENT WITH WAKE FOREST PRIMATE CENTER



Department of Pathology
Section on Comparative Medicine

Thursday, December 12, 2019

Safety Considerations for Handling of Nonhuman Primate Tissues

J. Mark Cline, DVM, PhD
Professor of Pathology/Comparative Medicine
Diplomate, American College of Veterinary Pathologists

Fresh or Frozen Tissues

There are unique procedures and safety concerns surrounding the use of macaque tissues, primarily because of concerns regarding the zoonotic Cercopithecine Herpesvirus 1 ("Herpes B"). Special care should be used when handling fresh or frozen tissues, as many pathogens will survive freezing. A lab coat, gloves, face mask, and full eye protection (face shield or goggles) must be worn. Waste tissue must be incinerated. Instruments or surfaces exposed to the tissues must be disinfected using methods approved for the control of tuberculosis and herpesviruses. Gloves must be removed when leaving the work area, and hands washed. There can be no smoking, eating, or application of cosmetics in any laboratory area where nonhuman primate tissues are handled. Working in a biosafety cabinet is recommended if aerosols will be produced otherwise full personnel protective equipment is recommended.

If the person handling the tissues is injured in any way involving a break in the skin or exposure of the face to monkey tissues, immediate cleaning of the area is imperative, and medical attention should be sought. The guidelines in the attached document "Occupational Health Program for Personnel Caring for or Using Laboratory Animals and Animal Tissues/Fluids" are those used by Wake Forest University in working with hazardous animal tissues, and are provided for your information.

Fixed Tissues

Fixation should kill any infectious agents in the tissue; however, caution is recommended in handling even fixed tissues. If the tissues are formalin-fixed, a lab coat and gloves are required for handling them, and because of the cancer hazard associated with formaldehyde vapor, all work with fixed tissues should be done under a fume hood. A face shield or goggles should also be worn.

Please sign the following statement. No tissues can be sent until we have this document on file.

"I have read and understand this agreement and the attached guidelines, and I accept full responsibility for the proper handling of animal tissues obtained from Wake Forest University."

Signature:

A handwritten signature in black ink, appearing to read "Joshua M. Hayes".

Date:

12/12/2019

Printed Name:

Joshua M. Hayes

Wake Forest University Primate Center
Medical Center Boulevard, Winston-Salem, NC 27157-1040
Telephone 336 716 1564 • Fax 336 716 1515 • E-mail jmcline@wfubmc.edu

Department of Pathology
Section on Comparative Medicine

Thursday, December 12, 2019

Safety Considerations for Handling of Nonhuman Primate Tissues

J. Mark Cline, DVM, PhD
Professor of Pathology/Comparative Medicine
Diplomate, American College of Veterinary Pathologists

Fresh or Frozen Tissues

There are unique procedures and safety concerns surrounding the use of macaque tissues, primarily because of concerns regarding the zoonotic Cercopithecine Herpesvirus I ("Herpes B"). Special care should be used when handling fresh or frozen tissues, as many pathogens will survive freezing. A lab coat, gloves, face mask, and full eye protection (face shield or goggles) must be worn. Waste tissue must be incinerated. Instruments or surfaces exposed to the tissues must be disinfected using methods approved for the control of tuberculosis and herpesviruses. Gloves must be removed when leaving the work area, and hands washed. There can be no smoking, eating, or application of cosmetics in any laboratory area where nonhuman primate tissues are handled. Working in a biosafety cabinet is recommended if aerosols will be produced otherwise full personnel protective equipment is recommended.

If the person handling the tissues is injured in any way involving a break in the skin or exposure of the face to monkey tissues, immediate cleaning of the area is imperative, and medical attention should be sought. The guidelines in the attached document "Occupational Health Program for Personnel Caring for or Using Laboratory Animals and Animal Tissues/Fluids" are those used by Wake Forest University in working with hazardous animal tissues, and are provided for your information.

Fixed Tissues

Fixation should kill any infectious agents in the tissue; however, caution is recommended in handling even fixed tissues. If the tissues are formalin-fixed, a lab coat and gloves are required for handling them, and because of the cancer hazard associated with formaldehyde vapor, all work with fixed tissues should be done under a fume hood. A face shield or goggles should also be worn.

Please sign the following statement. No tissues can be sent until we have this document on file.

"I have read and understand this agreement and the attached guidelines, and I accept full responsibility for the proper handling of animal tissues obtained from Wake Forest University."

Signature: _____

Date: _____

Printed Name: _____

Wake Forest University Primate Center
Medical Center Boulevard, Winston-Salem, NC 27157-1040
Telephone 336 716 1564 • Fax 336 716 1515 • E-mail jmcline@wfubmc.edu

Occupational Health and Zoonotic Concerns When Using Laboratory Animals or Tissues

While not complete, this document identifies the zoonotic and infectious agents most likely to pose a health threat to employees, students, and visitors of the Wake Forest Baptist Medical Center. Persons working with or in close proximity to animals not covered in this summary should consult their supervisor regarding potential health hazards and appropriate precautions necessary to reduce the risk of animal-associated occupational injury or illness. These guidelines are to be followed by visitors, students, and house officers as well. As necessary, situations will be handled on a case-by-case basis in keeping with safety considerations and procedures for the humans and animals alike, and in keeping with the current regulatory requirements, e.g., CDC, OSHA, AAALAC, and TJC (The Joint Commission).

Please read this document thoroughly and ask any questions you may have. Your signature, witnessed by a supervisor and/or other designated individual, acknowledges that you have read the document and have had the opportunity to ask questions about its contents.

Isaac M. Hayes
Employee Name (Print)

[Signature]
Signature

12/12/2019
Date

[Signature]
Supervisor Name (Print)

Thomas E. Johnson
Signature

12/12/2019
Date

Document updated May 19, 2017

[Signature] MD
Andrea S. Fernandez, MD
Medical Director, Employee and Occupational Health Services

5/19/17
Date

[Signature]
Richard W. Young, DVM, Diplomate ACLAM
Director, Animal Resources Program

6-14-17
Date

Retain original in department and provide a copy to the employee/visitor.

Occupational Health and Zoonotic Concerns When Using Laboratory Animals or Tissues

While not complete, this document identifies the zoonotic and infectious agents most likely to pose a health threat to employees, students, and visitors of the Wake Forest Baptist Medical Center. Persons working with or in close proximity to animals not covered in this summary should consult their supervisor regarding potential health hazards and appropriate precautions necessary to reduce the risk of animal-associated occupational injury or illness. These guidelines are to be followed by visitors, students, and house officers as well. As necessary, situations will be handled on a case-by-case basis in keeping with safety considerations and procedures for the humans and animals alike, and in keeping with the current regulatory requirements, e.g., CDC, OSHA, AAALAC, and TJC (The Joint Commission).

Please read this document thoroughly and ask any questions you may have. Your signature, witnessed by a supervisor and/or other designated individual, acknowledges that you have read the document and have had the opportunity to ask questions about its contents.

Thomas E. Johnson [Signature] 12/12/2019
Employee Name (Print) Signature Date

Alexander Bradt (Section Head) [Signature] 12 DEC 19
Supervisor Name (Print) Signature Date

Document updated May 19, 2017

[Signature] MD 5/19/17
Andrea S. Fernandez, MD Date
Medical Director, Employee and Occupational Health Services

[Signature] 6-14-17
Richard W. Young, DVM, Diplomate ACLAM Date
Director, Animal Resources Program

Retain original in department and provide a copy to the employee/visitor.

APPENDIX D: CHART OF HEMATOPOIETIC STEM CELL DIFFERENTIATION

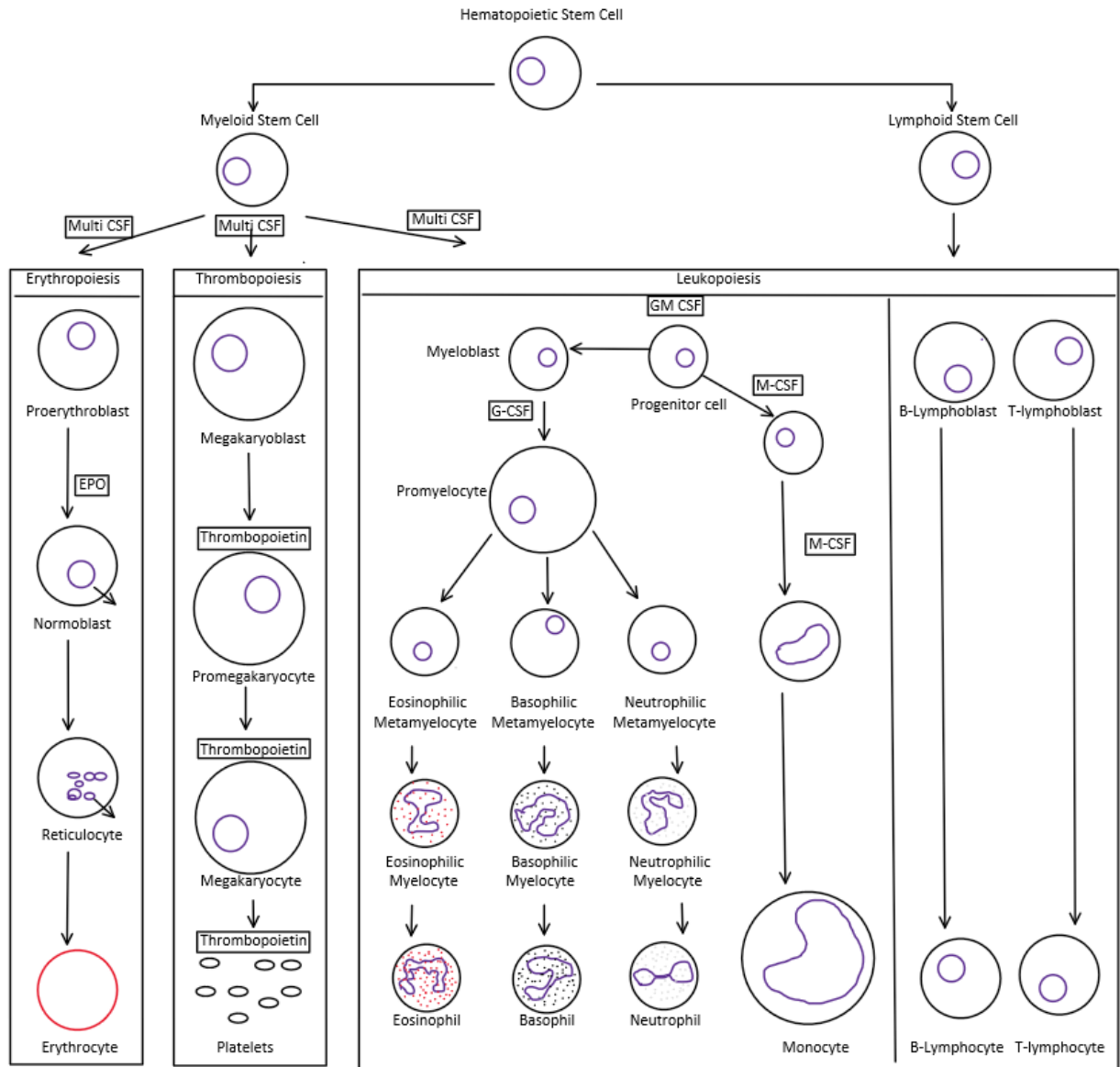


Figure 17. Hematopoietic stem cell differentiation into all components of the blood.

APPENDIX E: STATEMENT OF PERMISSION TO USE RHESUS MACAQUE IMAGES

Photo Release

I, Prof. J Mark Cline hereby grant and authorize Joshua M. Hayes and Thomas E. Johnson of Colorado State University, Department of Environmental and Radiological Health Sciences the right to utilize 2 images of rhesus macaques (see thumbnails below) provided by Wake Forest School of Medicine, Section on Comparative Medicine for limited purposes. This authorization of use is limited to the use of the photos as figures and in publication of Joshua Hayes' doctoral dissertation and use in presentation of the dissertation results. Any use of the photos outside of the prescribed uses is prohibited.

J Mark Cline

December 10, 2020

Printed Name

Date


Signature



APPENDIX F: RHESUS MACAQUE DATA TABLES AND MODELS FOR INDIVIDUALS
IN THE BIOKINETICS/PERSISTENCE STUDY

Table 7. Rhesus macaques dose response data.

Rhesus Macaque Dose Response Data				
Animal ID	Days Post Irradiation Blood Smear was Taken	Radiation Dose (Gy)	Number of PPHAs	PPHA %
1962	N/A	0	3	1.00
1965	N/A	0	5	1.67
1971	N/A	0	0	0.00
1973	N/A	0	4	1.33
1974	N/A	0	0	0.00
1975	N/A	0	2	0.67
1976	N/A	0	3	1.00
1977	N/A	0	1	0.33
1979	N/A	0	2	0.67
1982	N/A	0	0	0.00
1960	N/A	0	1	0.33
1967	N/A	0	0	0.00
1968	N/A	0	2	0.72
1969	N/A	0	1	0.33
1970	N/A	0	2	0.67
1972	N/A	0	1	0.33
2061	195	0	2	0.67
2065	195	0	2	0.67
1962	198	4	6	2.00
1965	193	4	10	3.34
1971	198	4	9	3.01
1973	193	4	9	3.00
1974	199	4	6	2.01
1975	192	4	10	3.34
1976	193	4	7	2.34
1977	192	4	9	3.00
1979	198	4	8	2.69
1982	199	4	6	2.00
2058	195	4	8	2.67
2059	195	4	8	2.67
2060	195	4	7	2.33
2062	195	4	8	2.67

2063	195	4	9	3.00
2064	195	4	6	2.00
2067	195	4	5	1.67
1892	223	6.4	14	4.67
1884	203	6.5	9	3.00
1885	196	6.5	8	2.67
1886	183	6.5	13	4.33
1904	210	6.5	11	3.67
1906	204	6.5	12	4.00
1917	203	6.5	10	3.33
1919	184	6.5	9	3.00
2056	209	6.5	12	4.00
1910	201	8	14	4.67
2053	217	8	16	5.33
1905	204	8.5	15	5.00
Average Days Post Irradiation= 198 ± 8.23				

Group 1 Biokinetics, Rhesus Macaques, Irradiation date 10/23/2016 (4Gy dose)

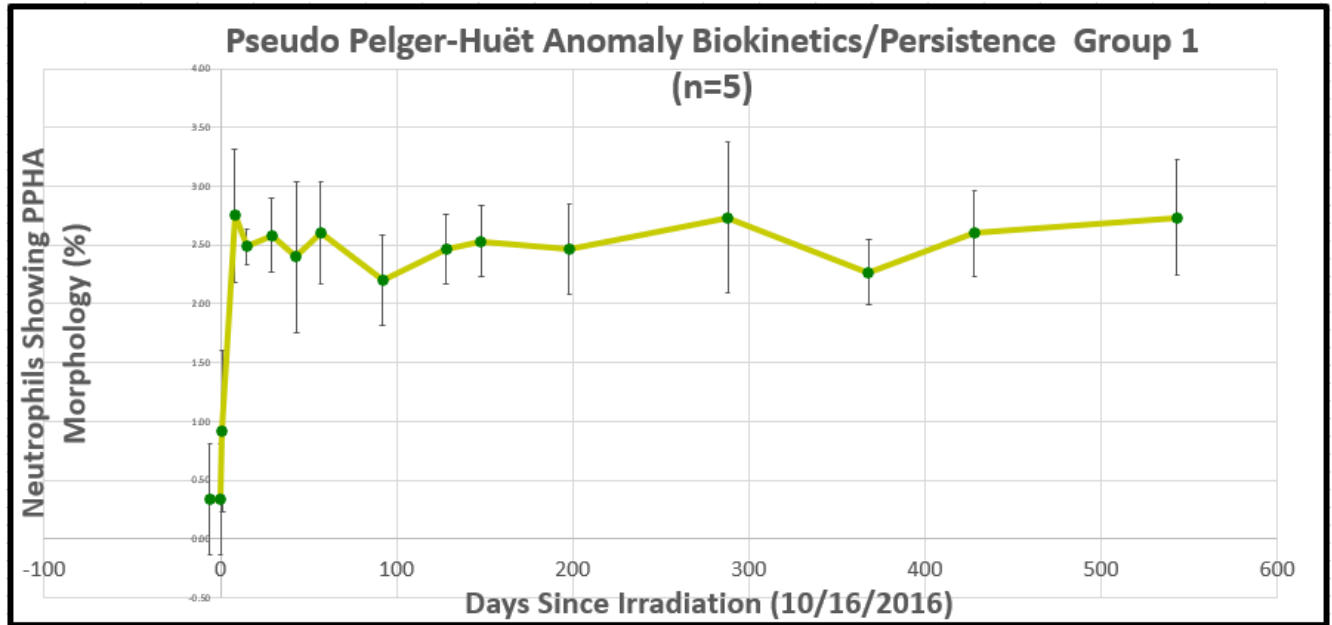


Figure 18. Rhesus macaque biokinetics/persistence, average PPHA concentration of group 1 (rhesus macaque ID 1962, 1971, 1974, 1979, & 1982).

Table 8. Rhesus macaque biokinetics/persistence, average PPHA concentration of group 1 (rhesus macaque ID 1962, 1971, 1974, 1979, & 1982).

Average Biokinetics/Persistence Group 1 (n=5)		
Days Since Irradiation	Average PPHA %	Std.Dev (±)
-6	0.33	0.47
0	0.33	0.47
1	0.92	0.69
8	2.75	0.57
15	2.49	0.15
29	2.58	0.32
43	2.40	0.64
57	2.60	0.43
92	2.20	0.38
128	2.47	0.30
148	2.53	0.30
198	2.47	0.38
288	2.73	0.64
368	2.27	0.28
428	2.60	0.37
543	2.73	0.49
659	2.67	0.47
829	2.73	0.72

1018	2.67	0.41
1125	2.83	0.19

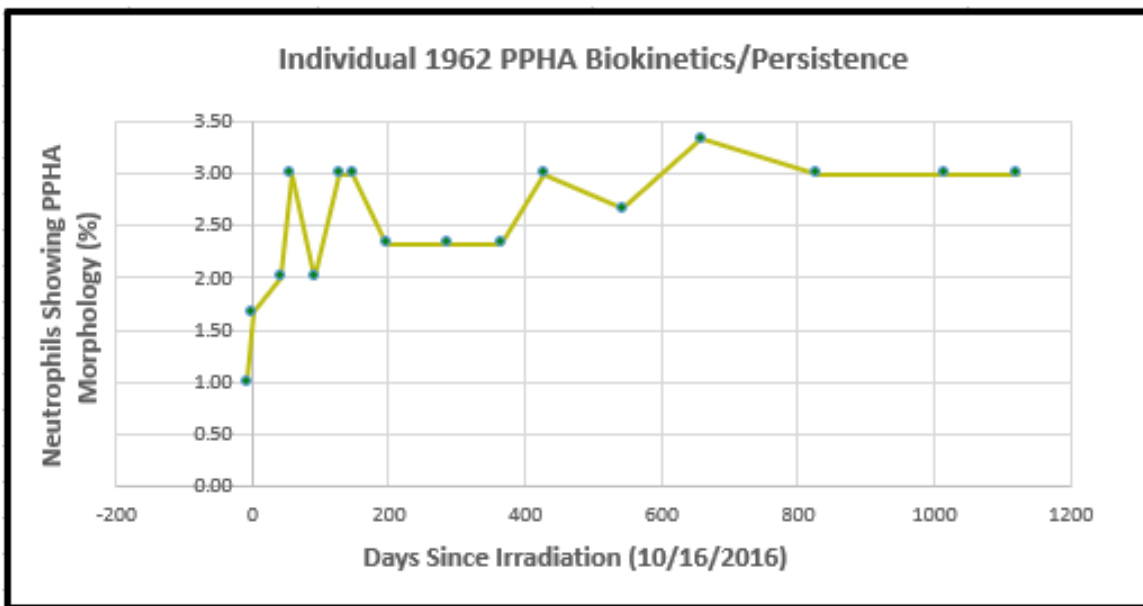


Figure 19. Biokinetics/persistence diagram for macaque 1962.

Table 9. Biokinetics/persistence for macaque 1962.

1962	
Days Post Irradiation	PPHA %
-6	1.00
1	1.67
43	2.00
57	3.00
92	2.00
128	3.00
148	3.00
198	2.33
288	2.33
366	2.33
428	3.00
544	2.67
659	3.33
829	3
1018	3
1124	3

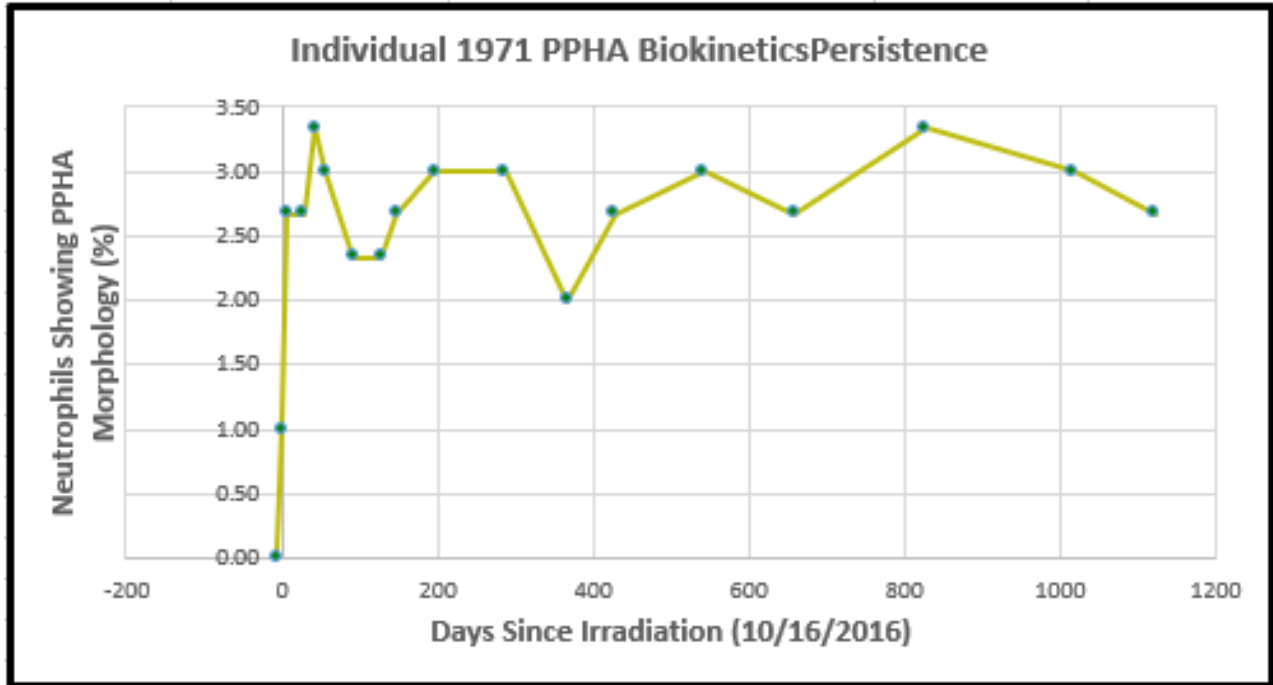


Figure 20. Biokinetics/persistence diagram for macaque 1971.

Table 10. Biokinetics/persistence for macaque 1971.

1971	
Days Post Irradiation	PPHA %
-6	0.00
1	1.00
8	2.67
29	2.67
43	3.33
57	3.00
92	2.33
128	2.33
148	2.67
198	3.00
288	3.00
368	2.00
429	2.67
544	3.00
659	2.67
829	3.33
1018	3.00
1124	2.67

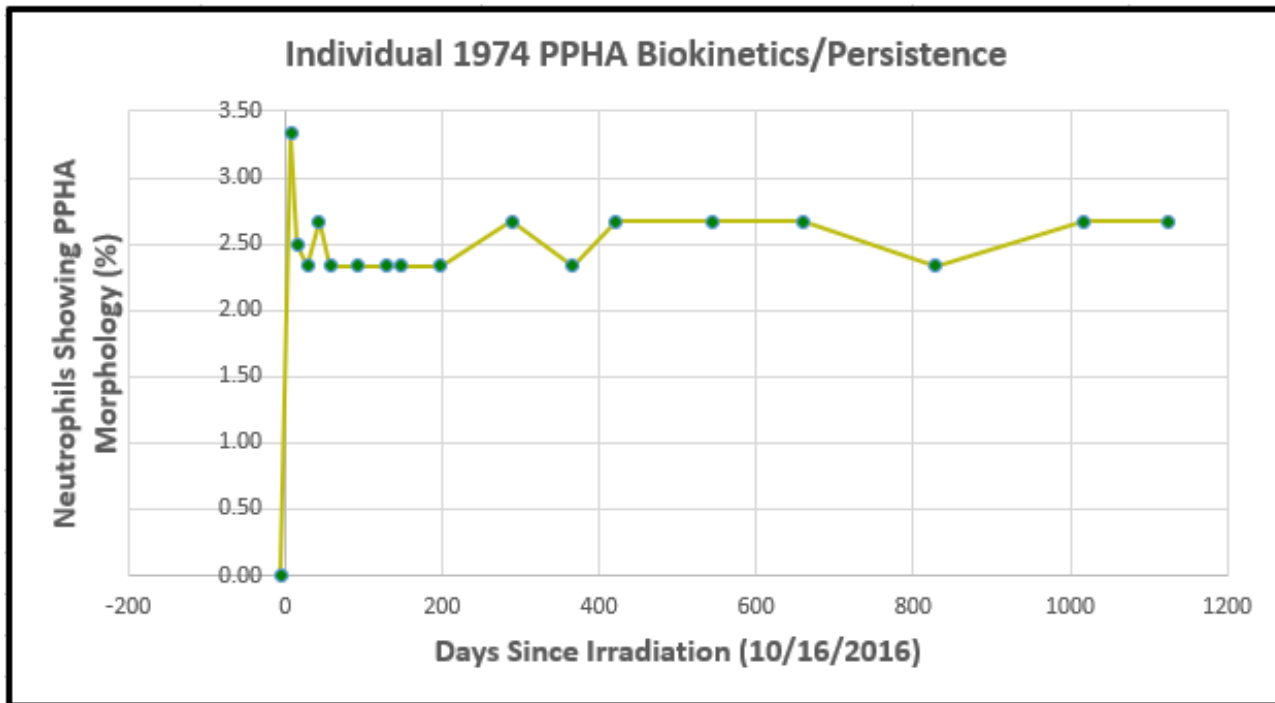


Figure 21. Biokinetics/persistence diagram for macaque 1974.

Table 11. Biokinetics/persistence for macaque 1974.

1974	
Days Post Irradiation	PPHA %
-6	0.00
8	3.33
15	2.50
29	2.33
43	2.67
57	2.33
92	2.33
128	2.33
148	2.33
198	2.33
288	2.67
366	2.33
421	2.67
543	2.67
659	2.67
829	2.33
1018	2.67
1124	2.67

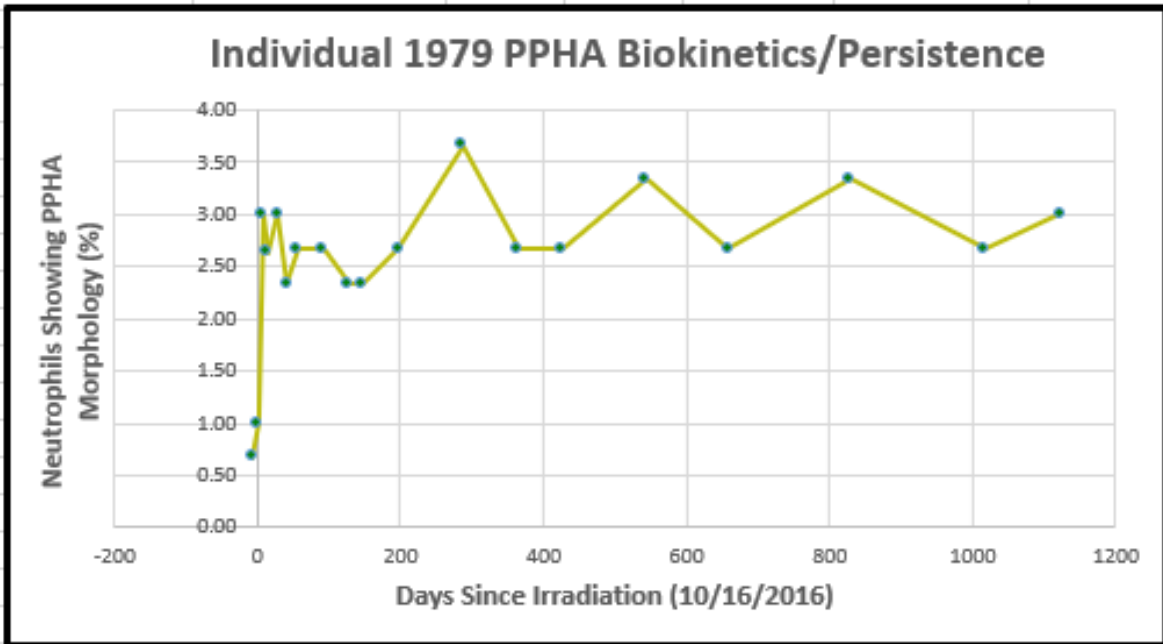


Figure 22. Biokinetics/persistence diagram for macaque 1979.

Table 12. Biokinetics/persistence for macaque 1979.

1979	
Days Post Irradiation	PPHA %
-6	0.67
1	1.00
8	3.00
15	2.63
29	3.00
43	2.33
57	2.67
92	2.67
128	2.33
148	2.33
198	2.67
288	3.67
366	2.67
428	2.67
544	3.33
659	2.67
829	3.33
1018	2.67
1124	3.00

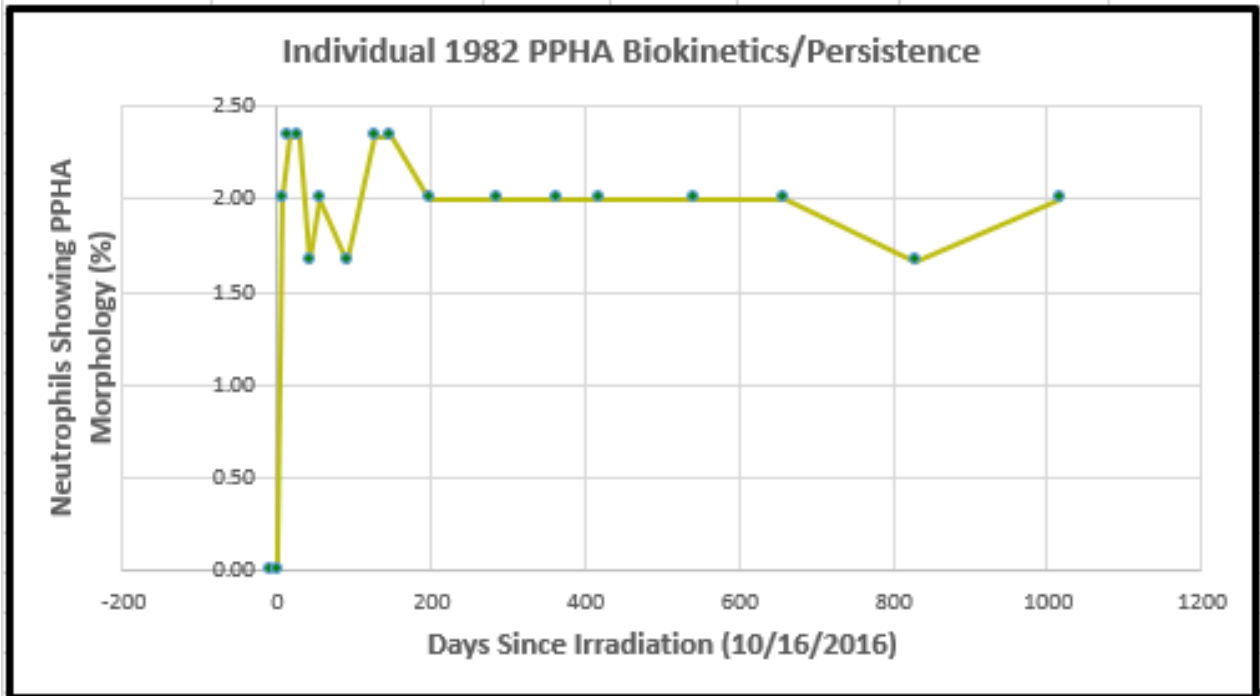


Figure 23. Biokinetics/persistence diagram for macaque 1982.

Table 13. Biokinetics/persistence for macaque 1982.

1982	
Days Post Irradiation	PPHA %
-6	0.00
1	0.00
8	2.00
15	2.33
29	2.33
43	1.67
57	2.00
92	1.67
128	2.33
148	2.33
198	2.00
288	2.00
366	2.00
421	2.00
543	2.00
659	2.00
829	1.67
1018	2.00

Group 2 Rhesus Macaques, Irradiation date 10/23/2016 (4Gy dose):

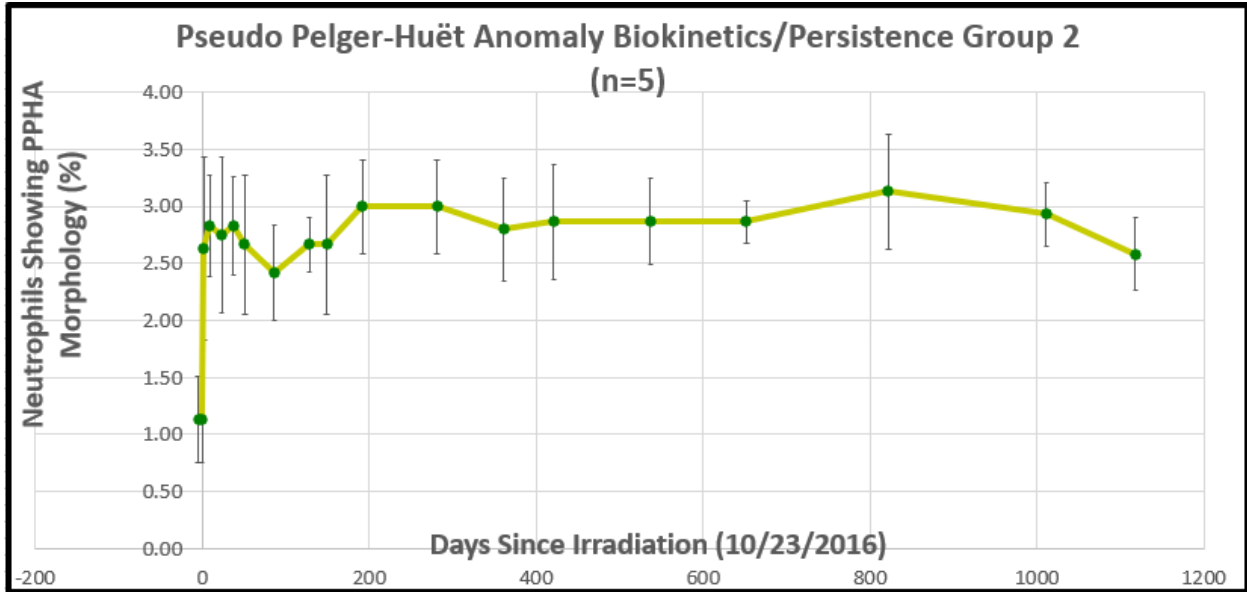


Figure 24. Rhesus macaque biokinetics/persistence, average PPHA concentration of group 2 (rhesus macaque ID 1965, 1971, 1975, 1976, & 1977).

Table 14. Rhesus macaque biokinetics/persistence, average PPHA concentration of group 2 (rhesus macaque ID 1965, 1971, 1975, 1976, & 1977).

Average Biokinetics/Persistence Group 2 (n=5)		
Days Post Irradiation	Average PPHA %	Std. Dev (±)
-5	1.13	0.38
0	1.13	0.38
2	2.63	0.80
9	2.83	0.44
23	2.75	0.69
37	2.83	0.43
51	2.67	0.61
86	2.42	0.42
128	2.67	0.24
149	2.67	0.61
192	3.00	0.41
281	3.00	0.41
361	2.80	0.45
421	2.87	0.51
537	2.87	0.38
652	2.87	0.18
822	3.13	0.51
1011	2.93	0.28
1118	2.58	0.32

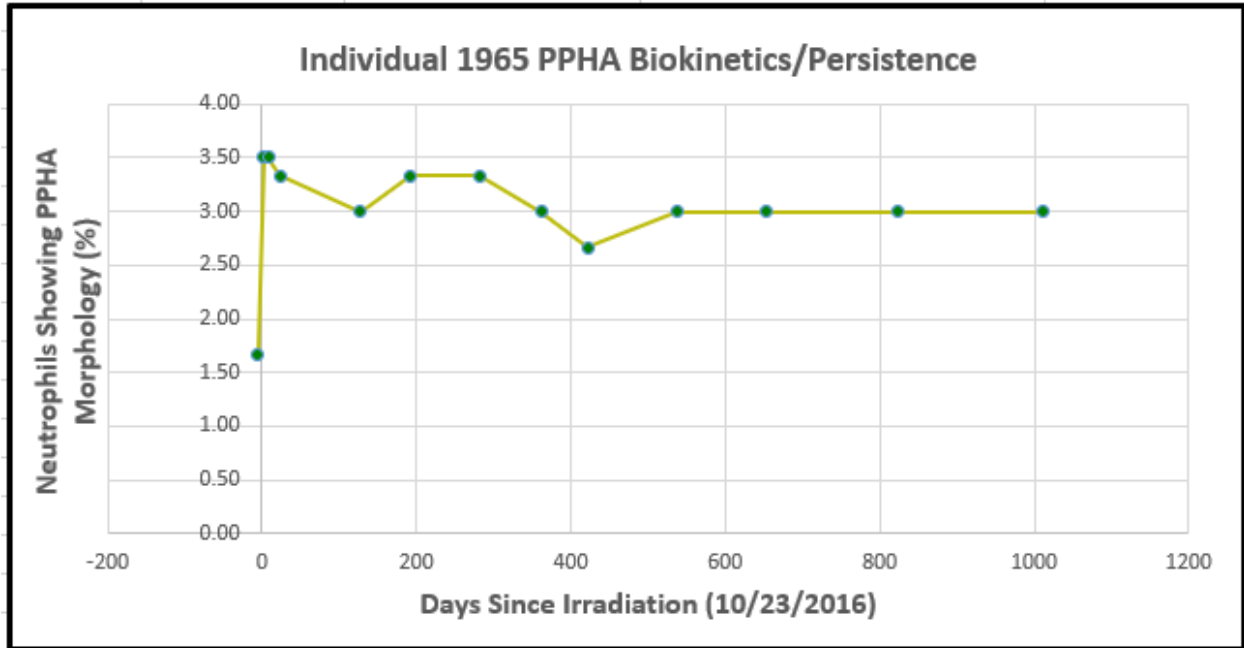


Figure 25. Biokinetics/persistence diagram for macaque 1965.

Table 15. Biokinetics/persistence for macaque 1965.

1965	
Days Post Irradiation	PPHA %
-5	1.67
2	3.50
9	3.50
23	3.33
128	3.00
192	3.33
281	3.33
361	3.00
422	2.67
537	3.00
652	3.00
822	3.00
1011	3.00

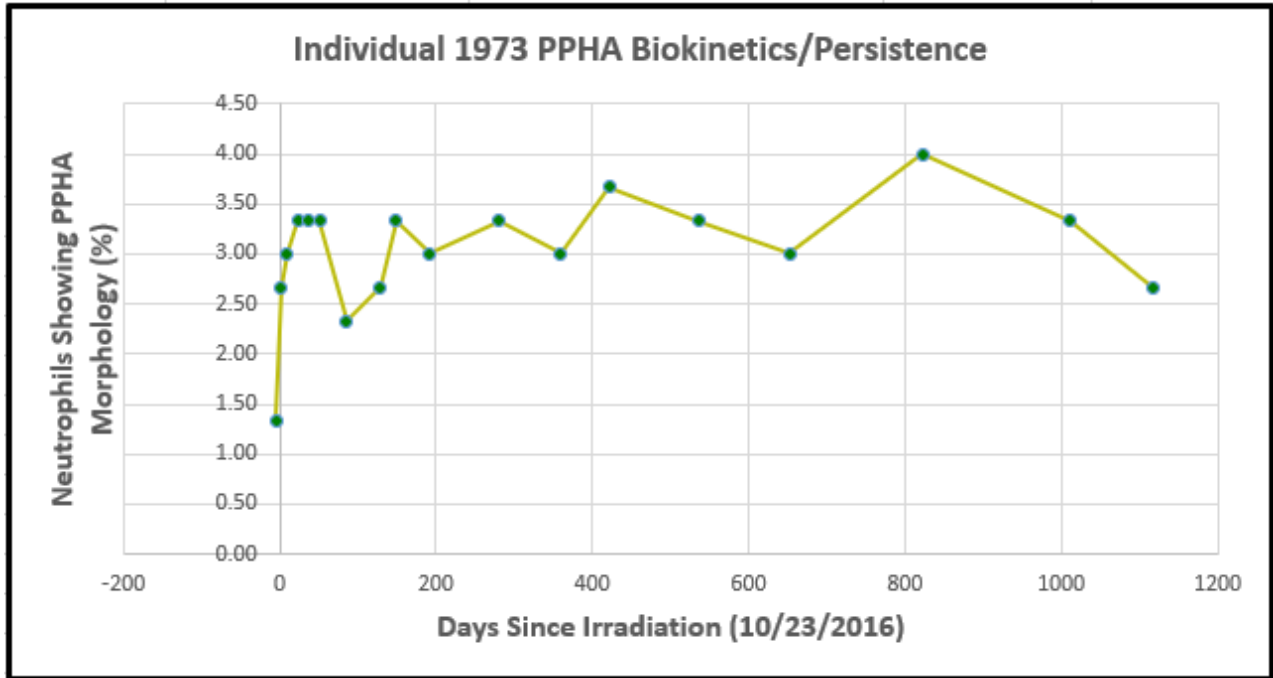


Figure 26. Biokinetics/persistence diagram for macaque 1973.

Table 16. Biokinetics/persistence for macaque 1973.

1973	
Days Post Irradiation	PPHA %
-5	1.33
2	2.67
9	3.00
23	3.33
37	3.33
51	3.33
86	2.33
128	2.67
149	3.33
192	3.00
281	3.33
359	3.00
421	3.67
536	3.33
652	3.00
822	4.00
1011	3.33
1117	2.67

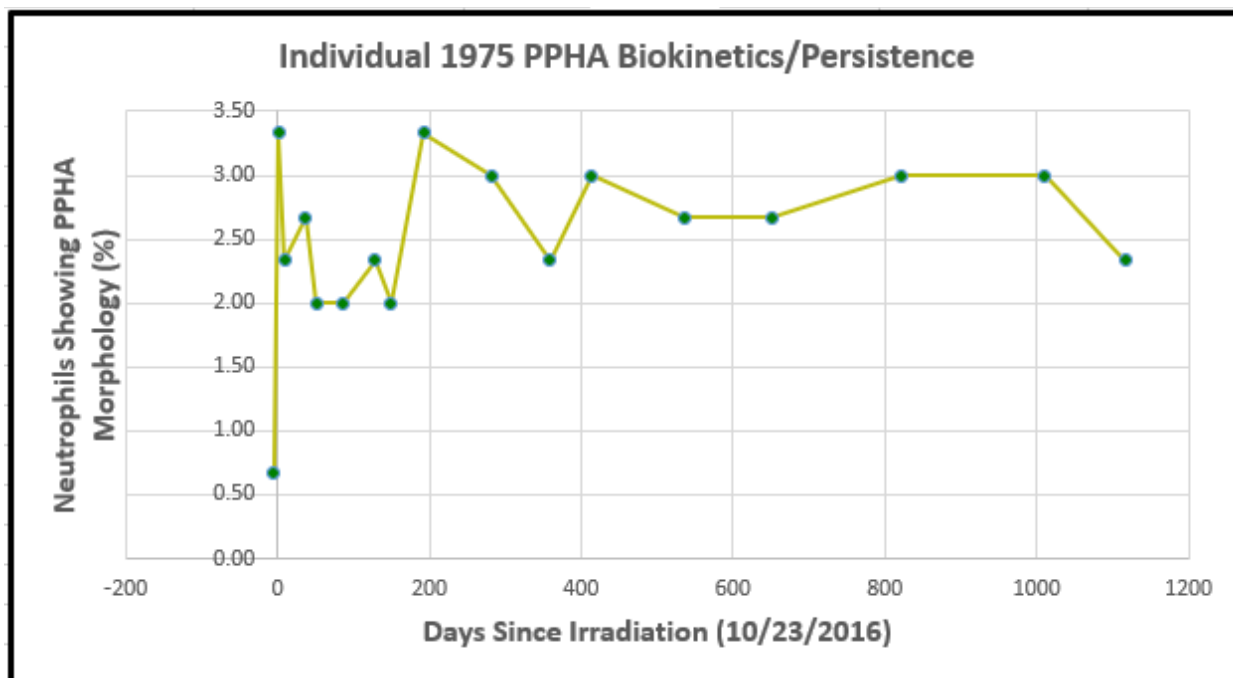


Figure 27. Biokinetics/persistence diagram for macaque 1975.

Table 17. Biokinetics/persistence for macaque 1975.

1975	
Days Post Irradiation	PPHA %
-5	0.67
2	3.33
9	2.33
37	2.67
51	2.00
86	2.00
128	2.33
149	2.00
192	3.33
281	3.00
359	2.33
414	3.00
536	2.67
652	2.67
822	3.00
1011	3.00
1117	2.33

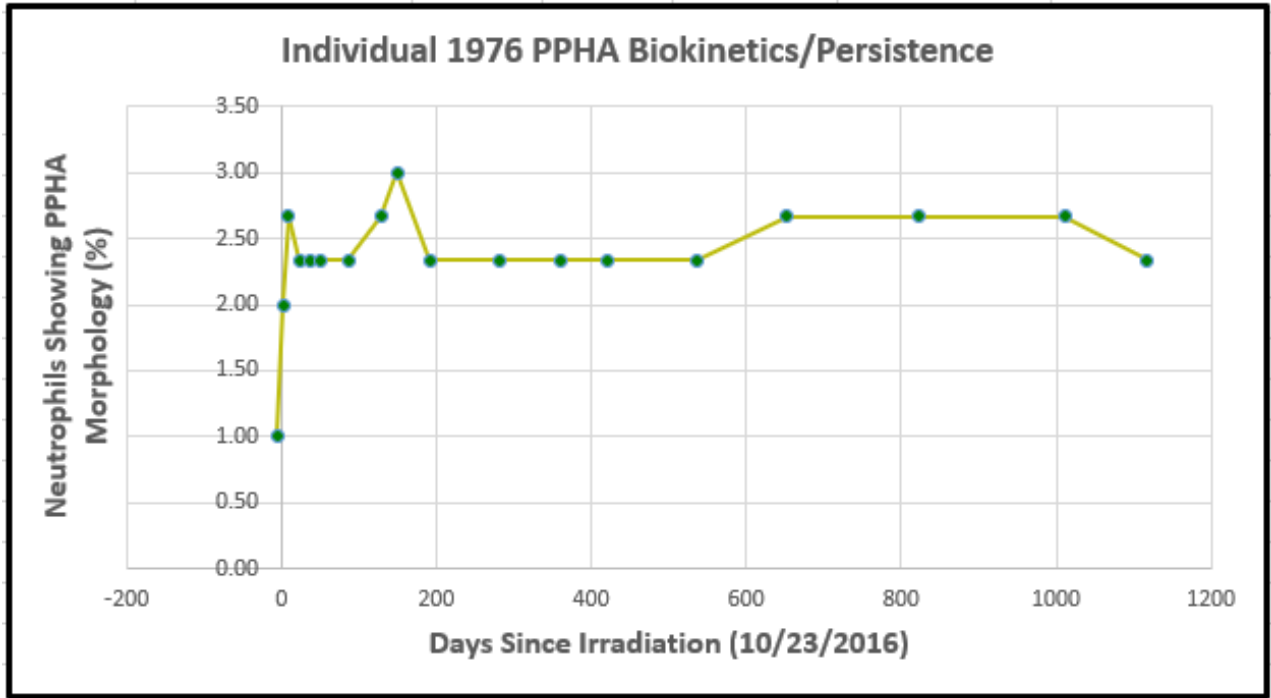


Figure 28. Biokinetics/persistence diagram for macaque 1976.

Table 18. Biokinetics/persistence for macaque 1976.

1976	
Days Post Irradiation	PPHA %
-5	1.00
2	2.00
9	2.67
23	2.33
37	2.33
51	2.33
86	2.33
128	2.67
149	3.00
192	2.33
281	2.33
359	2.33
421	2.33
537	2.33
652	2.67
822	2.67
1011	2.67
1117	2.33

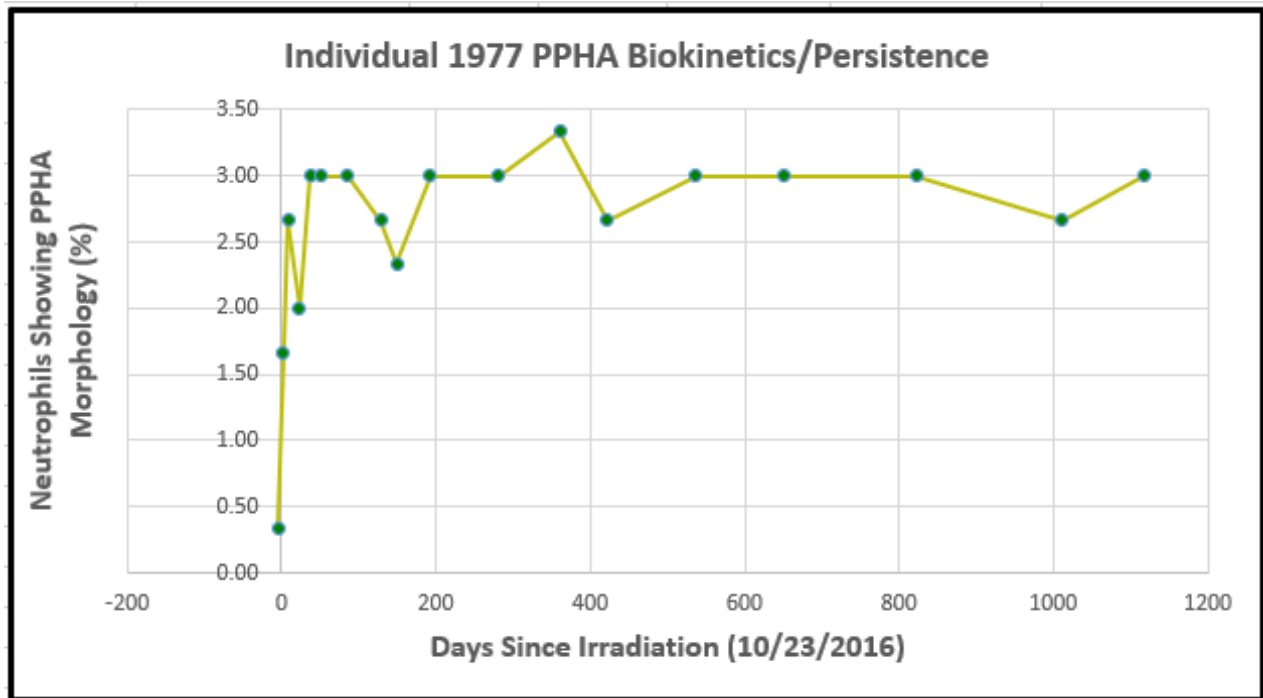


Figure 29. Biokinetics/persistence diagram for macaque 1977.

Table 19. Biokinetics/persistence for macaque 1977.

1977	
Days Post Irradiation	PPHA %
-5	0.33
2	1.67
9	2.67
23	2.00
37	3.00
51	3.00
86	3.00
128	2.67
149	2.33
192	3.00
281	3.00
361	3.33
422	2.67
537	3.00
652	3.00
822	3.00
1011	2.67
1117	3.00

APPENDIX G: MAKING A BLOOD SMEAR

1. Place a drop of blood that is roughly 10 μ L in volume near one end of a blood slide.
2. quickly take a second slide and while holding it at an angle above the slide containing the drop of blood contact the slide as seen in Figure 30.
 - a. It is important to do this quickly because the blood will coagulate rapidly in air.

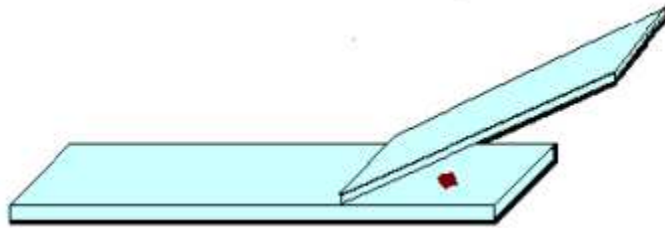


Figure 30. Placement of second slide in the process of creating a blood smear.

3. While ensuring that contact is maintained between the two slides draw the top slide back towards the blood drop slowly. Capillary action will cause the blood to spread out along the glass surface depicting in Figure 31.

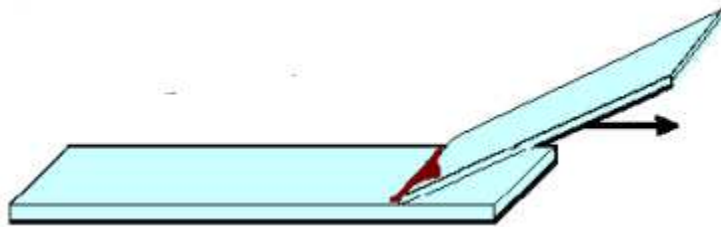


Figure 31. Drawing back the top slide as to contact the blood drop.

4. In a quick motion push the top slide forward. The blood with smear behind the slide in a uniform fashion as depicted in Figure 32. Ideally the resulting smear will have a feathered edge that will be the location of evaluation.

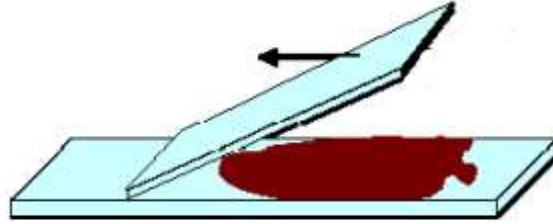


Figure 32. Placement of second slide in the process of creating a blood smear.

5. Allow the blood to dry and then using an eye dropper coat the smear in 100% methanol to fix the cells in place.
6. Return to the lab and see to Appendix H for Giemsa staining and cover slipping.

APPENDIX H: GIEMSA STAINING BLOOD SMEARS

1. Ensure that blood smears are fixed in methanol and properly dried and labeled.
 - a. If an ink pen is used for labeling methanol will cause the label to run. Write label with pencil and write over with a permanent marker once slides are fully prepared.
2. Prepare a 5% Giemsa stain in GURR
 - a. GURR buffer solution preparation:
 - i. Add 1 tablet to 100mL dH₂O → dissolve
 - ii. GURR buffer tablets can be seen in Figure 33.



Figure 33. GURR buffer tablets used in preparation of Giemsa stain

- b. Add 2.5mL Giemsa solution to 47.5mL GURR in a Coplin jar
3. Submerge slides in Giemsa solution for 45 minutes in a Coplin jar.
4. Rinse in fresh deionized H₂O. stained and rinsed blood smears can be seen in Figure 34.

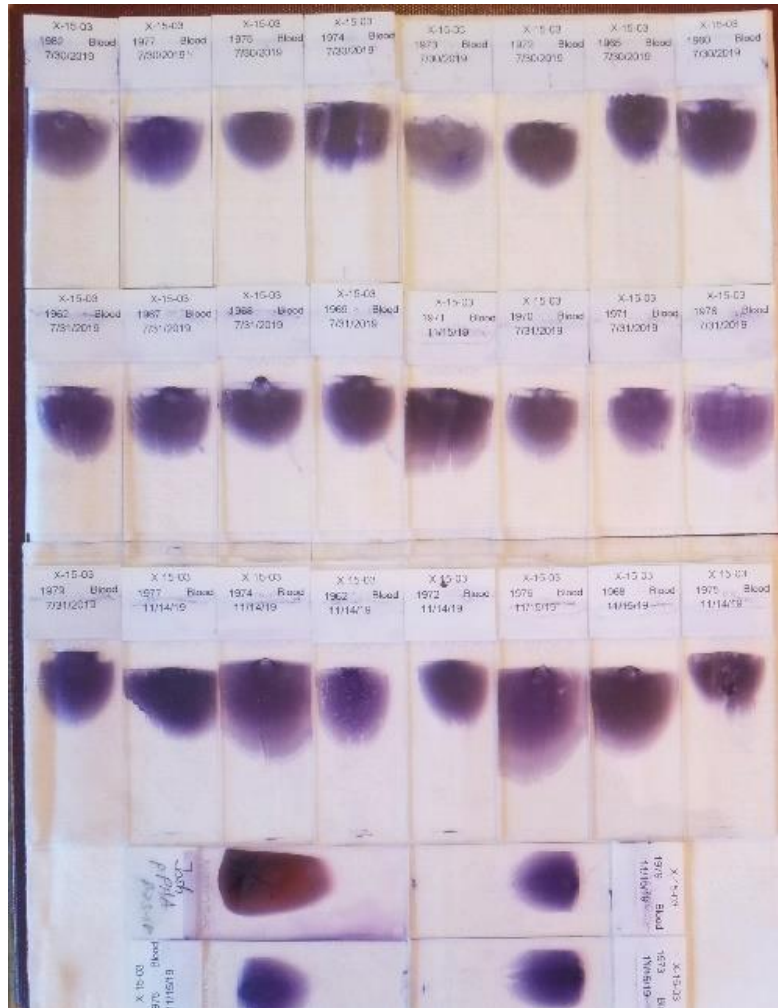


Figure 34. Giemsa stained blood smears.

5. Submerge slides in xylene to ensure all oils are removed.
6. Mount coverslip with Permount mounting medium.
 - a. Apply pressure to the coverslip to remove any air bubbles.
 - b. Clean any excess mounting medium that is forced out from under the coverslip.
7. Store in cool dry place. Avoid keeping them for extended periods of time in hot vehicles if transporting them.